



Published in final edited form as:

Chem Soc Rev. 2017 October 02; 46(19): 5771–5804. doi:10.1039/c7cs00195a.

The development of anticancer ruthenium(II) complexes: from single molecule compounds to nanomaterials

Leli Zeng^{1,2}, Pranav Gupta¹, Yanglu Chen³, Enju Wang⁴, Liangnian Ji², Hui Chao^{2,*}, and Zhe-Sheng Chen^{1,*}

¹College of Pharmacy and Health Sciences, St. John's University, New York, NY 11439, USA

²MOE Key Laboratory of Bioinorganic and Synthetic Chemistry, School of Chemistry, Sun Yat-Sen University, 510275, P. R. China

³Department of Chemistry, Princeton University, Princeton, New Jersey, NJ 08544, USA

⁴Department of Chemistry, St. John's University, New York, NY 11439, USA

Abstract

Cancer is rapidly becoming the top killer in the world. Most of the FDA approved anticancer drugs are organic molecules, while metallodrugs are very scarce. The advent of first metal based therapeutic agent, cisplatin, launched a new era in the application of transition metal complexes for therapeutic design. Due to their unique and versatile biochemical properties, ruthenium-based compounds have emerged as promising anti-cancer agents that serve as alternatives to cisplatin and its derivatives. The ruthenium(III) complexes have successfully been used in clinical research and their mechanisms of anticancer action have been reported in large volumes over the past few decades. Ruthenium(II) complexes have also attracted significant attention as anticancer candidates; however, only few of them have been reported comprehensively. In this review, we discuss the development of ruthenium(II) complexes as anticancer candidates and biocatalysts, including arene ruthenium complexes, polypyridyl ruthenium complexes, and ruthenium nanomaterial complexes. This review focuses on the likely mechanisms of action of ruthenium(II)-based anticancer drugs and the relationship between their chemical structures and biological properties. This review also highlights the catalytic activity and the photoinduced activation of ruthenium(II) complexes, their targeted delivery, and their activity in nanomaterial systems.

Graphical abstract

This review covers ruthenium(II) complexes as anticancer drugs in single molecules and nanomaterials including targets, mechanisms, SAR, PDT and nano-systems.

*Correspondent authors.



1. Introduction

Due to a rapid increase in cancer cases worldwide, there is an indispensable need for the development and screening of potential anticancer agents. In this regard, metal complexes hold potential as novel anticancer agents against a wide majority of cancer types.^{1–7} Cisplatin or cis-diamminedichloroplatinum(II) is the most widely known metal-based anticancer drug. Cisplatin has been shown to have efficacy against lung, head, ovarian, neck, and esophageal cancers.^{8–10} Although cisplatin and its derivatives are efficacious against the vast majority of cancers, they also produce non-cancer cell toxicity, thereby causing severe adverse effects, including peripheral neuropathy, hair loss and myelotoxicity in patients.^{11–17} The resistance of tumors to platinum decreases the efficacy of platinum-based or even renders them ineffective, causing treatment failure.^{18–22} In the design of new anticancer drugs,^{23–29} the ruthenium complexes have raised great interest and have been tested against a number of cancer cell lines,^{30–36} and are regarded as promising candidates for alternative drugs to cisplatin and its derivatives.

Ruthenium is a transition metal in group 8, the same chemical group as iron. Ruthenium has two main oxidation states, Ru(II) and Ru(III). Ruthenium(IV) compounds are also possible, but they are generally unstable due to their higher oxidation states.³⁷ The ruthenium ion is typically hexa-coordinated with octahedral coordination geometries. Generally, the thermodynamic and kinetic stability of Ru(III) complexes are lower than that of Ru(II) complexes, and the kinetics of the hydration of Ru(II/III) compounds depends significantly on the nature of their ligands and net charge.³⁸ Many Ru(III) compounds contain exchangeable ligands and require activation by the tumor microenvironment.³⁹ The antitumor properties of the Ru(III) complexes occur when they are reduced to their corresponding Ru(II) counterparts *in vivo*. Under biological circumstances of low oxygen concentration, acidic pH and high levels of glutathione, the Ru(II/III) redox potential can be altered, and thus, Ru(III) complexes can be readily reduced to Ru(II) complexes.^{40–42} As the first approved ruthenium complex in clinical trials, NAMI-A, [ImH][trans-RuCl₄(DMSO) (Im)] (Im = imidazole, DMSO = dimethylsulfoxide; Fig 1), has low potency in terms of direct cytotoxicity towards cancer cells *in vitro*; however, *in vivo*, it has significant efficacy in inhibiting tumor metastasis.^{43–48} The mechanism of action of NAMI-A remains to be elucidated. There are data suggesting that NAMI-A is capable of binding to DNA and RNA. It can bind to the histidine residues of serum albumin (has or bsA) under physiological conditions.^{49–51} However, the low therapeutic efficiency, the progressive disease in the clinical studies (phase I) and partial response (phase I/II) limited the further clinical use of

NAMI-A and resulted in the failure of the clinical investigations.⁵² Alessio *et al.* believed that the main reason of the failure is more philosophical, but nevertheless fundamental.⁵³ Subsequently, the KP1019 [trans-tetrachlorobis-(1H-indazole)ruthenate(III)] designed by the Keppler group entered clinical trial.^{54,55} But its low solubility limits its further development and its better soluble sodium salt KP1339 is currently undergoing clinical trials.⁵⁶

Recently, many organometallic Ru(II), inorganic Ru(II) and nanomaterial Ru(II) complexes have been designed and developed into anticancer drugs, with potent therapeutic properties.^{57–61} With the development of new technology, such as photodynamic therapy (PDT) and nanomaterials,^{62–69} Ru(II) complexes can be photophysical and bioactive, improving the efficacy and selectivity of Ru(II) complexes as anticancer drugs, as well as allowing for the elucidation of their mechanism of action. The Ru(II)-polypyridyl compound (TLD-1433) recently entered phase IB clinical trials as PDT agent in patients with bladder cancer at 2015.⁷⁰ Therefore, the direct study of Ru(II) complexes for cancer therapy contributes to the design of new metal-based drugs.

Generally speaking, the following options are viable in the design of ruthenium-based drugs: (i) constructing complexes with selective and specific targets; (ii) exploiting the potential targets and mechanisms; (iii) the evaluation of structure-activity relationships; (iv) exploiting prodrugs that can be activated by light; and (v) exploiting drug accumulation and activation at the tumour tissues with the nano drug-delivery system. This Review aims to present the reader with an impression of the latest progress of development of ruthenium complexes as anticancer agents as well as biocatalysts from single molecule compounds to nanomaterials. We present an overview of the field today, hoping that colleagues not only may taste a comprehensive development of ruthenium(II) complexes as metallodrugs, but that we can inspire more researchers to enter the charming field of metallodrugs.

2. The cellular uptake and potential targets of Ru(II) complexes

2.1 Cellular uptake

The uptake of ruthenium complexes by cancer cells or other cells is important for selective and effective cancer therapy. In order to move into living cells, molecules and atoms must cross or penetrate the cell membrane. The cell membrane contains diverse proteins and lipids, and it functions to regulate what substances enter into the cells. The general mechanisms of cellular uptake for small molecule drugs are shown in Fig. 2.⁷¹ Ru(II) complexes are known to enter cells through multiple mechanisms, such as passive diffusion, active transport, and endocytosis.⁷¹ However, it is noted that most nanostructured ruthenium complexes enter cells by endocytosis.^{72,73} Confocal laser scanning fluorescence microscopy, inductively coupled plasma mass spectrometry (ICP-MS), flow cytometry and transmission electron microscopy are often used to determine the intracellular accumulation of ruthenium complexes.⁷⁴ As the changes in ligands and hydrophobicity can modulate cellular uptake and cellular localization, the intracellular distribution of ruthenium complexes in cells have been discussed with regard to: (a) the net ionic charge, which can undergo change from anionic to cationic; (b) the degree of lipophilicity based on the octanol/water partition coefficient; (c) the structures and sizes of the ligands.⁷⁵

2.1.1 Localization in nucleus—The cell nucleus is an enclosed membranous organelle that exists in eukaryotic cells, containing nucleic acids and proteins. Typically, the nucleus is regarded as one of the most important organelles in eukaryotic cells. Ruthenium complexes have been shown to interact with nucleic acids and proteins via multiple binding modes in the nucleus.⁷³ The synthesis of Ru(II) complexes would represent an ideal scaffold for the optimization of therapeutic compounds targeted to the nucleus.⁷⁶ In order to allow Ru(II) complexes to target the nucleus, a nuclear targeting peptide D-octaarginine (D-R8) was conjugated to a Ru(II) complex.⁷⁷ The **Ru-D-R8** significantly enhanced cellular uptake compare to the Ru(II) complex and was found to preferentially accumulate in the nucleus at high concentration (15–20 μM). The authors speculated that a high concentration of **Ru-D-R8** could enter into the nucleus via a nonendocytic uptake mechanism. Similarly, the same research group found that **Ru-RrRK**, bearing a tetrapeptide, became localized in the nucleus at a high concentration (100 μM).⁷⁸ It should be noted that a low concentration of the conjugated Ru(II) complexes had a less cellular uptake. The above studies mainly focused on the direct imaging of the nucleus and the compounds did not have significant cytotoxic efficacy. Subsequently, Tan *et al.* designed three Ru(II) complexes containing a β -carboline alkaloid. These complexes were shown to penetrate into the cell nucleus and to have significant cytotoxic efficacy.⁷⁹ The most potent complex of this family had greater efficacy than cisplatin, and the mechanistic studies showed that reactive oxygen species (ROS), autophagy and increased sub-G1 phase arrest were involved in eliciting apoptosis. Recently, Chao *et al.* synthesized a new cycloruthenated $[\text{Ru}(\text{bpy})(\text{phpy})(\text{dppz})]^+$ (bpy=bipyridine, dppz = dipyridophenazine) by replacing the bpy ligand with the cycloruthenated ligand (Fig. 3), phpy (2-phenylpyridine) from the molecule $[\text{Ru}(\text{bpy})_2(\text{dppz})]^{2+}$. This compound readily entered into the nucleus and had IC_{50} values lower than cisplatin.⁸⁰

2.1.2 Localization in mitochondria—Although the nucleus is reported to be the key target for ruthenium complexes, many studies have demonstrated that the accumulation of some ruthenium complexes in the nucleus is far lower than that in other subcellular regions.^{74,81} Some nonnuclear targets, such as the cell surface, and especially mitochondria, have also been reported to be targets for the anticancer activity of some Ru(II) complexes. Mitochondria function plays a significant role in cellular metabolism and under certain cellular conditions, release molecules that can activate the extrinsic and intrinsic apoptotic pathways.⁸² Two key characteristics of mitochondria include mitochondrial DNA nucleoids anchored to the matrix side of the inner membrane, and the extremely negative membrane potential (–160 to –180 mV) caused by the proton gradient across its inner membrane.^{83–85} The negative potential of the inner membrane attracts lipophilic cations, including metal complexes such as the Ru(II) complexes. The lipophilicity of Ru(II) complexes can be modulated by adjusting the ligands and the valence of complexes, which partly affects the uptake and targeting of Ru(II) complexes. For examples, Gasser and co-workers found that $[\text{Ru}(\text{dppz})_2(\text{CppH})]^{2+}$ (**1a**, CppH = 2-(2'-pyridyl)pyrimidine-4-carboxylic acid) possesses two positive charges and accumulates in the mitochondria (Fig. 4). In addition, **1a** had significant anticancer efficacy in A2780 cancer cells, with an IC_{50} value of 2.8 μM , which was similar to that of cisplatin (IC_{50} : 2.9 μM).^{86, 87} Moreover, **1a** was more efficacious in cisplatin-resistant A2780/CP70 cells than cisplatin and less cytotoxic than cisplatin in healthy MRC-5 cells.⁸⁶ Dickerson and co-workers reported that the Ru(II) complex **1b**,

carrying an overall charge of +2, can localize to the mitochondria and induce rapid membrane depolarization and necrotic cell death.⁸⁸ In contrast, its analogue Ru(II) complex (**1c**), carrying an overall charge of -4, does not localize to the mitochondria and lacks efficacy as it does not localize to the mitochondria.⁸⁸ Chao *et al.* reported that the mitochondrial-targeting Ru(II) complexes, complexes **1d** to **1f**, induce cellular apoptosis via the mitochondrial pathway.^{89,90} In addition, the combination of mitochondrial-targeting and photodynamic therapy significantly increase the selectivity and anticancer efficacy of the Ru(II) complexes.⁹¹ Although many Ru(II) complexes target the mitochondria and induce cell apoptosis, most research has been directed towards DNA-targeting complexes. Therefore, there is potential for further study of mitochondrial-targeting Ru(II) complexes and the elucidation of their mechanisms for inducing cell apoptosis.

2.1.3 Localization in lysosomes—Lysosomes are spherical vesicles found in almost every eukaryotic cell and contain hydrolytic enzymes that degrade numerous biomolecules.⁹² Lysosomes play an essential role in many physiological processes and cell signaling pathways, including intracellular transport, protein degradation and recycling, endocytosis and apoptosis. Differing from two-membrane systems, such as cell membranes and mitochondria, lysosomes are single-membrane organelles. Lysosomes are an intracellular target and the final destination for numerous macromolecules, including drugs formulated as nanomaterials.⁹³ The luminal environment pH is 4.6–5.0 in lysosomes, which helps optimize hydrolysis and digestion. Because the cell membrane is typically impermeable to complexes larger than 1 kDa, and given that most medical nanomaterials range from tens to hundreds of nanometers in diameter, nanomaterials generally enter cells through an endocytic process.⁹³ In the endocytic process, nanomaterials are transported to the endosomes and then fuse with lysosomes, where the nanomaterials begin to degrade. Moreover, due to the acidic environment of lysosomes, some nanomaterials are designed to release ruthenium complexes or other drugs, preferentially in an acidic environment, to improve the stability and selectivity of the nanomaterial. Although lysosomes are regarded as the targets of nanomaterial drugs, some organometallics have been found to target organelles.^{94–97} The highly positively charged Ru(II) polypyridyl complex selectively localizes in the lysosomes, and can be used in photodynamic therapy as photosensitizers (PS).⁹⁸ Moreover, lysosomes participate in an autophagic process that is linked to carcinogenesis and resistance to chemotherapy.⁹⁹ Targeting these pathways could constitute a novel approach to cancer therapy.

2.2 The potential targets of ruthenium complex

There are some different molecules with special structures and distinct function, especially DNA and proteins, that have critical roles in determining cellular activity.^{76,100} The understanding of how ruthenium complexes interact with these two specific targets within cell is therefore important for exploring the anticancer mechanism and selecting the most potent ruthenium complex for selective and effective therapy.

2.2.1 DNA as a target—Cancer cells have a high rate of proliferation due to a loss of control of the normal restraints on cell cycle division. Also, cancer cell proliferation is regulated by DNA. Many ruthenium compounds are known to have high selectivity for

binding to DNA.^{101–105} The electron-deficient metal atoms in these complexes might act as electron acceptors for electron-rich DNA nucleophiles by the hydrolysis of ligands. Furthermore, Ru(II) complexes can bind to DNA via interaction with aromatic ligands. There are two main categories of binding modes between DNA and Ru compounds: covalent and noncovalent binding.¹ The covalent binding is irreversible and forms adducts consisting of DNA and Ru(II) complexes. For example, the complex $[(\eta^6\text{-arene})\text{Ru}(\text{en})\text{Cl}]\text{PF}_6$ (arene= biphenyl, en= ethylenediamine) can bind to the N7 atom in guanosine.¹⁰⁶ The covalent mode of binding in Ru–DNA distorts the DNA backbone, which impairs DNA replication and transcription. The non-covalent binding of Ru(II) complexes is usually reversible and occurs as electrostatic binding, intercalation, and groove binding, amongst which intercalation has received the most attention. Intercalation occurs when planar aromatic compounds are inserted between adjacent base pairs in the DNA double helix.¹⁰⁷ Many Ru(II) polypyridyl complexes can intercalate DNA with high affinity *in vitro*, and serve as DNA molecular probes. For example, the well known complex $[\text{Ru}(\text{bpy})_2(\text{dppz})]^{2+}$ was reported as a DNA light switch *in vitro*,¹⁰⁸ but this complex did not readily cross the cell membrane. Gill *et al.* reported that the multi-intercalator,¹⁰⁹ **2a**, can bind DNA with a binding constant of $2.5 \times 10^6 \text{ M}^{-1}$. Moreover, it can bind cellular DNA in fixed and membrane-permeabilized HeLa cells (Fig. 5).¹⁰⁹ Compound **2a** immediately stalled the progression of the replication fork in HeLa cells, resulting in the activation of DNA damage checkpoints and blocking the cell cycle between the G1 and S stage. This complex induced death in HeLa cells, with an IC_{50} value of $38 \text{ }\mu\text{M}$.¹⁰⁹ Önfelt *et al.* reported that the binuclear Ru(II) complex, $\Delta\text{-}\Delta [\mu\text{-C4}(\text{cpdppz})_2\text{-(phen)}_4\text{Ru}_2]^{4+}$ ($\text{C4}(\text{cpdppz})_2 = N,N'$ bis-(cpdppz)-1,4-diaminobut-ane; cpdppz = 12-cyano-12,13-carbonyl-11*H*-cyclopenta[*b*]-dipyrido[3,2-*h*:2',3'-*j*]phen-azine-12-carbonyl; phen = 1,10-phenanthroline), binds with high affinity to DNA ($K_b \sim 10^8 \text{ M}^{-1}$).¹¹⁰ The entry of this complex into the nucleus was facilitated by electroporation, and it induced the run apoptosis at 10^{-4} M . Thomas *et al.* showed that the dinuclear compound **2b** (Fig. 5) rapidly targets the nuclei of MCF-7 cancer cells via a non-endocytic mechanism. However, its IC_{50} value, after 24 h of incubation with MCF-7 cells, was $138 \text{ }\mu\text{M}$.^{111,112}

2.2.2 Proteins as targets—The primary cellular target of ruthenium complexes is DNA. However, data also indicates that certain proteins may be targets for ruthenium complexes, especially protein kinases.^{113–116} It is well known that certain enzymes play key roles in metabolic pathways associated with intercellular uptake, cancer cell proliferation, and cell death. The targeting of these biological processes with metal complexes has shown promising anticancer efficacy (Fig. 6).¹¹⁷ Ru(II) complexes have the potential to inhibit protein kinases due to their facile, three-dimensional structure and physicochemical properties. These Ru(II) complexes are highly stable, kinetically inert and stable in biological environments. The targeting capability and diverse functions of ruthenium complexes can be realized by modification of the ligands.^{118,119} In the early work of Dwyer and colleagues, the Ru(II) polypyridyl complex **3a** and **3b** were designed to act as acetylcholinesterase (AChE) inhibitors by a combination of electrostatic and hydrophobic interactions between the Ru(II) complexes and the peripheral anionic site of AChE.¹²⁰ Generally, most of the Ru(II) complexes bind to the active site of enzymes through their biologically active ligands. The natural organic product staurosporine is a potent ATP-

competitive inhibitor of protein kinase.^{121,122} Meggers and co-workers designed several ligands that retained the active core of staurosporine and coordinated this to ruthenium and this yielded compound **3c**, **3d** and **3e** which were inhibitors of the protein kinases Pim1, MSK1, and GSK3R, respectively.^{123,124} The kinetic inertness of the coordination bonds allowed these Ru(II) compounds to successfully mimic the organic product staurosporine, thereby inhibiting these protein kinases. The binding of ATP and the active core of staurosporine was illustrated by the co-crystal structures of the protein kinase Pim-1 with the Ru(II) complexes, which verified that the ruthenium ion only has a structural role and is not involved in binding with the active site of ATP.^{125–128} Similarly, Dyson *et al.* designed a compound, **3f**, which contains a benzimidazole-phenoxazine derivative that significantly inhibited P-glycoprotein (P-gp). **3f** was shown to inhibit P-gp activity and thus has the potential to attenuate multidrug resistance due to the overexpression of P-gp.¹²⁹ Dyson *et al.* also designed **3g** and its analogues that contained ethacrynic acid (EA) ligands that inhibited glutathione-S-transferase (GST) in A2780 and cisplatin-resistant A2780cisR cell lines.¹³⁰

Respondek *et al.* developed a novel method to inhibit the activity of cysteine protease by using the photoactive **3h** containing the cysteine protease inhibitor Ac-Phe-NHCH₂CN.¹³¹ As a result of binding to the Ru(II) center, the nitriles of Ac-Phe-NHCH₂CN were caged, and thus **3h** could not bind to cysteine protease (Fig. 6). However, when **3h** was irradiated, it released Ac-Phe-NHCH₂CN, which can potently inhibit the cysteine proteases papain and cathepsin B. This method provides a novel approach to control the activity of enzymes. In addition, the identification of cellular target proteins is a major challenge in drug development. However, Hartinger *et al.* first identify 15 cancer-related proteins that associated with the observed antimetastatic ruthenium organometallic complex based on 1,3,5-triaza-7-phosphaadamantane (RAPTA) by chemical proteomic.¹¹⁶ As shown in Fig. 7, this methodology has broad applicability beyond RAPTA complexes and enables, for the first time, the direct identification of intracellular interactions of metallodrugs with proteins.

3. Cell death process

Cell death can occur via several mechanisms (Fig. 8).¹³² Apoptosis is primarily induced by the activation of two pathways in cells, the intrinsic and extrinsic (death receptor-mediated) pathways.¹³² The intrinsic pathway, also known as the mitochondria-mediated pathway, is activated by DNA damage, oxidative stress and endoplasmic reticulum (ER) stress.¹³³ These stimuli can induce the mitochondrial release of the cytochrome c, which can activate the apoptotic protease activating factor 1, and regulate other proteins involved in apoptosis. Chen and Chao *et al.* conducted experiments to determine the effect of Ru(II) complexes on the intrinsic pathway of apoptosis.^{89,90,134,135} Typically, non-apoptotic cell death occurs by necrosis and ER stress.¹³² The process of autophagy is regulated by autophagy-related (ATG) proteins and the role of autophagy in cancer is complex and is contextually dependent.¹³⁶ For example, autophagy can inhibit or facilitate cell death. The process of necrosis differs from the apoptosis in a number of ways.¹³⁷ Interestingly, certain stimuli that induce apoptosis can also cause necrosis, such as ROS. It has been shown that Ru(II) complexes can induce autophagy and necrosis, as well as apoptosis.^{138–140}

4. Arene ruthenium(II) complexes

Arene ruthenium(II) complexes are also called piano stool complexes.¹⁴¹ Sadler and Dyson are the pioneers in the field of anticancer arene ruthenium complexes.^{142,143} Arene Ru (II) complexes have the general formula $[(\eta^6\text{-arene})\text{Ru}(\text{X})(\text{Y})(\text{Z})]$, as shown in Fig. 9. Common arene rings include benzene (ben), methylisopropyl benzene (cym), biphenyl (bip) and dihydroanthracene (dha). The ligands X and Y can be two monodentate ligands or one bidentate ligand, and Z is usually a leaving group, such as a halogen.¹⁴⁴ The arene is regarded as the core component of arene Ru(II) complexes. Furthermore, the arene rings are hydrophobic, which facilitates the entry of Ru(II) complexes into cells. The arene rings determine the electron distribution of the Ru(II) complex, which affects the stability of the Ru(II) complexes. However, the hydrolysis of Ru-Z bonds is also affected by pH and the concentration of Z in the environment. The water solubility and volume of the chelating ligand and leaving group can also affect the anticancer efficacy of arene Ru (II) complexes.¹⁴¹

4.1 Arene Ru(II) complexes with *N,N*-chelating ligands

Common *N,N*-chelating ligands include aliphatic diamine, aromatic diamine and pyridine derivatives. The arene ruthenium complexes containing ethylenediamine (en) chelating ligands have been studied systematically by Sadler.⁵⁸ Sadler's group reported that variation in the leaving group, the *N,N*-chelating ligand and the arene ring, can have a significant effect on chemical and biological activity.⁵⁸ The complex $[(\eta^6\text{-C}_6\text{H}_5)\text{Ru}(\text{en})\text{Cl}]^+$ (**4a**, Fig. 10) had anticancer efficacy against A2870 cancer cells, with an IC_{50} value of 17 μM .⁵⁸ Another compound, **4b**, was synthesized by replacing the benzene with a more hydrophobic biphenyl group, and **4b** had similar anticancer efficacy compared to carboplatin in A2780 cells.⁵⁸ In order to gain insight into the mechanism of arene Ru(II) complexes as anticancer drugs, Chen and co-workers reported the recognition of nucleic acid derivatives with the compound $[(\eta^6\text{-C}_6\text{H}_5)\text{Ru}(\text{en})\text{X}]$, where arene = Bip, Tha, Dha, Cym or Ben, X = Cl^- or H_2O .¹⁰⁶ At neutral pH, pseudo-octahedral diamino arene Ru(II) complexes were found to discriminate between G and A nucleobases. In kinetic studies (pH 7.0, 298 K, 100 mM NaClO_4), the rates of reactions of cGMP (3', 5'-cyclic-GMP) with X (Cl^- or H_2O) decreased according to arene present as follows: Tha > Bip > Dha, Cym > Ben (Scheme 1). The cytotoxicity study showed of the family $[(\eta^6\text{-C}_6\text{H}_5)\text{Ru}(\text{en})\text{Cl}]^+$ was distinctly correlated to the above reactions rates.¹⁰³ These findings indicate that diamine NH_2 groups, the hydrophobic arene, and the chlorine leaving group all have important roles in the interaction of nucleic acids with arene Ru(II) complexes. In addition, Romero-Caneló *et al.* determined the activity of iodido versus chlorido *N,N*-chelated arene Ru(II) complexes with imino-pyridine ligand.²⁶ The subtle changes in the monodentate ligands (Cl, I) can lead to major changes in cellular metabolism and mechanisms of anticancer efficacy. The iodido complex, **4d**, was more potent and selective than the chlorido analogue, **4c**, towards cancer cell lines and was not cross-resistant to platinum-based drugs. Moreover, these two halido ligands were found to affect cellular uptake of the arene Ru(II) complexes.¹⁴⁵ The chloride complex, **4c**, was largely taken up through active transport, whereas the iodide complex **4d** entered cells through passive transport. After 24 h of drug exposure, the ruthenium accumulation of **4d** was 1.6 times greater than that of **4c** in A2780 cells.¹⁴⁵ Additional experiments showed

that the ABC transporter P-gp contributed to the efflux of **4c**, but had little effect on the cellular efflux of **4d**, indicating that the passive transport may help drugs circumvent some resistance mechanisms. Montani *et al.* determined the antitumor activity of **4e** *in vivo* and found that **4e** effectively inhibited the growth of A17 triple negative breast cells transplanted into mice.¹⁴⁶ **4e** was rapidly eliminated from the liver, kidney and bloodstream due to its high hydrosolubility, and it has with excellent therapeutic efficacy and minimal adverse effects. Immunohistological studies showed a significant reduction in the number of tumor-infiltrating regulatory T cells caused by **4e**.

Chow *et al.* synthesized a more effective arene Ru(II) compound, **4g**, compared to cisplatin, by using high-throughput screening.¹⁴⁷ Compound **4g** displayed low micromolar IC₅₀ values against A2780, A2780cisR, MCF7, HCT116 and SW480 cells. The authors also found that the water-soluble and stable half-sandwich arene Ru(II) Schiff-base (RAS) complexes, **4f** and **4g**, can induce non-apoptotic programmed cell death (PCD) through the ER stress pathway.¹⁴⁸ The mechanism of action was significantly different between the two complexes, despite modest structural variations. **4g** elicited ROS-mediated ER stress, while **4f**'s efficacy was independent of ROS. These two complexes were more efficacious against apoptosis-resistant cells compared to clinical drugs such as oxaliplatin. This work provides the basis for targeting ER stress modulation using Ru(II) complexes to bypass apoptosis resistance. Recently, the same group study of the relationship between the structures and cytotoxicities of a series of arene Ru(II) Schiff-base (RAS) complexes was conducted.¹⁴⁹ They reported that the RAS complexes with more hydrophobic ligands displayed higher intercellular accumulation. For example, **4g**, with more hydrophobic π -donating arene ligands, accumulated 7.5-fold more than the least hydrophobic compound, **4i**. **4g** exhibited more than a 150-fold increase in cytotoxicity compared to **4i** in HCT116 cells. The authors also found that **4h** accumulated 3 times less than **4f**, but had a higher cytotoxicity, which suggested that the higher cytotoxicity was partially correlated to the intercellular uptake of the RAS complexes. In addition, **4j** and **4k**, with more π -acidic 3-CF₃ or 3-Cl substituent groups, were more likely to be hydrolyzed compared to **4g**, which had a 4-OMe substituent group. Further experiments indicated that all of the RAS complexes induced p53-independent cytotoxicity. Therrien *et al.* designed hydrazinyl-thiazolo arene Ru(II) complexes and these compounds were more cytotoxic to HeLa, A2780 and A2780cisR cells compared to cisplatin and oxaliplatin.¹⁵⁰ The representative complexes, **4l** and **4m**, were induced HeLa cell death by disrupting mitochondrial membranes and damaging the nucleus. The biological activity of the two compounds was first evaluated using microarray gene expression assay and ingenuity pathway analysis. **4l** and **4m** affected p53 signaling, which induced apoptosis. In addition, **4l** and **4m** activate the genes that correlate with overcoming cisplatin-resistance, such as PRMT2, FAS, ZMAT3, BBC3/PUMA, and PDCD4. It is hypothesized that **4l** and **4m** will surmount cisplatin resistance in ovarian cancer therapy.

In addition, Betanzos-Lara *et al.* investigated the effect of arene Ru(II) complexes on DNA. Their results indicated that arene Ru(II) complexes [(*p*-cym)Ru(bpm)(py)][PF₆]₂ (where *p*-cym = para-cymene, bpm = 2,2'-bipyrimidine and py = pyridine) can selectively photodissociate a monodentate ligand (py) when excited by visible light.¹⁵¹ Betanzos-Lara *et al.* also studied the relationship between photoactivity and structure of the arene Ru(II)

pyridine and pyridine-derivative complexes with *N,N*-chelating ligands. These complexes can activate the release of its monodentate ligands by photoirradiation to increase the activities of these photoactivatable arene ruthenium complexes.¹⁵² They found that increasing the electron-donating substituents in the Py ring moderately increased the extent of the photoinduced hydrolysis. In contrast, more electron-donating substituents on the arene ring increased both the extent and the rate of photoinduced hydrolysis, and increasing the aromatic *N,N*-chelating ligands decrease the extent of photoinduced hydrolysis. These complexes were only tested for cytotoxicity in the dark, with the IC₅₀ values in the range of 9.0–60 μM in A2870 cells.¹⁵² However, Wang *et al.* reported that the ferrocenyl pyridine-based arene Ru(II) complex, **5a**, was an efficacious photosensitizer that killed cancer cells (Fig. 11).¹⁵³ Interestingly, this complex could produce both hydroxyl radicals and ¹O₂ as well as photoinduced monodentate ligand dissociation upon visible light irradiation (> 400 nm). The complex produced DNA photodamage under light irradiation and had significant photoactivated anticancer efficacy, at 70 μM and irradiated for 30 min, decreased the viability of SKOV3 and A549 cells by 70% and 62%, respectively. In addition, the same research group also determined the effect of substituents on the photoactivity of the [(η⁶-*p*-cymene)Ru(dpb)(py-R)]²⁺ (Fig. 11).¹⁵⁴ The complexes induced DNA photocleavage and DNA photobinding by photoinduced ligand dissociation and ¹O₂. The magnitude of ¹O₂ production by the complexes was: **5e** > **5f** > **5d** > **5h** ≈ **5c** ≈ **5b**, and the order of ligand dissociation rates were: **5h** > **5f** > **5e** > **5d** > **5c** > **5b**. **5e** produced the most potent phototoxicity under irradiation in A549 cells. It was reported that the difference in the photoactivities may result from the influence of the substituent groups on the energy levels of ³MLCT and ³MC, and the energy gaps between ³MLCT, ³MC and ³IL.

4.2 Arene Ru(II) complexes with *N,O*-, *O,O*- and *C,N*- ligands

N,O-chelating ligands, including tetrahydroisoquinoline, select amino acid ligands, and the *O,O*-ligands, are common β-diketonate and pyrone ligands.¹⁵⁵ Chelopo *et al.* determined the anticancer efficacy of several arene Ru(II) complexes containing 1,2,3,4-tetrahydroisoquinoline amino alcohol ligands (**6a–6d**, Fig 12) in the human cancer cell lines MCF-7, A549, and MDAMB-231.¹⁵⁶ These complexes were moderately efficacious against only MCF-7 cells, with the lowest IC₅₀ value of 34 μM for complex **6d**. These complexes displayed much lower activity (> 250 μM) in the normal MDBK cells.¹⁵⁶ The results indicated that certain Ru(II) *N,O*-complexes are cytotoxic in certain cancer cell lines but do not elicit significant toxic effects in normal cells. Sadler *et al.* determined the structure-activity relationships in cytotoxic arene Ru(II) complexes containing *N,O*-, and *O,O*-chelating ligands (Fig. 12, Scheme 2).¹⁵⁷ Their results indicated that the amino acidato (*N,O*-) complexes were inactive in A2780 cells, with IC₅₀ values > 100 μM. However, the *O,O*-chelated arene Ru(II) complexes were efficacious in A2780 cells (Scheme 2). Most of the *O,O*-chelated arene Ru(II) complexes were poorly soluble and had a moderate rate of hydrolysis. Their efficacy was significantly dependent upon the substituent and the arene ring. The IC₅₀ values of neutral Ru(II) acetylacetonate (acac) complexes in A2780 cells had the following differences in efficacy, depending upon the arene: *p*-cymene, biphenyl, dihydroanthracene < benzene, indan.¹⁵⁷ The effect of substituents in the acac backbone has been investigated in *p*-cymene complexes, where the IC₅₀ values vary with the acac substituents in the order: Ph, *tert*-butyl < Me, Me/naphthyl < CF₃, Ph/phenyl.¹⁵⁷ In general,

acac-type complexes have low cytotoxicity, poor aqueous solubility and rapid hydrolysis compared to the ethylenediamine analogs, which is likely due to the protonation and irreversible displacement of the acac derivatives under some conditions.

A series of water-soluble iminophosphorane Ru(II) complexes were synthesized by Frik *et al.* Most of the complexes were found to be more cytotoxic than cisplatin in several human cancer cell lines.¹⁵⁸ The most effective complex, **6k**, produced a 56% decrease in tumor size in mice with xenografted breast carcinoma MDA-MB-231 cells, with low systemic toxicity after 28 days of treatment (14 doses of 5 mg/kg, every other day). Pharmacokinetic studies indicated that **6k** appeared rapidly in plasma, with high uptake in the breast tumor tissues compared to the kidneys and liver. Mechanistic studies indicated that this complex did not interact with DNA or inhibit protease cathepsin B and induced cell death mainly through canonical or caspase-dependent apoptosis, independent of p53. Ru(II) complexes with *N,O*-ligands were synthesized by Lord *et al.*¹⁵⁹ Most of the complexes were cytotoxic effect in HT-29 and MCF-7 cell lines, with significantly greater efficacy in A2780 and A2780cisR cells. In addition, the complexes were also cytotoxic to the hypoxic HT-29 cells. The complexes were found to inhibit the thioredoxin reductase (TrxR), with IC₅₀ values in the nanomolar range, in combination with significant single-strand DNA breaks. The representative, **6l**, was the most active against all cancer cell lines (IC₅₀ = 1.9 μM for MCF-7 cells) and **6l** was ~3-fold more efficacious than cisplatin against A2780cisR cells.

Dyson *et al.* also designed another two arene Ru(II) complexes, **7a** and **7b**, with *O,O*-ligands (see Fig. 13).¹⁶⁰ **7b** was more cytotoxic than **7a** in A2780 cells (IC₅₀ = 22.4 and 73 μM, respectively). These two complexes could selectively inhibit the migration of MDA-MB-231 tumor cells. Moreover, the compounds displayed more potent antivasular effects *in vivo* (chicken chorioallantoic membrane) model compared to RAPTA-C. The Turel group discussed the anticancer efficacies of a series of fluorinated *O,O*-ligands arene Ru(II) compounds with different monodentate ligands (Cl, pta, Fig. 13).¹⁶¹ They found that all complexes were efficacious against two cancer cell models (ovarian, osteosarcoma), but did not produce toxic effect nonmalignant keratinocytes. The analogues of pta Ru(II) complexes showed lower cellular Ru accumulation, but higher efficacy, especially in the osteosarcoma cells, compared to the chloride analogues. All chlorido complexes significantly induced ROS production, DNA damage, and apoptosis. Although the pta compounds did not significantly induce ROS production, they blocked cell cycle progression in the G0/G1 phase. **7c** and **7c-I** had the highest cytotoxicity in ovarian CH1 cells, with IC₅₀ values of 17 μM and 8 μM, respectively. Pettinari *et al.* determined the anticancer efficacies of arene Ru(II) complexes (**7i-7q**, Fig. 13), with the 4-(biphenyl-4-carbonyl)-3-methyl-1-phenyl-5-pyrazolonate ligand and different monodentate ligands (Cl, CH₃OH, pta).¹⁶² The nature of the monodentate ligands were critical in terms of the DNA binding affinities of the Ru(II) complexes, with a rank order of: pta analogues > CH₃OH analogues > chloride analogues. They found that the three Ru(II) complexes with a hexamethyl benzenearene ring (hmb) had IC₅₀ values of 9–34 μM in cancer cells, whereas the other Ru(II) complexes were much less active. The three hexamethylbenzene-Ru(II) complexes induced cell apoptosis by activating caspases. The active complexes produced DNA fragmentation, accumulation of pro-

apoptotic proteins (i.e. p27, p53, p89 PARP fragments), and the down-regulation of the antiapoptotic protein Bcl-2.

Typically, arene Ru(II) complexes with *C,N*-cyclometalated ligands are more efficacious than cisplatin as anticancer compounds. Yellol and co-workers synthesized some neutral benzimidazole *C,N*-cyclometalated arene Ru(II) complexes (see Fig. 14), and these complexes were efficacious in HT29, T47D, A2780 and A2780cisR cancer cell lines.¹⁶³ The IC₅₀ value of **8a**, a representative compound, was 2.18 μM in HT29 cancer cells, indicating that it is more efficacious than cisplatin (IC₅₀: 9 μM). Further studies indicated that **8a** induces a high rate of apoptosis, good accumulation, S-phase cell cycle arrest, strong binding to HSA at sites I and II, and weak binding to DNA in the minor groove. Subsequently, Yellol *et al.* determined the effects of varying substituents (H, Me, F, CF₃, MeO, NO₂, and Ph) in the R4 position of the phenyl ring of 2-phenylbenzimidazole chelating ligand on the anticancer efficacy of the complexes.¹⁶⁴ The hydrolysis of the ruthenium–chlorido bond was relatively rapid for **8c**, **8d**, and **8h**. The relative hydrophobicities, according to RP-UPLC-QTOF-MS studies, were: **8d** < **8c** < **8h**. There was no distinct variation in the cytotoxicities for these complexes due to the substitutions, but the CF₃ substitution was found to increase the efficacy of **8e** in almost all of the cell lines.¹⁶⁴ Most of these compounds were more efficacious than cisplatin in A427 and HT29 cell and were able to kill A2780cisR cells with IC₅₀ values of 0.96–3.26 μM.

4.3 Arene Ru(II) complexes with RAPTA ligands

RAPTA compounds are characterized by a monodentate phosphane ligand pta (1,3,5-triaza-7-phosphaadamantane) and a η^6 -arene ligand bound facially to the metal center, with the general formula $[(\eta^6\text{-arene})\text{Ru}(\text{X})(\text{Y})(\text{pta})]$, where X and Y are most commonly chlorine.¹⁴¹ The hydrophilic pta ligand had good aqueous solubility and is preferentially protonated in a low pH environment. RAPTA derivatives containing two chloride ligands were susceptible to hydrolysis in a low chloride environment.¹⁶⁵ RAPTA-C is the prototype of this class of organometallic, half-sandwich compounds and had properties similar to the toluene derivative RAPTA-T. *In vitro*, RAPTA-C and RAPTA-T lack significant cytotoxicity, but they inhibited lung metastasis in CBA mice bearing the MCa mammary carcinoma, while having only mild effects on the primary tumor.^{166,167} Weiss *et al.* recently reported that RAPTA-C can reduce the growth of primary tumors in preclinical models for ovarian and colorectal carcinomas.¹⁵⁶ When administered daily, at a relatively low dose (0.2 mg/kg), RAPTA-C significantly reduced the growth of A2780 cells transplanted onto the chicken chorioallantoic membrane (see Fig. 15). RAPTA-C had similar efficacy in LS174T colorectal carcinoma in athymic mice, albeit at a higher dose. This complex restricted microvessel density and was cleared from the organs and the bloodstream.¹⁶⁸

RAPTA must undergo hydrolysis to be active *in vivo*, and the extent of hydrolysis depends upon the pH and the amount of chloride present in solution. The chloride ligands of RAPTA-C were replaced with bidentate oxalate to create RAPTA derivatives (**9a–9f**, Fig. 16) that were more inert towards hydration, and some of these complexes displayed efficacy similar to RAPTA-C *in vitro*.¹⁶⁹ However, the RAPTA derivatives were highly cytotoxic in A2780

and A2780cisR cell lines (IC₅₀ 0.14–1.15 and 0.27–1.18 μ M, respectively) and all the complexes with curcuminoid ligands were more efficacious than cisplatin.¹⁶⁹

It was first hypothesized that DNA was the primary target of the RAPTA derivatives.¹⁷⁰ Allardyce *et al.* reported that RAPTA-C exhibited pH-dependent DNA damage; the pH where damage was greatest was significantly correlated with the pH environment of the cancer cells.¹⁷⁰ As shown in Fig. 17, Davey *et al.* found that the RAED-C complex preferentially targets the DNA of chromatin with cytotoxic effects.¹⁷¹ However, the relatively non-cytotoxic antimetastasis RAPTA-C was found to interact with the proteins in A2780 cells and formed protein-Ru(II) complex adducts. About 85% of the adducts resulting from the total intracellular ruthenium content were bound to histone proteins, and the authors hypothesized that histone lesions may contribute to the efficacy of this compound.¹⁷¹ Recently, Dyson and Davey *et al.* firstly found that the RAPTA-T can combine with auranofin to yield a synergistic activity in killing cancer cells via the allosteric cross-talk in chromatin.¹⁷² In addition, the RAPTA derivatives inhibited the activity of glutathione transferase, lysozyme, cathepsin B (Cat B) and TrxR.¹⁷³ Thus, RAPTA complexes can readily react with proteins and inhibit enzymes, but there is no significant correlation between this reactivity and toxicity in cancer cells. Dyson *et al.* postulated that the RAPTA derivatives induced cell death via multiple modes of action.¹⁷³

4.4 Multinuclear arene Ru(II) complexes

The introduction of ligands with multiple ligand-binding sites enables arene Ru(II) compounds to occur in multinuclear complexes.^{174,175} The lipophilicities and water solubilities of the new multinuclear ruthenium complexes with large positive charges are distinct from the mononuclear arene ruthenium complexes. Multinuclear ruthenium compounds mainly contain dinuclear, trinuclear, tetranuclear, hexanuclear, octanuclear, or supermolecular derivatives.¹⁷⁶ Among the multinuclear arene ruthenium complexes, dinuclear complexes have a variety of significant biological effects. Keppler *et al.* designed a series of dinuclear arene Ru(II) complexes and investigated the relationships related to spacer length, lipophilicity, modes of action and cell toxicity (Fig. 18A).^{177,178} Increasing the chain length of the dinuclear arene Ru(II) complexes from 2 to 6 and 12 CH₂ groups, increased the lipophilicity and the *in vitro* efficacy, respectively. The most potent dinuclear compound, **10f**, had an IC₅₀ of 0.29 μ M in SW480 cancer cells and there was no cross-resistance between oxoplatin and **10f** in three oxoplatin-resistant cell lines (5637-oxo, SISO-oxo, and KYSE70-oxo).¹⁷⁷ The mechanism study indicated that DNA molecules were the main targets for the dinuclear arene Ru(II) compounds. The dinuclear arene Ru(II) complexes were rapidly hydrolyzed to predominantly form diaqua species that interacted with transferrin, indicating proteins were potential targets. Brabec and co-workers reported that the dinuclear arene Ru(II) complexes with long linkers bind DNA by forming intrastrand and interstrand cross-links in one DNA molecule in the absence of proteins and that they can crosslink two DNA duplexes, as well as proteins, to DNA—a feature not observed for other antitumor ruthenium complexes.¹⁷⁹ Gras *et al.* designed some thiophenolato-bridged dinuclear arene Ru(II) complexes (Fig. 18B) and found the complexes to be highly cytotoxic in A2780 and A2780cisR cells, with IC₅₀ values in the submicromolar range.¹⁸⁰

Another feature of multinuclear arene Ru(II) compounds is supramolecular self-assembly: the spontaneous association of two or more moieties under equilibrium conditions into stable, structurally well-defined aggregates through either covalent or non-covalent interactions.¹⁸¹ These compounds can form both two-dimensional and three-dimensional structures. Generally, these supramolecular arene ruthenium compounds have large charges, good solubility in water and a large, hollow space capable of encapsulating guest molecules.¹⁸² These multinuclear arene ruthenium compounds have antitumor efficacy in certain cancer cells. The Therrien and Barea research groups reported that some *p*-cymene ruthenium-based metalla-cycles (see Fig. 18C) have significant biological activity and the metalla-cycles had IC₅₀ values in the micromolar range in A2780 cancer cells.^{174,183} In addition, the three-dimensional cages on these multinuclear compounds can serve as drug delivery vectors to control the release of the guest molecule, and may become a new platform for future development of efficacious anticancer drugs.^{184–186} Schmitt *et al.* used the water-soluble Ru(II) metalla-cage, **10g**, to deliver hydrophobic porphyrin molecules to cancer cells (Fig. 18D).¹⁸² After photoactivation, there was a significant increase in cellular cytotoxicity.

5. Ruthenium(II) polypyridyl complexes

Recently, many studies have reported that ruthenium(II) polypyridyl complexes have a number of significant biological properties.^{187–190} Most Ru(II) polypyridyl complexes have excellent reactivity, imaging capability, binding ability, and redox chemistry, giving them potential as diagnostic and therapeutic drugs for cancer. These ruthenium complexes frequently contain *N,N*-chelating ligands with octahedral structures, and they are kinetically inert. Ru(II) polypyridyl complexes can reversibly interact as probes or inhibitors with important biological molecules including DNA, proteins and RNA. The interaction of ruthenium complexes with biological molecules often leads to damage or toxicity to the biological targets. In addition, many Ru(II) polypyridyl complexes have photophysical and photothermal properties, including a large stoke shift, long luminescent lifetime, significant two-photon absorbing and photostability, which endows Ru(II) polypyridyl complexes with the properties of photosensitization for use in cancer photodynamic therapy (PDT).^{68,191} PDT is a non-invasive and effective method for localized tumor treatment. PDT, as a new multi-modality treatment platform, requires both a non-toxic photosensitizer and a harmless light source which matches the absorption spectrum of the photosensitizer. PDT can cause a direct effect on cancer cells, inducing cell death by necrosis or apoptosis.

5.1 Ru(II) tris(polypyridyl) complexes

The Ru(II) polypyridyl complexes frequently contain chelating ligands such as polypyridine, 1,10-phenanthroline and their derivatives.¹⁹⁰ These coordinated, saturated Ru(II) tris(bidentate) complexes are lipophilic and cationic, and are strictly octahedral in their geometry. The unique construction of their three-dimensional and molecular geometries contribute to a variety of biological properties of the ruthenium complex.¹⁹² It has been more than 65 years since the biological activity of Ru(II) polypyridyl complexes was first reported by Dwyer *et al.*¹²⁰ Dwyer and co-workers demonstrated that different types of enantiomeric Ru(bpy)₃²⁺ and Ru(phen)₃²⁺ have different biological activity. Ji *et al.*

designed a number of Ru(II) tris(polypyridyl) complexes as potential anticancer drugs and systematically investigated the interactions between Ru(II) complexes and DNA molecules.¹⁹⁰ As a source of positive charge and stable molecule construction, most Ru(II) tris(polypyridyl) complexes interact electrostatically with various biomolecules. The intercalating action of the Ru(II) polypyridyl complexes with DNA is a classical and frequent mechanism of anticancer activity.¹⁹³

Barton *et al.* reported that Δ -[Ru(bpy)₂dppz]²⁺ could bind to both mismatched and well-matched sites in the oligonucleotide 5'-(dCGGAAATTACCG)2-3'.¹⁹⁴ Furthermore, the complex [Ru(bpy)₂dppz]²⁺ was unable to permeate cells due to its poor lipophilicity. Strategies using either conjugation to cell-penetrating peptides, lipophilic ancillary ligands, such as dip or biochemical compounds (carbonyl cyanide p-(trifluoromethoxy) phenylhydrazone, pentachlorophenol and tolfenamic acid) have been used to increase the membrane permeability of the Ru(II) complexes.^{74,77,195} Barton *et al.* systematically explored the cellular uptake of dppz Ru(II) polypyridyl complexes and reported that the complex [Ru(dip)₂(dppz)]²⁺ entered the cell by passive diffusion.^{76,196} The cellular uptake of the complex appeared to be facilitated by the lipophilic dip ligand. Overall, the Ru(II) complexes with the greatest lipophilicity exhibited the highest uptake and [Ru(dip)₂(dppz)]²⁺ mainly accumulated in the mitochondria and ER.^{76,196}

The modification of ligands also affected the uptake and intracellular localization of ruthenium complexes. Gill *et al.* changed the ligands of the ruthenium complexes, and found that the modification of lipophilicity and cellular uptake by modulating ligands has the great effect on the cytotoxicity and intercellular targets of Ru(II) complexes.¹⁹⁷ Compound **1e** targeted the cell nucleus in the MCF-7 cells, with an IC₅₀ value of 138 μ M. However, its analogue, with more hydrophobic ligands, targeted the cellular membrane structures in MCF-7 cells, with an IC₅₀ value of 7.0 μ M.¹⁹⁷ Recently, Zeng *et al.* reported that the chiral structures of Ru(II) complexes can also affect the intercellular localization of the complexes (Fig. 19). Their study showed that the complex **A-11**, mainly located in the cell nucleus, slightly inhibited the growth of MDAMB-231 cancer cells.¹⁹⁸ However, **A-11** was mainly enriched in the cytoplasm and produced no significant cytotoxicity in MDAMB-231 cells. These results demonstrated that the ligands can affect the anticancer efficacy of Ru(II) complexes by affecting their uptake and intracellular localization.

In addition, both the Liu and Chen group designed a series of mitochondria-targeted, Ru(II) complex **12a-12e** (see Fig. 20), based on a 2-phenylimidazo[4,5-f][1,10]phenanthroline (PIP) Ru(II) polypyridyl complex. Their results indicated that these complexes induced apoptosis by a mitochondrial pathway.¹⁹⁹⁻²⁰⁴ Moreover, the Chen group found that **12f** triggered cell apoptosis via the extrinsic pathway by inducing the activation of caspase-9.²⁰⁵ This complex firstly accumulated on cell membranes by a transferrin receptor-mediated endocytosis, promoting access to the cell cytoplasm and ultimately, the nucleus. Notably, the complex possessed more prolonged circulation time in the blood, comparable antitumor efficacy and significant lower toxicity *in vivo* experiments in mice, compared to cisplatin.

The luminescent complex, **12g**, was used as a theranostic compound by Cardoso *et al.*²⁰⁶ This complex was taken up in high amounts by HCT116 cells. In addition, it was cytotoxic

in HCT116/p53^{+/+} and HCT116/p53^{-/-}, with IC₅₀ values of 0.1 and 0.7 μ M, respectively. The cytostatic mechanism indicated that the complex induced cell cycle arrest in the G1 phase in both cell lines, and it activated proapoptotic PARP in p53^{-/-}, but not in p53^{+/+} cells. Chao *et al.* reported that mixed ligand Ru(II) complexes had potent activity against a variety of tumor cell lines.⁸⁹ The Ru(II) complex **1d** accumulated preferentially in the mitochondria of HeLa cells. Furthermore, **1d** induced apoptosis via the mitochondrial pathway, with an IC₅₀ value of 7.9 μ M after 48 h of incubation, which involved ROS generation, mitochondrial membrane potential depolarization and activation of Bcl-2 and caspase family members.⁸⁹ Recently, MacDonnell *et al.* determined the cytotoxicity of **12h** in H358, HCC2998, HOP-62, Hs766t cells, *in vitro*, under normoxia (18% O₂) and hypoxia (1.1% O₂).²⁰⁷ The cytotoxicity of **12h** was increased in Hs766t and HOP-62 cells under hypoxia compared to normoxia; however, neither H358 and HCC2998 cells were significantly affected by **12h**. The authors hypothesized that a mechanistic model where single-strand cleavage of the DNA-bound complex was due to redox-cycling mediated by the concentration of GSH and O₂ in a low O₂ environment.

However, other mechanisms are assumed to be operative and Ru(II) complexes also have anticancer efficacy by inhibiting topoisomerases,^{208–210} G-quadruplex stabilizers,^{211–213} telomerase,^{214–216} histone deacetylase, and thioredoxin reductase,^{217,218} as well as stabilizing G-quadruplexes in DNA.

5.2 Cyclometallated Ru(II) complexes

Generally, the cyclometallated ligands are *N*- and *C*- donors.²¹⁹ The metal-to-ligand bond distances of Ru-C are significantly shorter than that of Ru-N, and the binding of cyclometallated ligands with Ru is very stable.^{220,221} In addition, the cyclometalation can decrease the valence charge of the Ru(II) complexes, which contributes to an increase in the lipophilicity and cellular uptake of Ru(II) complexes. Therefore, the cycloruthenated complexes may be more stable in biological systems and exhibit distinct biological activities compared to non-cycloruthenated complexes (see Fig. 21, Table 1).²²² Loeffler *et al.* evaluated the biological effects of cycloruthenated complexes in 2005 and reported that some cycloruthenated complexes display significant efficacy as antitumor compounds *in vitro*, compared to the anticancer efficacy of cisplatin.²²³ Subsequently, Meng *et al.* reported that the cycloruthenated complex, **13b** inhibited the growth of various tumors implanted in mice more efficaciously than cisplatin.²²⁴ Further experiments indicated that this complex induced cell death through at least two pathways: the DNA damage/p53 and the ER stress/CHOP pathways.²²⁴ Recently, Licona *et al.* reported that **13b** could interact with histones to induce cell death. Three histones (H3.1, H2A, H2B) were regarded as possible targets for **13b**.²²⁵

Pfeffer and group reported the synthesis and biological applications of cycloruthenated compounds. The synthesized cycloruthenated complexes produced significant cytotoxic effects in mammalian tumor cells that were similar to cisplatin and were less likely to produce neurotoxicity compared to cisplatin.^{226,227} Fetzter *et al.* synthesized a series of cycloruthenated compounds with *N*-*C*-*N* and *N*-*N*-*C* pincer derivatives (Fig. 21).²²⁸ Most of the compounds were tested for their *in vitro* antitumor efficacy, which ranged from good to

excellent. Several of these compounds had IC₅₀ values in the nanomolar range.²²⁸ The efficacy of the aforementioned cycloruthenated compounds was tentatively correlated to their Ru^{III/II} redox potential and lipophilicity (log *P*).²²⁸

In addition, Peña *et al.* reported some cycloruthenated compounds were cytotoxic, and their cytotoxic efficacy in the dark was similar to that of cisplatin.²²⁹ The compound **13x**, was 6 times more than cisplatin, and it disrupted the mitochondria membrane potential. Although Peña *et al.* reported that **13p** is not an optimal compound for PDT due to its high cytotoxicity in the dark and its lack of photochemical sensitivity.²³⁰ They found a 7-fold increase in the cytotoxicity of cycloruthenated complex **13p** upon irradiation with light at 639 nm.

Chao *et al.* reported the efficacy of novel cycloruthenated compounds in different cancer cell lines. Interestingly, the Ru(II) complexes **13s** to **13x** had lower IC₅₀ values against HeLa cells, resulting from an increase of the volume of the chelating ligands, which is partly due to the larger chelating ligands which produces higher cellular uptake and stronger interactions with DNA.^{80,229,231} Recently, the same group also designed some cycloruthenated compounds with significant potency in hypoxic and cisplatin-resistant cancer cell lines.^{232,233} Complex **13y-5** (see Fig. 21) was efficacious against hypoxic HeLa cancer cells (IC₅₀ = 0.53 μM).²³² This complex was 46-times more potent than cisplatin (IC₅₀ = 24.62 μM) in HeLa cells.²¹⁵ The hydrophobicity and cellular uptake of the complexes were consistent with their cytotoxicity. They also postulated that the cycloruthenated compounds have the potential to surmount drug resistance.²³²

The mechanism of action and subcellular localization of the cycloruthenated compounds, **13k** and **13l**, in cancer cells and normal cells was reported by Klainer *et al.* (see Fig. 21).²³⁴ They first tested and compared the intrinsic luminescence of cycloruthenated compounds with an anionic cyclometalated 2-phenylpyridine chelate or neutral aromatic chelating ligands, using a special charge-coupled camera instrument.²³⁴ Both **13k** and **13l** had nonselective interactions with DNA, RNA and BSA *in vitro*. **13k** had reduced cellular uptake and cytotoxicity due to its improved water solubility compared to **13l**. Further studies showed that **13l** preferentially accumulated in the ER and induced H₂AX phosphorylation, as well as expression of CHOP/UPR and SATB₂ (signaling pathways). **13l** entered into cells via passive transport (at high concentration, 10 μM) and active/facilitated transport (at low concentration, 5 μM). **13l**, at 5 μM, accumulated to a greater level in glial A172 cancer cells compared to normal cells (neurons or glial cells), which may have resulted from the above mentioned transport modes. **13l** had some selectivity for glial cancer cells compared to healthy glial cells, with IC₅₀ values of 0.25 μM and 1.2 μM, respectively.²³⁴ Mechanistic studies indicated that multi-mode ER stress mechanisms and mitochondrial stress responses were involved in producing **13l**'s cytotoxic efficacy in the cancer cells. This work provides novel and critical information on the molecular mechanisms and direct targets of organoruthenium compounds.

5.3 Ru(II) polypyridyl complexes for PDT

Recently, a variety of Ru(II)polypyridyl complexes have been reported to have excellent photoactive properties, with certain compounds having enhanced cytotoxicity following light irradiation, providing a platform for relatively selective and improved tumor therapy (see Fig. 22, Table 2).^{235–237} The mechanism of action for most photoactive Ru(II) compounds involves: ligand dissociation and ROS/¹O₂ (reactive singlet oxygen).^{63,238} The ligand dissociation property is regarded as an O₂-independent mechanism, and the Ru(II) dyes can undergo photoinduced ligand dissociation, which allows the Ru(II) dyes to bind DNA, typically resulting in DNA damage.²³⁸ For the ROS/¹O₂ mechanism, the Ru(II) complexes enter excited states under light irradiation, giving them the potential for producing ROS or ¹O₂ by electron/energy transfer. Moreover, ROS or ¹O₂ can produce direct damage to cancer cells.⁶³

5.3.1 Ligand dissociation—The research groups of Turro and Sadler reported that Ru(II) complexes can lose the ligands following light irradiation, allowing them to covalently bind DNA to produce phototoxicity.^{239,240} They hypothesized that this class of complexes may provide valuable leads for new photoactivatable, antitumor Ru(II) complexes. I Turro et al. recently reported that irradiation of the cycloruthenated complex, **13b**, at 690 nm, resulted in an IC₅₀ value of 70 nM, representing a 14-fold increase in toxicity relative to the IC₅₀ obtained in the dark.²⁴¹ Furthermore, glutathione (GSH) facilitated ligand exchange of the cycloruthenated complex **13b**, with solvent DMSO-*d*₆ molecules. Intracellularly, in the absence of DMSO, a ligand exchange may result in the covalent binding of the complex to DNA and other biomolecules to produce phototoxicity. In order to increase the toxicity of the Ru(II) complex, Turro *et al.* used a dual-action therapeutic compound, 5-cyanouracil (5CNU), as a photoreleased ligand to combine with Ru obtain a photodynamic compound, **14a**.²⁴² **14a** binds to DNA following light (≥395 nm) irradiation and release of the 5CNU ligand, damaging HeLa cancer cells. The above mentioned research group also designed a new tris-heteroleptic, **14b**, and this complex was more photocytotoxic due to both ¹O₂ production and ligand exchange upon irradiation.²⁴³ This dual-action is useful for increasing the efficacy of photochemotherapy drugs.

Bonnet *et al.* first obtained two Ru(II) complex prodrugs by using a tetrapyridyl biqbp ligand and two *trans* monodentate ligands.²⁴⁴ The complexes **14c** and **14d** had *trans* geometries and the *trans* ligands were found to be photosubstituted by water under green light irradiation. The complexes were well taken up and had mild cytotoxicity in A431 and A549 cells in the dark. In contrast, when **14c** and **14d** were activated by green light irradiation, they produced significant cytotoxic, with EC₅₀ (EC = effective concentration) values below 1 μM and a PI of up to 22 for complex **14c**. Recently, the same group designed a photosensitive Ru(II) complex **14e**.²⁴⁵ The complex was found to have similar cytotoxicity as cisplatin in the dark and increased photocytotoxicity after 24 h incubation with blue light activation. Interestingly, the complex had monomer characteristics at a low concentration (< 3.5 μM) and it released the monodentate ligand under blue light activation. However, the complex formed supramolecular aggregates by self-aggregation at high concentrations (> 3–5 μM), which could induce non-apoptotic cell death by permeabilizing cell membranes and extracting membrane proteins and cell lipids.

Two photoactive $[\text{Ru}(\text{bpy})_2(\text{L})]^{2+}$ complexes (**14f**, **14g**), with sterically clashing ligands, were designed by Glazer *et al.*²⁴⁶ The complexes were inert until activated by visible light, which induces ligand loss and covalent modification of DNA.²⁴⁶ Mechanistically, **14f** lost the 6,6'-dimethyl-2,2'-bpy ligand and **4g** lost the 2,9-dimethyl-dpq (dpq: dipyrldo[3,2-f:2',3'-h]-quinoxaline) under light irradiation. The photo-ejection kinetics was 30-fold faster for **14f** compared to **14g**. A greater than 100-fold increase in cytotoxicity of these two complexes occurred with light activation in HL60 and A549 cancer cells. Glazer *et al.* also found that Ru(II) polypyridyl complexes (**14h**, **14i**), with biquinoline ligands, could photobind DNA following the loss of the biquinoline ligands in the presence of visible and near infrared light.²⁴⁷ These two complexes were cytotoxic in HL60 cancer cells after irradiation with near infrared light, with phototoxicity indices (PI) of 3.32 and 9.2, for **14h** and **14i**, respectively. Recently, the same group designed two novel, strained Ru(II) polypyridyl complexes (**14j**, **14k**), containing a 2,3-dihydro-1,4-dioxino[2,3-f]-1,10-phenanthroline ligand (dop), and these two complexes selectively lost a methylated ligand when irradiated with light > 400 nm.²⁴⁸ The compound **14k** was 1880-fold more cytotoxic in HL60 cancer cells upon activation by light and was 19-fold more potent than cisplatin.²⁴⁸ Glazer *et al.* hypothesized that this O_2 -independent mechanism and ligand dissociation in photoactive metal complexes can simultaneously provide effective and selective phototherapy and overcome diminished efficacy due to hypoxia in the core of the tumor.^{65,249}

5.3.2 ROS/ $^1\text{O}_2$ —As most Ru(II) complexes have high photostability and long fluorescence lifetimes, they can produce ROS or $^1\text{O}_2$ when irradiated by light. The Ru(II) polypyridyl complex elevates ROS production, resulting in the efficient cleavage of supercoiled DNA and damage to certain biomarkers.⁶³ Swavey *et al.* designed several Ru(II) polypyridyl complexes with porphyrin derivative ligands.^{250,251} The Ru(II) porphyrin complex, **14i**, efficiently cleaved supercoiled DNA and induced apoptosis in melanoma cells after irradiation with light, while normal cells were unaffected. Ke *et al.* also designed a mitochondria-specific, porphyrin-Ru(II) conjugate (**14m**), with high a luminescence and a high singlet oxygen quantum yield.²⁵² The porphyrin-Ru(II) complex held a large two-photon absorption cross section σ value of 1104 GM (GM = $10^{-50} \text{ cm}^4 \text{ photon}^{-1} \text{ molecule}^{-1}$) upon light irradiation 800 nm. This complex was used to sensitize the formation of $^1\text{O}_2$, with high $^1\text{O}_2$ quantum yields (0.93) upon irradiation at 424 nm. This complex could kill 80% of HK-1 cells at a concentration of 1 μM and a light dose of 3 J/cm^2 . After a 5 minute flash excitation by an 850 nm laser on cells loaded with 5 μM of this complex, 90% of the HeLa cells were deformed or had lost their integrity.

Gasser's group recently inactivated **1a** by attaching it to a photo-labile protecting group (PLPG).⁸⁷ Upon UV-A exposure, **1a** was released from the PLPG and had effective phototoxicity. In addition, two other light sensitive Ru(II) polypyridyl complexes (**14n** and **14o**) were tested for photosensitization efficacy.²⁵³ The two complexes had significant PDT activity in HeLa cancer cells, with IC_{50} values of 25.3 μM for **14o** and 0.62 μM for **14n** under light irradiation (420 nm, 6.95 J/cm^2). Moreover, both complexes showed significant antimicrobial PDT activity against the *Staphylococcus aureus* and the *Escherichia coli*.²⁵³ Recently, the same group reported that **14o** localized in the nucleus of various cancerous and

normal cells, but only produced cytotoxicity upon irradiation.²⁵⁴ This complex induced the production of ROS, causing DNA damage, cell cycle arrest and cell death. Importantly, the complex had a 3.6-fold increase in its phototoxicity against mitotic cells. This dual mode of cell death upon photo irradiation of the complex may open new avenues in PDT. Cloonan *et al.* designed a new Ru(II) PDT candidate, **14q**, that efficiently entered cells by incorporation of 1,4,5,8-tetraazaphenanthrene ancillary ligands and the lipophilic aromatic pdppz ([2,3-h]dipyrido[3,2-a:2',3'-c]phenazine) ligand.²⁵⁵ The complex entered into cells via an energy-dependent mechanism and was localized in mitochondria, lysosomes and ER. The complex was nontoxic to HeLa cells, with an IC₅₀ value 70 μM in the dark, and cellular clearance occurred within 96 h. However, it had significant photoactivity against HeLa cells, with an IC₅₀ value 8.8 μM upon visible light activation. Further studies showed that the complex could induce DNA photocleavage and caspase-dependent and ROS-dependent apoptosis upon light activation. Recently, Bonnet *et al.* obtained two highly photosensitive Ru(II)-based anticancer prodrugs. The complexes contained either a D- or L-glucose.²⁵⁶ The D-glucose, **14r**, was present in the mitochondria and had significant photocytotoxicity in A549 cells, with an IC₅₀ value of 0.72 μM due to both ¹O₂ production and ligand exchange upon irradiation at 454 nm.

McFarland *et al.* designed and tested the PDT efficiency of Ru(II) polypyridyl complexes that had the lowest-lying ³IL-based excited states, with remarkably long lifetimes (from 22 to 270 μs), by linking pyrenylethynylene derivatives ligands,^{257–259} which made the complexes hold higher ¹O₂ quantum yields compared to [Ru(bpy)₃]²⁺. These complexes interacted with DNA via intercalation and produced photocleavage of DNA *in vitro* at submicromolar concentrations when irradiated with visible light. These photosensitizers had highly potent photocytotoxicities in melanoma, HL60 and bacterial cells at very low concentrations. Compounds **14s** induced cell death in a HL60 cells, and the LC₅₀ (LC = lethal concentration) went from 262 μM in the dark to less than 0.15 μM upon visible light irradiation.²⁵⁸ Another class of Ru(II) polypyridyl complexes, with polythiophene chains of variable lengths, were obtained and studied by the same group.^{1,260} These compounds gave access to a low-lying, ³IL excited state and a strong interaction with plasmid DNA. These complexes were also found to possess high ¹O₂ quantum yields that increase with polythiophene chain length, and the complex, **14t-III**, was found to targeted DNA in HL60 cells, inducing = DNA photodamage.¹ The cytotoxicity of this family in the dark was very low, with an EC₅₀ > 300 μM in the dark. However, there was a 200-fold increase cytotoxicity after light exposure compared to dark conditions as n was increased (n = 1 to 4) in polythiophene chain. Furthermore, animal survival was significantly increased after the administration of **14t-III** and **14u-III**. The complex **14u-III** is currently undergoing human phase IB clinical trials.^{1,70} Interestingly, McFarland's group found that the family of **14v**, containing the π-expansive dppn (benzo[i]dipyrido[3, 2-a: 2', 3'-c]phenazine) ligand, also shared the properties of low-energy and long-lived ³IL excited states, and had efficient photodynamic activity in HL60 cancer cells.²⁶¹ In addition, a photoactive cycloruthenated complex [Ru(bpy)₂(pbpn)]⁺, **14x**, was developed by replacing dppn with the π-expansive cyclometalating ligand pbpn (4,9,16-triazadibenzo (a,c-naphthacene)).²⁶² This complex displayed intense green ligand-centered fluorescence from inside the cell. This complex had very weak to no room temperature phosphorescence, extremely short phosphorescence state

lifetimes (< 10 ns), low singlet oxygen quantum yields (0.5–8%) and lack of cytotoxicity in the dark ($EC_{50} > 300$ μ M). However, it had significant phototoxicity in cancer cells, with an IC_{50} in the nanomolar range.²⁶² The authors postulated that 3IL excited states affected the phototoxicity of **14x**. Moreover, three cycloruthenated compounds of *N-C-N*pincer were designed by Tabrizi *et al.* The compounds showed high uptake and effective photocytotoxicity in HeLa cells under light irradiation (350 nm) with the formation of 1O_2 and hydroxyl radicals.²⁶³

Recently, Chao *et al.* developed an efficacious cancer therapy by combining PDT with targeting.⁶⁸ They found that **15a**, (Fig. 23) with a triphenylphosphine (TPP) group, highly targeted mitochondria and was activated by 2 photons.²⁶⁴ **15a** had an IC_{50} value as low as 9.6 μ M in one-photon PDT ($\lambda_{irr} = 450$ nm, 12 J cm⁻²) and an IC_{50} of 1.9 μ M in two-photon PDT ($\lambda_{irr} = 830$ nm, 800 J cm⁻²) towards 3D HeLa, with multicellular spheroidal tumors (MCTSs). In addition, several highly charged Ru(II) complexes (**15c–15e**), were designed as two-photon photosensitizers by the same group.⁹⁸ The three complexes were found to localize in the lysosomes via an endocytotic uptake pathway. **15c** produced significant phototoxicity upon irradiation (800 nm, 10 J/cm²) in 3D HeLa MCTSs, with an IC_{50} value as low as 1.9 μ M. Thus **15c** has the potential to be used for two-photon photodynamic therapy. Moreover, Chao's group utilized a GSH-activatable Ru(II)-azo photosensitizer, (**15b**), for two-photon PDT.²⁶⁵ **15b** did not show luminescence but exhibited a strong luminescence after incubation in HeLa cells due to the activation of intracellular GSH. **15b** accumulated to a significant extent in mitochondria and could produce ROS in HeLa cells upon two-photon irradiation (810 nm, 100 mW). In dark conditions, **15b** lacked significant cytotoxicity in 3D HeLa MCTSs ($IC_{50} > 100$ μ M). In contrast, **15b** was significantly cytotoxic in MCTSs, with an IC_{50} value as low as 5.71 μ M upon two-photon irradiation.²⁶⁵ The Chao *et al.* study demonstrated that the combination of organelle-targeting and two-photon activation provides a valuable paradigm for developing Ru(II) complexes for PDT applications.

6. Ruthenium(II)-based nanomaterial systems

Over the years, numerous strategies have been used to deliver Ru(II)-based metal complexes into cancer cells. However, their particle size and specificity have always been major obstacles for effective tumor targeting. Nanomaterials represent a wide range of nanoscaled, hybrid components that are linked together by covalent or non-covalent interactions. Recently, nanomaterials have been developed for a variety of biomedical applications for the treatment and imaging of diseases.²⁶⁶ Drug encapsulation into nanomaterials can provide significant improvements in pharmacokinetics, solubility, toxicity and biodistribution when compared to freely administered molecules.²⁶⁷ Importantly, once nanomaterial drugs are injected into the bloodstream, they preferentially accumulate in solid tumors due to the enhanced permeation and retention (EPR) effect.^{268–290} Past studies have shown that encapsulating Ru(II) metal complexes in a nanomaterial system improves their targeting and delivery into tumor cells. Ru(II) complexes in nanomaterial systems play four main roles: (a) to control the release of payloads (drugs) with better efficiency; (b) to work as drugs or catalysts in the nanomaterial systems; (c) to improve the photothermal efficacy and the

stability of nanomaterials and (d) to act as theranostic tools to track the import of nanomaterials through luminescence imaging.

6.1 Ru(II)-selenium nanoparticles

Due to its biocompatibility, rapid degradation, low toxicity, facile synthesis, selenium has evolved as one of the most commonly used nanosystems to deliver drugs.²⁷¹ Moreover, selenium shows promising chemopreventative efficacy when used as a nanosystem to deliver chemotherapeutic drugs such as 5-fluorouracil and doxorubicin.^{272,273} Several selenium nanoparticle systems have been utilized to deliver Ru(II) complexes as anti-cancer compounds. The Ru(II) complex, **RuPOP**, produced significantly greater anticancer efficacy and lower toxicity compared to cisplatin, but its use was limited due to poor aqueous solubility.²⁷⁴ Liu *et al.* loaded **RuPOP** in selenium-based nanoparticles (Fig. 24A) and determined its anti-cancer efficacy.²⁷⁴ They developed pluronics (a group of block copolymers that are amphiphilic) based on the ruthenium complex antagonism of the folate receptor and formulated a selenium-based nanosystem. This formulation (**FA-SeNPs**) entered cells via endocytosis. Furthermore, 20 μM of **FA-SeNPs** had significant cellular uptake after 8h of incubation in doxorubicin-resistant R-HepG2 cells. The intracellular translocation was achieved in 1 h and the pluronic-bound ruthenium was released in acidic conditions. *In vitro*, **FA-SeNPs** had significant cytotoxicity in the parental and drug-resistant hepatocellular carcinoma cell lines, with IC_{50} values of 0.33 and 0.24 μM , respectively.²⁷⁴ The mechanistic experiments indicated that **FA-SeNPs** induced cell apoptosis by up-regulating the level of ROS in cells to activate the MAPK and AKT pathways. Moreover, 0.48 μM of **FA-SeNPs** decreased the expression level of major drug efflux transporters, namely, ABCB1, ABCC1, and ABCG2 and induced apoptosis by stimulating the sub-G1 phase of the cell cycle. This work suggests that **FA-SeNPs** are significantly more cytotoxic in cancer cells compared to normal cells and this system may provide a suitable approach for surmounting multidrug resistant cancers.

A key study by Sun *et al.* demonstrated the anti-angiogenic effects of Ru-SeNPs, which are luminescent ruthenium selenium nanoparticles (Fig. 24B).²⁷⁵ The chicken chorioallantoic membrane (CAM) assay *in vivo* was used to evaluate the anti-angiogenic effects of **Ru-SeNPs**. At 50 μg , the nanoparticles significantly reduced the angiogenesis in the chorioallantoic membrane, compared to the control. Moreover, **Ru-SeNPs** inhibited the proliferation of the following cancer cell lines: prostate PC-3, MCF-7, human umbilical vein endothelial cells (Huvec), SW480, and HepG2, with $\text{IC}_{50\text{s}}$ in the range of 3–20 $\mu\text{g}/\text{ml}$. A concentration-dependent increase in apoptosis occurred in HepG2 cells after 24 h of exposure to **Ru-SeNPs**. Furthermore, an inhibition of the phosphorylation of FGFR1, Erk1/2, and AKT validated the anti-angiogenic effects of **Ru-SeNPs**.²⁷⁵ Another study indicated that the anti-angiogenic effects of ruthenium-thiol selenium nanoparticles (**Ru-MUA@Se**) by the same group (Fig. 24C).²⁷⁶ **Ru-MUA@Se** directly suppressed HepG2 tumor growth, with no significant body weight loss, and also blocked blood vessel growth *in vivo* by decreasing microvessels. **Ru-MUA@Se** entered the cells via a clathrin-mediated endocytosis pathway. This system was shown to inhibit mitochondrial membrane function and induce ROS formation in HepG2 cells. Moreover, there was a significant reduction in tumor angiogenesis and low-systemic toxicity in HepG2 tumor.

6.2 Ru(II)-gold nanomaterials

Gold nanomaterials have been a topic of significant interest due to their interesting surface plasmon resonance (SPR) properties.^{277–282} The functionalized gold nanostructures have the properties of good biocompatibility, small size and shape-dependence, and they have proven to be a versatile platform for a wide range of biomedical applications. Similarly, Ru(II)-polypyridyl complexes, due to their photophysical properties, high luminescence and large two-photon absorption cross sections, have emerged as promising theranostic tools for cancer treatment.^{283–285} In addition, there are two excellent examples for Ru(II) complex functionalized gold nanomaterials as anticancer compounds for photothermal therapy (PTT). Zhang *et al.* developed the gold nanoparticles for PTT by grafting two-photon luminescent Ru(II) complexes to the surface of gold nanoparticles as antenna molecules (Fig. 25A).²⁸⁶ The **Ru@AuNPs** converted NIR (808 nm) light to heat ($\Delta T = 9.4\text{--}38.5\text{ }^{\circ}\text{C}$), with high photothermal therapy efficiency ($\Delta T = 38.5\text{ }^{\circ}\text{C}$, $\eta = 33.3\%$), which was well over the required temperature increase for efficient cancer photothermal therapy. More importantly, the *in vivo* experiments indicated that **Ru@AuNPs**, as PTT compounds, had significant tumor ablation efficacy. Indeed, under diode laser (808 nm) irradiation at the power density of 0.8 W/cm^2 for 5 min, tumors shrunk gradually or disappeared individually after 10 days of treatments.²⁸⁶ This study with Ru(II) complex modifications provides an effective solution for overcoming the typically poor NIR absorbance and low photostability (melting effect) of gold nanoparticles in PTT. Recently, the same group developed two novel gold nanostructures to get the Ru(II)-functionalized gold nanorods, (**AuNRs@Ru**) and nanostars (**AuNTs@Ru**) (see Fig. 25B).²⁸⁷ **AuNRs@Ru** and **AuNTs@Ru** had higher photothermal stability and photothermal efficiency compared to pure **AuNRs** and **AuNTs** ($\Delta T_{\text{AuNRs@Ru}} = 41.1\text{ }^{\circ}\text{C}$, $\Delta T_{\text{AuNTs@Ru}} = 38.9\text{ }^{\circ}\text{C}$; $\Delta T_{\text{AuNRs}} = 21.0\text{ }^{\circ}\text{C}$, $\Delta T_{\text{AuNTs}} = 19.2\text{ }^{\circ}\text{C}$). **AuNRs@Ru** and **AuNTs@Ru** exhibited efficacious photothermal therapy both *in vitro* and *in vivo* under low power (808 nm laser, 0.25 W cm^{-2}), which suggested that the two candidates have potential application as cancer therapy through photothermal destruction.

6.3 Ru(II)-silica composites

Silica has long been used as a nanocarrier to deliver drugs for therapeutic uses.^{288,289} Silica nanoparticles are non-toxic to cells and readily undergo endocytosis in acidic liposomes. The release of these nanoparticle in specific pH environments, photon activation, redox activation, and tumor targeting, makes them an ideal nanocarrier for Ru(II) complexes and other drugs. Frasconi *et al.* developed ruthenium-silica nanoparticles (Fig. 26A), with enhanced cellular uptake and photoactivation.²⁹⁰ 1 The Ru(II) complex was linked covalently to the mesoporous silica nanoparticles (**MSNPs**) to form **MSNPs2** by coordination of the monodentate ligand (3-isocyanato-propylethoxysilane with 4-(aminomethyl)-benzonitrile).²⁹⁰ The **MSNPs2** showed rapid cellular uptake and the ruthenium complexes were rapidly released and transformed upon light irradiation into a cytotoxic aqua complex that formed monoadducts with DNA. In addition, the **MSNPs2** could load paclitaxel with an 82% uptake efficiency and 35% release efficiency. Cytotoxicity studies showed that empty **MSNPs2** had no significant cytotoxicity against MDAMB-231 cells. In contrast, light activation enhanced the cytotoxicity of docetaxel-loaded **MSNPs2** significantly in MDA-MB-468 and MDAMB-231 breast cancer cell lines but had no effect on the cytotoxicity of

free paclitaxel. Moreover, a photoactive drug delivery system, using only low light intensity, was developed by He *et al.* by grafting mesoporous silica coated **UCNPs** (lanthanide-doped upconverting nanoparticles) with Ru(II) complexes.²⁹¹ The photoactive and blue light-cleavable Ru(II) complexes were grafted to the surface of the **UCNPs** to generate **DOX-UCNP@mSiO₂-Ru** (Fig. 26B).²⁹¹ The concept of this system is that the **UCNPs** can convert NIR light (~980 nm) to UV and visible light which subsequently activates Ru(II) complexes to initiate photoreactions, releasing doxorubicin. Approximately 27% of doxorubicin and 59% Ru(II) complexes in this system can be released after 974 nm light irradiation, with 0.35 mW cm⁻² for 5 hours. Using the same irradiation condition, NIR irradiation of **DOX-UCNP@mSiO₂-Ru** for 10–30 min reduced cell viability to 40–29%. No obvious burn wound was observed when the light intensity was lower than 1 mW cm⁻². The results of the above experiments indicate that the **UCNPs** may be an efficacious and safe therapy strategy using low intensity NIR light.

Knežević *et al.* used multifunctionalized, porous silicon nanoparticles (**pSiNPs**) to deliver the photosensitized ruthenium complex for PDT (Fig. 26C).²⁹² This ruthenium complex had good two photon absorption at 800 nm, yielding a ROS that killed cancer cells upon light irradiation. In addition, polyethylene glycol (**PEG**) was added to the surface of the nanoparticles to improve the dispersibility and biocompatibility of **pSiNP-Ru-PEG-Man**.²⁹² Cytotoxicity studies indicated that 87% of MCF-7 cancer cells died at 80 mg/mL⁻¹, following a 5 h pre-incubation upon 800 nm irradiation of **pSiNP-Ru-PEG-Man**. Recently, He *et al.* developed silica nanoparticle as a carrier for delivering anticancer Ru(II) complexes.²⁹² The **RGD** (arginine-glycine-aspartic acid) peptide, which targets the $\alpha\text{v}\beta3$ integrin receptor, was attached to the surface of the mesoporous silica nanoparticles to improve their selectivity for cancer cells compared to and cells.²⁹³ The nanoparticle system, **RuPOP@MSNs** (Fig. 26D), released Ru(II) complexes much faster at pH 5.3 than at pH 7.4, with a 63.3% release for pH 5.3 and 43.1% for pH 7.4 after 12 days.²⁹³ Under a fluorescence microscope, **RuPOP@MSNs** was shown to enter the cells through endocytosis and release the Ru(II) complexes from lysosomes into the cytosol. The nanoparticle system had unprecedented, enhanced cytotoxicity in cancer cells overexpressing the integrin receptor and the mechanistic studies indicated that ROS overproduction induced by **RuPOP@MSNs** was involved in the cancer cell apoptosis through the regulation of AKT and MAPK signaling pathways.

6.4 Ru(II)-carbon nanotubes

Carbon nanotubes (**CNTs**) are one-dimensional, columniform structures of wrapped graphene sheets, forming tubular architectures. Single-walled nanotubes (**SWNTs**) and multiwalled nanotubes (**MWNTs**) are two main types of carbon nanotubes that can have high structural perfection.²⁹⁴ Single-walled nanotubes (**SWNTs**) are formed by a single graphite sheet seamlessly wrapped into a cylindrical tube. Multi-walled carbon nanotubes (**MWCNT**) contain several graphene sheets, leading to multiple concentric tubes of different diameters.^{295,296} Carbon nanotubes have unique properties that make them a highly promising system for biomedical application, as they can be used to deliver therapeutic drugs and diagnostic agents into cells.^{297,298} However, carbon nanotubes can also absorb

light in the near-infrared region as photosensitizers and can kill cancer cells by localized photothermal effects.²⁹⁹

Wang *et al.* determined if nanostructured **RuPOP@MWCNTs** (Fig. 27A) are efficacious in surmounting multidrug resistance and radio resistance in cancer cells.³⁰⁰

RuPOP@MWCNTs was formed by loading a potent anticancer Ru(II) polypyridyl complex (**RuPOP**) in multiwalled carbon nanotubes via π - π interactions and by formation of a hydrogen bond. The **RuPOP@MWCNTs** entered cells via endocytosis and enhanced the selective cellular uptake of **RuPOP** in HepG2 and multidrug-resistant R-HepG2 cells. A concentration-dependent cell apoptosis occurred in HepG2 and R-HepG2 cells with the **RuPOP@MWCNTs**. The IC₅₀ values of **RuPOP@MWCNTs** against R-HepG2 and HepG2 cells were 40 and 100 ng/mL, respectively. However, **RuPOP@MWCNTs** had significantly lower cytotoxicity towards L02 normal liver cells at the same concentration. Importantly, the nanosystem was found to significantly enhance the anticancer efficacy of clinically used X-rays in R-HepG2 cells through induction of apoptosis and G0/G1 cell cycle arrest, which involved the generation of ROS. Moreover, the nanosystem effectively reduced the toxic side effects of loaded drugs and prolonged the blood circulation of **RuPOP** *in vivo*.

Zhang *et al.* used the single-walled carbon nanotube, loaded with Ru(II) complexes (Fig. 27B) for bimodal photothermal and photodynamic therapy, with near-infrared (808nm) irradiation.³⁰¹ The carbon nanotube nanosystem had a high photothermal conversion efficiency of ~39.4% for **Ru1@SWCNTs** and 38.3% for **Ru2@SWCNTs**.³⁰⁰ The nanosystem can convert NIR (808 nm) light to heat (creating temperature changes from 20.3 to 58.5 °C for **Ru1@SWCNTs** and from 20.2 to 56.6 °C for **Ru2@SWCNTs**), a marked improvement from pure **SWCNTs** (where temperatures changed from 20.2 °C to 44.2 °C). The Ru(II) complex in the system can be released from the **Ru@SWCNTs** upon irradiation (808 nm, 0.25 W/cm²). Furthermore the released Ru(II) complexes produced ¹O₂ upon two photon laser irradiation (808 nm, 0.25 W/cm²). Cytotoxicity studies *in vitro* indicated that the **Ru@SWCNTs** (50 µg/mL) could kill all the HeLa cells under 808 nm laser irradiation at 0.25 W/cm² for 5 min. More importantly, the tumors in nude mice shrank gradually or disappeared individually after 15 days of intratumoral injection with 100 µL of an aqueous dispersion of 1 mg/mL of **Ru@SWCNTs** upon the irradiation (808 nm laser).

6.5 The organic and biomaterial Ru(II) nanomaterials

Due to its biocompatibility and biodegradability, poly-(DL-lactic-co glycolic acid) (PLGA) is widely used as a nanocarrier to deliver drugs. Boeuf *et al.* encapsulated Ru(II) photosensitizers in PLGA-based nanosystems and determined their cytotoxicity in C6 glioma cells.³⁰² The ruthenium-PLGA nanoparticles typically released a lower amount of the ruthenium complexes in phosphate buffer of pH 7.4 at 37 °C. In contrast, the nanoparticle systems exhibited faster release of the ruthenium complexes upon light irradiation. After exposure to a pulsed laser at 740 nm, the released Ru(II) complexes produced ¹O₂ and had potent cytotoxicity in the C6 glioma cells. Moreover, light exposure to PLGA-based ruthenium nanoparticles enhanced the cytotoxicity in C6 cells by ~ 60%, supporting the notion that ruthenium-PLGA nanoparticles could be good candidates for two-

photon-excited PDT applications in the future. In an effort to improve the blood circulation times and increase in the cellular uptake of polymetallo drugs, Wu *et al.* used the poly(ethylene glycol) (PEG) block to bind metal ruthenium to form a nanoparticle, **PolyRu**, via self-assembly.³⁰³ The **PolyRu** efficiently accumulated at the tumor sites through the enhanced permeability and retention (EPR) effect. Furthermore, **PolyRu** released anticancer Ru(II) complexes and generate cytotoxic $^1\text{O}_2$ and inhibited the growth of tumors under 656 nm red light, with minimal systemic toxicity.

Zhou *et al.* investigated the anticancer efficacy of functionalized Ru(II) nanoparticles (**RuNPs**) loaded with luminescent Ru(II) complexes (**RuBB**) and epigallocatechingallate (**EGCG**).⁷² The nanoparticle system (**RuBB-loaded EGCG-RuNPs**) displayed red fluorescence and were entered SMMC-7721 liver cancer cells by 67LR-mediated endocytosis, with drug accumulation in the cytoplasm after 6 h.⁷² However, some of the nanoparticles were found in the nucleus after 12 h of incubation; the gradual accumulation indicated that the nucleus is a potential organelle target of the nanoparticles. Moreover, the nanoparticles significantly inhibited migration and invasion of the liver cancer cells and induced apoptosis by generating ROS and activating both the intrinsic and extrinsic apoptotic pathways. *In vivo* studies indicated that **RuBB-loaded EGCG-RuNPs** (50 $\mu\text{g}/\text{mouse}$) decreased the average tumor volume to 23% of the control level after 15 days of treatment.

In addition, a **3P-Ru/PbPS** nanocapsule system for delivering the tris (1,10-phenanthroline) Ru(II) complex (**3P-Ru**) to tumor cells based on a pH-sensitive Poly (2-diisopropyl-aminoethyl methacrylate)-blockpoly (2-aminoethyl methacrylate hydrochloride) was designed by Chen *et al.*³⁰⁴ This system released 35% of the **3P-Ru** in the nanocapsule in a pH 7.4 solution after 48 h of dialysis. However, the release rate reached 65% in a solution at pH 6.5, indicating a selective and rapid release in acidic environments. The **3P-Ru/PbPS** system delivered the **3P-Ru** into gliomas cells with high efficiency and inhibited U251 cell proliferation in a concentration-dependent manner via an apoptosis pathway. More importantly, the **3P-Ru/PbPS** system significantly decreased tumor growth in tumor-bearing mice, resulting in smaller tumor volumes (5 mm^{-3}), compared to mice treated for 8 days with PBS (25 mm^{-3}), **PbPS-NC** (26 mm^{-3}) and **PEG-Ru-NC** (20 mm^{-3}) mice.

Recently, Chakraborty *et al.* used the TPP-functionalized bloodplasma protein serum albumin (HSA) as the targeting peptide to combine with a Ru(II) complex to serve as a new photosensitizer (**cHSA-PEO-TPP-Ru**) (Fig. 28).³⁰⁵ **cHSA-PEO-TPP-Ru** produced an ~8-fold improvement in $^1\text{O}_2$ quantum yields and a five times higher TP action cross section compared to the single Ru(II) complex. **cHSA-PEO-TPP-Ru** was highly localized in mitochondria. **cHSA-PEO-TPP-Ru** had potent phototoxicity, with an IC_{50} value of 34.9 nM against HeLa cells after light irradiation for 5 min (470 nm, $\sim 20 \text{ mW}/\text{cm}^2$) and had a significantly high PI of 250. Further study indicated that **cHSA-PEO-TPP-Ru** had effective antileukemic activity, which occurred by decreasing cell proliferation and clonogenic property of the myeloid leukemic cell line OCI-AML3. However, **cHSA-PEO-TPP-Ru** was less toxicity to normal bone marrow cells compared to leukemic cells.

In addition, there are other nanomaterials functionalized with Ru(II) complexes for cancer treatments, such as nanographene oxide,³⁰⁶ polymers,³⁰⁷ DNA origami and liposomes.^{308–311} These Ru(II) complex, functionalized-nanomaterials were safety and efficacious. Although further research, including clinical studies, is needed to verify these results, these examples serve as the basis of new developments for treating cancer.

7. Ru(II) complexes for bioorthogonal catalysis

The sections above presented ruthenium complexes as anticancer drugs or drug delivery systems, which play the role of reagents and direct targeting of tumor cells. Furthermore, ruthenium complexes could also be used as catalysis in biological system. The field, called bioorthogonal catalysis, has extended our understanding and is useful in imaging and drug development. Bioorthogonal chemistry allows for the occurrence of chemical reactions inside living cells without interfering with native biochemical processes. Thus, for this reason, bioorthogonal catalysts should selectively recognize specific functional, unnatural groups and catalyze the chemical reaction, especially in living systems. The catalyst needs to balance reactivity and stability. As a result, there is a lack of efficient bioorthogonal catalysts available today that match these crucial criteria.³¹² The design of bioorthogonal synthetic catalyst/substratepairs, which can passively diffuse into cells for use as tools in chemical biology studies, is a highly formidable challenge that has only recently started to be investigated.³¹³ Recently, unique opportunities, arising from the catalysis of transition metals,^{314,315} have been explored.

Metal ruthenium complexes represent a powerful toolkit for selective synthesis and lysis of chemical bonds, thus offering plentiful physicochemical properties. It is possible that Ru(II) complexes may serve as catalysts in bioorthogonal chemistry. Based on how they enter into cells, Ru(II) complexes could also be cataloged into direct catalysis and nano-systems.

7.1 Ru(II) complexes as catalytic agents

Within the last decade, significant attention has been centered around improving the biocompatibility of a Cu(I)-catalyzed bioorthogonal reaction in living cells. Meanwhile, additional transition metals, such as palladium or ruthenium, have been examined as alternative sources to facilitate a bioorthogonal conjugation reaction in living cells.³¹⁶ Current concepts of bioorthogonal chemistry have largely centered on ‘bond formation’ reactions between two mutually reactive bioorthogonal handles (Fig. 29). Recently, in a reverse strategy, a collection of ‘bond cleavage’ reactions has emerged with excellent biocompatibility.³¹⁷ In 2006, Meggers *et al.* reported allylcarbamate cleavage in living cells using Ru(II) complexes (**Ru1**).³¹⁸ In addition, researchers in the above group made progress towards synthesizing organometallic Ru(II) complexes for the catalytic uncaging of allyloxycarbonyl-protected amines under biologically relevant conditions and within living mammalian cells (**Ru2**).^{312,313} To find a catalyst with an improved activity, they screened a set of ruthenium complex and found that catalytic efficiency is fine-tuned by ligand-modifications (**Ru3–Ru5**).³¹⁹ Using those Ru(II) complexes catalysts, the fluorescence development was more pronounced in the presence of thiophenol, yielding a 10-fold increase within 15 min in the cytoplasm of HeLa cells.³¹³

Sadhu *et al.* developed a luminescent Ru(II) complex that labeled proteins, enabling the direct visualization and photocatalytic reduction of arylazide in live cells.³²⁰ Hsu *et al.* reported that a bioorthogonal precatalyst Ru(II) complex cleaves a novel caged bioluminescence probe in luciferase-transfected 4T1 cells. The rate of the probe release and enzymatic turnover could be evaluated in 4T1 cells using a luciferase reporter system.³²¹ With this method, researchers could measure the catalytic cleavage of a pro-probe and intracellular enzyme-mediated turnover of the released probe. This approach provides a set of critical metrics to observe the performance of biological catalysts and caging strategies for analogously cleavable pro-drugs.³²¹ Similarly, Mascarenas *et al.* developed a Ru(II) catalyst in the mitochondria of living cells by integrating the phosphonium-targeting moieties to Ru(II) complexes.³²² This metal catalysts was had significant catalytic efficacy and produced a smooth and rapid ruthenium-dependent depolarization of the mitochondria.

Sadler and colleagues summarized the design approaches of catalytic metallodrugs. Of special interest was the development of redox-modulating drugs, including the thiol oxidation and transfer hydrogenation reactions.³²³ The complexes $[(\eta^6\text{-arene})\text{Ru}(\text{azpy})\text{I}]$ (where arene = biphenyl, and azpy = *N,N*-dimethylphenyl- or hydroxyphenyl-azopyridine) were highly cytotoxic to A2780 and A549 cell lines, with IC₅₀ values from 2–6 μM .³²⁴ The replacement of iodide by chloride dramatically decreased the cytotoxicity of the arene Ru(II) complexes.³²⁵ Intriguingly, the iodide Ru(II) complexes were catalysts in reactions with the tripeptide glutathione ($\gamma\text{-L-Glu-L-Cys-Gly}$).³²⁴ In addition, millimolar concentrations of glutathione were oxidized to glutathione disulfide in the presence of micromolar concentrations of Ru(II) complexes (Fig. 30A), significantly influencing intracellular redox processes. In addition, the same group also reported that another class of Ru(II) complexes with a chelated sulfonylethylamine ligand can convert coenzyme NAD⁺ into NADH in the presence of formate, thereby modulating the NAD⁺/NADH redox couple, as depicted in Fig. 30B.³²⁶ The efficacy of the arene Ru(II) sulfonamidoethyleneamine complexes toward ovarian cancer cells was enhanced by up to 50-fold in the presence of low, non-toxic concentrations of formate. The IC₅₀ of this Ru(II) complex towards A2780 cells decreased from 13.6 μM (in the absence of formate), to 1.0 μM , in the presence of 2 mM formate, making the complex equipotent to cisplatin.³²⁶ Catalytic reactions in cancer cells offer a new strategy for the design of safe, Ru-based anticancer drugs that may contribute to further insight into the mechanism of cell death. The catalytic metallodrugs may offer the prospect of low-dose therapy and a challenging new design strategy for future exploration.³²³

Currently, the catalytic efficiency of most precious-metal organometallic catalysis within living cells or in the presence of cell lysates has not been maximized. There are two major restrictions for organometallic catalysis in a cellular environment: 1) the catalyst and enzymes would affect each other and 2) even millimolar concentration of glutathione in cells under aerobic conditions would inhibit the precious metals catalytic activity.³²⁷ Enzymes have evolved to be efficient biocatalysts, and with the development of protein engineering, researchers have the potential obtain powerful tools to exploit more metallo-enzymes combined with natural proteins.³²⁸ The undeniable advantage of signal amplification through catalytic turnover has been successfully exploited in the area of enzyme-based bio-imaging and sensing.³²⁹

7.2 Ru(II) complexes as nano-catalytic system

In the sections above, results indicated that by combining ruthenium complexes and Au nanoparticles, the metallodrug could enter into living cells more easily and effectively. Au nanoparticles (AuNPs) provide non-toxic carriers for drug and gene delivery applications. In these systems, the gold core imparts stability to the assembly, while the monolayer allows tuning of surface properties, such as charge and hydrophobicity.²⁷⁹ The adaptable functionalization of both selective and specific recognition elements and environmentally responsive optoelectronic properties of AuNPs can be utilized to accomplish the transduction of the binding event with appropriate affinity and selectivity toward target analytes. Functionalized AuNPs may be both molecular receptor and signal transducer in a single sensing motif, thereby simplifying the sensor design while improving the sensitivity.²⁸² All of the characteristics are present in bioorthogonal catalysis. Utilizing the well known property of thiols to bind to gold nanoparticles, researcher could produce facile access to multivalent, functional systems anchored on support. In addition, this complex would be soluble, with limited mobility and conformational restraint, thereby being suitable to act cooperatively in a catalytic process.²⁸¹ Thus, various research groups have reported that Ru(II) form complexes with traditional gold nanoparticles, which are so-called nanozymes (see Fig. 31).

Recently, researchers have altered the surface of AuNPs with a variety of unnatural molecules such as sialic acids with azide groups, acylhydrazide, amine, or azide moieties.^{330,331} Supramolecules were also introduced onto gold nanoparticles to target different sites in cells and control the size of NPs.³³² The new *in vivo* targeting strategy of nanoparticles, based on bioorthogonal, copper-free click chemistry, greatly broadens nano applications.³³³ The catalytic efficiencies of ruthenium complex nanoparticles in solutions and in cells have been measured and compared by Rotello *et al.*³³⁴ This bioorthogonal catalysis can be used not only in therapeutic applications, but also in treating noncancerous, chronic diseases. The system introduces biomimetics into bioorthogonal chemistry, providing a new platform for imaging and therapeutic applications, as well as combining pharmacological treatments with human made synthetic tools.³³³

8. Conclusions and future perspectives

Ru(II) compounds have highly promising anticancer activity in *in vitro* and *in vivo* models. Compared to platinum(II) compounds, ruthenium can be coordinated at two additional axial sites and it tends to form octahedral compounds. In general, the ligand combination and coordination geometry between ruthenium and its ligands mainly determine the activity of ruthenium compounds, mostly in their reactivity, hydrophobicity, binding, cellular uptake and intracellular distribution. In this regard, several different Ru(II) compounds in this review have been reported to have high selectivity and targeting, ultimately improving efficiency in cancer cells and minimizing toxicity in normal cells. Further studies of ruthenium compounds should investigate structure-activity relationships (SARs) to determine how modifying different functional groups on the ligands affect the anticancer efficacy of the complexes. As expected, most of the ruthenium complexes are lipophilic and hold positive charge, which facilitates their diffusion across the cell membrane, which is

composed of negatively-charged and similarly lipophilic phospholipids. In addition, DNA, proteins and mitochondria often contain negative charges, allowing ruthenium complexes to selectively target these biomolecules or organelles and have significant efficacy. However, the ruthenium complexes must be non-toxic or relatively less toxic in normal tissue before use in patients. Simply modulating the ligands or increasing the lipophilicity and the charge of ruthenium complexes does not decrease their adverse effects, limiting their clinical application.

The introduction of PDT allows for the design of additional Ru(II) complexes with enhanced anticancer efficacy and higher selectivity. Ruthenium complexes have been proven to be effective photosensitizers for PDT due to the relatively long lifetimes of their excited states and efficient, low-energy visible-infrared light absorption. PDT has been shown to have high efficacy and minimal adverse effects, and has also been used to overcome resistance in tumor cells. Ru(II) complexes have long $^3\text{MLCT}$ -based, excited states, with a luminescent lifetime of 1.1 μs and ^3IL -based excited states, with remarkably long and tunable lifetimes (from 22 to 270 μs).³³⁵ These lifetimes is sufficient to produce ROS, which kill cancer cells upon light irradiation. Moreover, the use of O_2 -independent, Ru(II) complex photosensitizers may kill hypoxic tumors with enhanced cytotoxicity. Many Ru(II) complexes have efficient two-photon absorption in the NIR or IR region. These Ru(II) complexes were developed into the photosensitizers for two-photon absorption PDT, with less photodamage and a maximum tissue penetration depth. These Ru(II) complexes have the potential to be the next-generation photosensitizer compounds for PDT. Therefore, the characterization of Ru(II) complexes, with excellent physicochemical properties, remains urgent. In parallel with these advances in chemistry, improvement in the methods of irradiation should further improve the efficacy of Ru(II) complexes for PDT.

In this review, we discussed typical nanostructured Ru(II) complexes. The application of nanostructures improves the delivery and penetration of Ru(II) complexes,^{336,337} thus increasing the concentration in cells. For example, the combination of nanomedicine and Ru(II) complexes yields significant anticancer efficacy in drug resistant cancer cells as they are not substrates for MDR transporters. The encapsulation and delivery of Ru(II) complexes with nanomaterials may also improve certain pharmacological barriers relevant to drugs such as bioavailability, targeting ability, solubility, degradation and adverse effects. In addition, the Ru(II) complexes are designed to allow the nanomaterial systems to control the release of drugs and maintain efficacy within an acidic tumor environment. Despite the major benefits of the nano-functionalization of Ru(II) complexes in cancer therapy, nanomaterials also produce a certain level of toxicity in normal cells. The physical properties of nanomaterials affect the efficacy and toxicity of the nanomaterials. Therefore, further research should investigate the structure-activity relationship in nanostructured Ru(II) complexes. Finally, new ideas and breakthroughs in nano-functionalized complexes are expected to produce safer and more efficacious anticancer drugs.

Finally, we briefly discussed the role of Ru(II) complexes as bioorthogonal catalysts. With the formation and especially lysis of chemical bond, Ru(II) complexes accelerate biochemical reactions in living systems without interfering with normal physiological processes. The metallo-drugs could directly function at the specific groups, and also be

delivered to cellular targets in encapsulated nanoparticles. With the development of protein engineering, it is essential that we integrate more transitional metal-based biological catalysts with natural biomolecules. By combining fluorescence with Ru complex moieties, we hypothesize that we can realize a real-time tracking of catalysts in cells, which would greatly improve our understanding of biological processes.

The complete mechanisms of action of the Ru(II) complexes are diverse and still poorly understood. However, this review delineates a number of different mechanisms where Ru(II) complexes have efficacy in certain cancers, with the ultimate goal of obtaining clinically acceptable candidates in the near future. We also believe that the design of metallo-drugs based on nanomaterials have potential as anticancer treatments.³³⁸ Also, we anticipate that metallodrugs will foster interdisciplinary research among organometallics, oncology, photochemistry, biology and nanomedicine.

Acknowledgments

We thank Dr. Charles R. Ashby, Jr. (St. John's University, New York) for reviewing and editing the article. We thank Juanjuan Huang (Sun Yat-Sen University), for making the graphic image. We thank the support from Department of Pharmaceutical Sciences, College of Pharmacy and Health Sciences, St. John's University and International Program for Ph.D. Candidates, Sun Yat-Sen University. This work was also supported by National Institute of Health-USA (Nos. 1R15CA143701 and 1R15GM116043-01), the National Science Foundation of China (Nos. 21471164 and 21525105), the 973 program (Nos. 2014CB845604 and 2015CB856301), and the Fundamental Research Funds for the Central Universities.

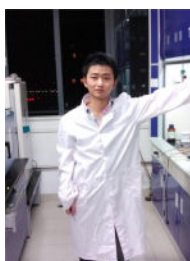
Biographies



Enju Wang received her PhD degree from ETH-Zurich in 1989 under the guidance of the later Prof. Simon in Analytical Chemistry. She joined Kagoshima University as a Research associate before her Post-doctoral research in the University of Michigan with Dr. Meyerhoff in 1992. She then joined the faculty at St. John's University in 1993 as an assistant professor and became full professor in 2005. She is the author of over 30 peer reviewed publications and 3 book chapters. Her current research interest is focused on developing Os/Ru-complex based optical sensors for Heparin and DNA polyanion sensing and detection.



Hui Chao received his PhD degree from Sun Yat-Sen University in 2000 under the guidance of Prof. Liangnian Ji. Subsequently, he joined the faculty at Sun Yat-Sen University. During 2000-2003, he attended Hong Kong University of Science and Technology every year as a short-term visiting scholar. In 2004-2005, he conducted postdoctoral work with Prof. F. A. Cotton at Texas A&M University. He was promoted to full professor in Sun Yat-Sen University in 2007. He is the author of over 180 peer reviewed publications and 4 book chapters. His current research interest is focused on metal-based anticancer complexes and bioimaging agents.



Leli Zeng received his MS degree in 2013 at XiangTan University and he worked under the supervision of Prof. Hui Chao from 2013 to 2017 at Sun Yat-Sen University, where he received his PhD degree in June, 2017. During 2016-2017, he had a one-year's study on the multidrug resistance under the guidance of Prof. Zhe-Sheng Chen at St. John's University. His primary work is focused on the design of ruthenium-based cancer drugs and nanodrugs, as well as the study of drug resistance.



Liangnian Ji was elected as a member of the Chinese Academy of Sciences in 2003. Prof. Ji is actively involved in bioinorganic chemistry research. He has designed and synthesized over 600 new coordination compounds. The results have been published in over 700 research papers, 3 monographs and 15 Chinese invention patents. Prof. Ji has been invited to be an organizing committee or advisory committee member in more than 10 international

conferences or symposia on bioinorganic chemistry. He is also on the editorial board or an advisory member for 8 international or national chemical journals.



Pranav Gupta received his Bachelor's degree in Pharmacy from Gurukul University and Master's degree in Pharmacology from St. John's University. He has worked as a graduate student researcher at St. Johns' University and has been a STEM mentor with the New York Academy of Sciences. He has published original research articles and invited reviews and book chapters in peer reviewed journals. Most recently, he is working on developing novel inhibitors to overcome chemotherapeutic multidrug resistance under Dr. Zhe-Sheng Chen.



Yanglu Chen graduated from Princeton University in 2017 with a Bachelor's degree in Chemistry. She has also conducted research at Fox Chase Cancer Center, St. John's University, the National Institutes of Health, University of Melbourne, and Rockefeller University, with interests ranging from immunology to genomics to nanomedicine. Most recently, she uses ultrafast spectroscopy to study photo-induced nanotheranostics under Professor Gregory Scholes.



Zhe-Sheng Chen received MS (Sun-Yat-Sen-University), PhD (Kagoshima-University). He had postdoctoral training at Fox-Chase-Cancer-Center. He joined St. John's University in 2004 as an assistant professor. He is a full professor and director of Institute for Biotechnology. He is an editor-in-chief of Journal of Cancer Research Updates, and New Developments on Chemistry, an editor of African Journal of Pharmacy and Pharmacology, an editorial board member of 26 journals and a reviewer of ~190 journals. He is an Ad-hoc

reviewer of grants including NIH, New Zealand, Poland, China, Hungary, Netherlands and Canada etc. He established research projects to study ABC transporters and MDR.

References

1. Shi G, Monro S, Hennigar R, Colpitts J, Fong J, Kasimova K, Yin H, DeCoste R, Spencer C, Chamberlain L. *Coord Chem Rev.* 2015; 282:127–138.
2. Garbutcheon-Singh KB, Grant MP, Harper BW, Krause-Heuer AM, Manohar M, Orkey N, Aldrich-Wright JR. *Curr Top Med Chem.* 2011; 11:521–542. [PubMed: 21189131]
3. Tao Y, Li M, Ren J, Qu X. *Chem Soc Rev.* 2015; 44:8636–8663. [PubMed: 26400655]
4. Li F, Collins JG, Keene FR. *Chem Soc Rev.* 2015; 44:2529–2542. [PubMed: 25724019]
5. Muhammad N, Guo Z. *Curr Opin Chem Biol.* 2014; 19:144–153. [PubMed: 24608084]
6. Johnstone TC, Suntharalingam K, Lippard SJ. *Chemi Rev.* 2016; 116:3436–3486.
7. Liu Z, Sadler PJ. *Acc Chem Res.* 2014; 47:1174–1185. [PubMed: 24555658]
8. Jamieson ER, Lippard SJ. *Chem Rev.* 1999; 99:2467–2498. [PubMed: 11749487]
9. Chu G. *J Biol Chem.* 1994; 269:787–790. [PubMed: 8288625]
10. Cepeda V, Fuertes MA, Castilla J, Alonso C, Quevedo C, Pérez JM. *Anti-Cancer Agents Med Chem.* 2007; 7:3–18.
11. Sledge G, Loehrer PJ, Roth BJ, Einhorn LH. *J Clin Oncol.* 1988; 6:1811–1814. [PubMed: 3199166]
12. Arany I, Safirstein RL. *Semin Nephrol.* 2003; 23:460–464. [PubMed: 13680535]
13. Florea A-M, Büsselberg D. *Cancers.* 2011; 3:1351–1371. [PubMed: 24212665]
14. Galluzzi L, Senovilla L, Vitale I, Michels J, Martins I, Kepp O, Castedo M, Kroemer G. *Oncogene.* 2012; 31:1869–1883. [PubMed: 21892204]
15. Zheng YR, Suntharalingam K, Johnstone TC, Yoo H, Lin W, Brooks JG, Lippard SJ. *J Am Chem Soc.* 2014; 136:8790–8798. [PubMed: 24902769]
16. Suntharalingam K, Song Y, Lippard SJ. *Chem Commun.* 2014; 50:2465–2468.
17. Graf N, Bielenberg DR, Kolishetti N, Muus C, Banyard J, Farokhzad OC, Lippard SJ. *ACS nano.* 2012; 6:4530–4539. [PubMed: 22584163]
18. Dhar S, Gu FX, Langer R, Farokhzad OC, Lippard SJ. *Proc Natl Acad Sci.* 2008; 105:17356–17361. [PubMed: 18978032]
19. Dhar S, Liu Z, Thomale J, Dai H, Lippard SJ. *J Am Chem Soc.* 2008; 130:11467–11476. [PubMed: 18661990]
20. Liang XJ, Meng H, Wang Y, He H, Meng J, Lu J, Wang PC, Zhao Y, Gao X, Sun B. *Proc Natl Acad Sci.* 2010; 107:7449–7454. [PubMed: 20368438]
21. Fong TTH, Lok CN, Chung CYS, Fung YME, Chow PK, Wan PK, Che CM. *Angew Chem, Int Ed.* 2016; 55:11935–11939.
22. Cao ZT, Chen ZY, Sun CY, Li HJ, Wang HX, Cheng QQ, Zuo ZQ, Wang JL, Liu YZ, Wang YC, Wang J. *Biomaterials.* 2016; 94:9–19. [PubMed: 27088406]
23. Abid M, Shamsi F, Azam A. *Mini-Rev Med Chem.* 2016; 16:772–786. [PubMed: 26423699]
24. Schmid WF, John RO, Arion VB, Jakupec MA, Keppler BK. *Organometallics.* 2007; 26:6643–6652.
25. Hearn JM, Romero-Canelón I, Qamar B, Liu Z, Hands-Portman I, Sadler PJ. *ACS Chem Biol.* 2013; 8:1335–1343. [PubMed: 23618382]
26. Romero-Canelón I, Salassa L, Sadler PJ. *J Med Chem.* 2013; 56:1291–1300. [PubMed: 23368735]
27. Zhu Z, Wang X, Li T, Aime S, Sadler PJ, Guo Z. *Angew Chem, Int Ed.* 2014; 53:13225–13228.
28. Liu Z, Romero-Canelón I, Qamar B, Hearn JM, Habtemariam A, Barry NPE, Pizarro AM, Clarkson GJ, Sadler PJ. *Angew Chem, Int Ed.* 2014; 53:3941–3946.
29. Ye RR, Tan CP, He L, Chen MH, Ji LN, Mao ZW. *Chem Commun.* 2014; 50:10945–10948.
30. Zhang CX, Lippard SJ. *Curr Opin Chem Biol.* 2003; 7:481–489. [PubMed: 12941423]
31. Kostova I. *Curr Med Chem.* 2006; 13:1085–1107. [PubMed: 16611086]

32. Smith GS, Therrien B. *Dalton Trans.* 2011; 40:10793–10800. [PubMed: 21858344]
33. Liu P, Jia J, Zhao Y, Wang K. *Mini-Rev Med Chem.* 2015; 16:272–289.
34. Furrer J, Süss-Fink G. *Coord Chem Rev.* 2016; 309:36–50.
35. Levina A, Mitra A, Lay PA. *Metallomics.* 2009; 1:458–470. [PubMed: 21305154]
36. Hartinger CG, Jakupec MA, Zorbas-Seifried S, Groessl M, Egger A, Berger W, Zorbas H, Dyson PJ, Keppler BK. *Chem Biodiversity.* 2008; 5:2140–2155.
37. Duan L, Fischer A, Xu Y, Sun L. *J Am Chem Soc.* 2009; 131:10397–10399. [PubMed: 19601625]
38. Abid M, Shamsi F, Azam A. *Mini-Rev Med Chem.* 2016; 10:772–786.
39. Dragutan I, Dragutan V, Démonceau A. *Molecules.* 2015; 20:17244–17274. [PubMed: 26393560]
40. Hartinger CG, Groessl M, Meier SM, Casini A, Dyson PJ. *Chemical Society Reviews.* 2013; 42:6186–6199. [PubMed: 23660626]
41. Antonarakis ES, Emadi A. *Cancer Chemother Pharmacol.* 2010; 66:1–9. [PubMed: 20213076]
42. Minchinton AI, Tannock IF. *Nat Rev Cancer.* 2006; 6:583–592. [PubMed: 16862189]
43. Bergamo A, Zorzet S, Gava B, Sorc A, Alessio E, Iengo E, Sava G. *Anti-cancer drugs.* 2000; 11:665–672. [PubMed: 11081461]
44. Jones SL. *Arch Psychiat Nurs.* 1999; 13:1–2.
45. Sava G, Gagliardi R, Cocchietto M, Clerici K, Capozzi I, Marrella M, Alessio E, Mestroni G, Milanino R. *Pathol, Oncol Res.* 1998; 4:30–36. [PubMed: 9555118]
46. Bacac M, Vadori M, Sava G, Pacor S. *Cancer Immunol, Immun.* 2004; 53:1101–1110.
47. Bergamo A, Gava B, Alessio E, Mestroni G, Serli B, Cocchietto M, Zorzet S, Sava G. *Int J Oncol.* 2002; 21:1331–1338. [PubMed: 12429985]
48. Debidda M, Sanna B, Cossu A, Posadino AM, Tadolini B, Ventura C, Pintus G. *Int J Oncol.* 2003; 23:477–482. [PubMed: 12851698]
49. Pacor S, Zorzet S, Cocchietto M, Bacac M, Vadori M, Turrin C, Gava B, Castellarin A, Sava G. *J, Pharmacol Exp Ther.* 2004; 310:737–744. [PubMed: 15075381]
50. Chen J, Chen L, Liao S, Zheng K, Ji L. *J, phys, chem, B.* 2007; 111:7862–7869. [PubMed: 17579393]
51. Bacac M, Hotze AC, van der Schilden K, Haasnoot JG, Pacor S, Alessio E, Sava G, Reedijk J. *J Inorg Biochem.* 2004; 98:402–412. [PubMed: 14729322]
52. Rademaker-Lakhai JM, van den Bongard D, Pluim D, Beijnen JH, Schellens JH. *Clin Cancer res.* 2004; 10:3717–3727. [PubMed: 15173078]
53. Alessio E. *Eur J Inorg Chem.* 2017; 2017:1549–1560.
54. Hartinger CG, Zorbas-Seifried S, Jakupec MA, Kynast B, Zorbas H, Keppler BK. *J Inorg Biochem.* 2006; 100:891–904. [PubMed: 16603249]
55. Hartinger CG, Jakupec MA, Zorbas-Seifried S, Groessl M, Egger A, Berger W, Zorbas H, Dyson PJ, Keppler BK. *Chem Biodiversity.* 2008; 5:2140–2155.
56. Bytzek AK, Koellensperger G, Keppler BK, Hartinger CG. *J Inorg Biochem.* 2016; 160:250–255. [PubMed: 26993078]
57. Wang F, Habtemariam A, van der Geer EPL, Fernández R, Melchart M, Deeth RJ, Aird R, Guichard S, Fabbiani FPA, Lozano-Casal P, Oswald IDH, Jodrell DI, Parsons S, Sadler PJ. *Proc Natl Acad Sci.* 2005; 102:18269–18274. [PubMed: 16352726]
58. Morris RE, Aird RE, del Socorro Murdoch P, Chen H, Cummings J, Hughes ND, Parsons S, Parkin A, Boyd G, Jodrell DI. *J Med Chem.* 2001; 44:3616–3621. [PubMed: 11606126]
59. Rodrigues FP, Carneiro ZA, Mascharak P, Curti C, da Silva RS. *Coord Chem Rev.* 2016; 306:701–707.
60. Kwong WL, Lam KY, Lok CN, Lai YT, Lee PY, Che CM. *Angew Chem.* 2016; 128:13722–13726.
61. Montani M, Pazmay GVB, Hysi A, Lupidi G, Pettinari R, Gambini V, Tilio M, Marchetti F, Pettinari C, Ferraro S. *Pharmacol Res.* 2016; 107:282–290. [PubMed: 27038531]
62. Fan W, Huang P, Chen X. *Chem Soc Rev.* 2016; 45:6488–6519. [PubMed: 27722560]
63. Mari C, Pierroz V, Ferrari S, Gasser G. *Chem Sci.* 2015; 6:2660–2686.
64. Dickerson M, Howerton B, Bae Y, Glazer EC. *J Mater Chem B.* 2016; 4:394–408.

65. Glazer EC. *Isr J Chem.* 2013; 53:391–400.
66. Shen Y, Shuhendler AJ, Ye D, Xu JJ, Chen HY. *Chem Soc Rev.* 2016; 45:6725–6741. [PubMed: 27711672]
67. Vajpayee V, Yang YJ, Kang SC, Kim H, Kim IS, Wang M, Stang PJ, Chi KW. *Chem Commun.* 2011; 47:5184–5186.
68. Chen Y, Guan R, Zhang C, Huang J, Ji L, Chao H. *Coord Chem Rev.* 2016; 310:16–40.
69. Barry NPE, Sadler PJ. *ACS nano.* 2013; 7:5654–5659. [PubMed: 23837396]
70. <http://theralase.com/pressrelease/health-canada-approvesclinical-trial-application-anti-cancer-drug/>.
71. Gill MR, Thomas JA. *Chem Soc Rev.* 2012; 41:3179–3192. [PubMed: 22314926]
72. Zhou Y, Yu Q, Qin X, Bhavsar D, Yang L, Chen Q, Zheng W, Chen L, Liu J. *ACS Appl Mater Interfaces.* 2016; 8:15000–15012. [PubMed: 26018505]
73. Liang R, Wei M, Evans DG, Duan X. *Chem Commun.* 2014; 50:14071–14081.
74. Puckett CA, Barton JK. *J Am Chem Soc.* 2007; 129:46–47. [PubMed: 17199281]
75. Puckett CA, Ernst RJ, Barton JK. *Dalton Trans.* 2010; 39:1159–1170. 65. [PubMed: 20104335]
76. Komor AC, Barton JK. *Chem Commun.* 2013; 49:3617–3630.
77. Puckett CA, Barton JK. *J Am Chem Soc.* 2009; 131:8738–8739. [PubMed: 19505141]
78. Puckett CA, Barton JK. *Bioorg Med Chem.* 2010; 18:3564–3569. [PubMed: 20430627]
79. Tan C, Lai S, Wu S, Hu S, Zhou L, Chen Y, Wang M, Zhu Y, Lian W, Peng W. *J Med Chem.* 2010; 53:7613–7624. [PubMed: 20958054]
80. Huang H, Zhang P, Yu B, Chen Y, Wang J, Ji L, Chao H. *J Med Chem.* 2014; 57:8971–8983. [PubMed: 25313823]
81. Groessl M, Zava O, Dyson PJ. *Metallomics.* 2011; 3:591–599. [PubMed: 21399784]
82. Green DR, Reed JC. *Science.* 1998; 281:1309. [PubMed: 9721092]
83. Hoye AT, Davoren JE, Wipf P, Fink MP, Kagan VE. *Acc Chem Res.* 2008; 41:87–97. [PubMed: 18193822]
84. Yousif LF, Stewart KM, Kelley SO. *Chembiochem.* 2009; 10:1939–1950. [PubMed: 19637148]
85. Bhat TA, Kumar S, Chaudhary AK, Yadav N, Chandra D. *Drug Discov Today.* 2015; 20:635–643. [PubMed: 25766095]
86. Pierroz V, Joshi T, Leonidova A, Mari C, Schur J, Ott I, Spiccia L, Ferrari S, Gasser G. *J Am Chem Soc.* 2012; 134:20376–20387. [PubMed: 23181418]
87. Joshi T, Pierroz V, Mari C, Gemperle L, Ferrari S, Gasser G. *Angew Chem, Int Ed.* 2014; 53:2960–2963.
88. Dickerson M, Sun Y, Howerton B, Glazer EC. *Inorg Chem.* 2014; 53:10370–10377. [PubMed: 25249443]
89. Qian C, Wang JQ, Song CL, Wang LL, Ji LN, Chao H. *Metallomics.* 2013; 5:844–854. [PubMed: 23483103]
90. Wang JQ, Zhang PY, Qian C, Hou XJ, Ji LN, Chao H. *J Biol Inorg Chem.* 2014; 19:335–348. [PubMed: 24287874]
91. Liu J, Chen Y, Li G, Zhang P, Jin C, Zeng L, Ji L, Chao H. *Biomaterials.* 2015; 56:140–153. [PubMed: 25934287]
92. Luzio JP, Pryor PR, Bright NA. *Nat Rev Mol Cell Biol.* 2007; 8:622–632. [PubMed: 17637737]
93. Cho K, Wang X, Nie S, Shin DM. *Clin Cancer Res.* 2008; 14:1310–1316. [PubMed: 18316549]
94. He L, Tan CP, Ye RR, Zhao YZ, Liu YH, Zhao Q, Ji LN, Mao ZW. *Angew Chem, Int Ed.* 2014; 53:12137–12141.
95. He L, Li Y, Tan CP, Ye RR, Chen MH, Cao JJ, Ji LN, Mao ZW. *Chem Sci.* 2015; 6:5409–5418.
96. Qiu K, Liu Y, Huang H, Liu C, Zhu H, Chen Y, Ji L, Chao H. *Dalton Trans.* 2016; 45:16144–16147. [PubMed: 27722346]
97. Qiu K, Huang H, Liu B, Liu Y, Huang Z, Chen Y, Ji LN, Chao H. *ACS Appl Mater Interfaces.* 2016; 8:12702. [PubMed: 27152695]

98. Huang H, Yu B, Zhang P, Huang J, Chen Y, Gasser G, Ji L, Chao H. *Angew Chem*. 2015; 127:14255–14258.
99. Kroemer G, Jäätelä M. *Nat Rev Cancer*. 2005; 5:886–897. [PubMed: 16239905]
100. Casini A, Mastrobuoni G, Ang WH, Gabbiani C, Pieraccini G, Moneti G, Dyson PJ, Messori L. *Chemmedchem*. 2007; 2:631–635. [PubMed: 17366652]
101. Zhao R, Hammitt R, Thummel RP, Liu Y, Turro C, Snapka RM. *Dalton Trans*. 2009:10926–10931. [PubMed: 20023923]
102. Zeng L, Xiao Y, Liu J, Tan L. *J Mol Struct*. 2012; 1019:183–190.
103. Aird RE, Cummings J, Ritchie AA, Muir M, Morris RE, Chen H, Sadler PJ, Jodrell DI. *Br J Cancer*. 2002; 86:1652–1657. [PubMed: 12085218]
104. Pascu GI, Hotze AC, Sanchez-Cano C, Kariuki BM, Hannon MJ. *Angew Chem*. 2007; 119:4452–4456.
105. Wu K, Hu W, Luo Q, Li X, Xiong S, Sadler PJ, Wang F. *J Am Soc Mass Spectrom*. 2013; 24:410–420. [PubMed: 23404464]
106. Chen H, Parkinson JA, Morris RE, Sadler PJ. *J Am Chem Soc*. 2003; 125:173–186. [PubMed: 12515520]
107. Turro C. *Proc Natl Acad Sci*. 2011; 108:17573–17574. [PubMed: 21997210]
108. Friedman AE, Chambron JC, Sauvage JP, Turro NJ, Barton JK. *J Am Chem Soc*. 1990; 112:4960–4962.
109. Gill MR, Harun SN, Halder S, Boghoozian RA, Ramadan K, Ahmad H, Vallis KA. *Sci Rep*. 2016; 6:31973. [PubMed: 27558808]
110. Önfelt B, Göstring L, Lincoln P, Nordén B, Önfelt A. *Mutagenesis*. 2002; 17:317–320. [PubMed: 12110628]
111. Gill MR, Garcia-Lara J, Foster SJ, Smythe C, Battaglia G, Thomas JA. *Nat Chem*. 2009; 1:662–667. [PubMed: 21378959]
112. Baggaley E, Gill MR, Green NH, Turton D, Sazanovich IV, Botchway SW, Smythe C, Haycock JW, Weinstein JA, Thomas JA. *Angew Chem*. 2014; 126:3435–3439.
113. Zhang L, Carroll P, Meggers E. *Org Lett*. 2004; 6:521–523. [PubMed: 14961613]
114. Meggers E. *Chem Commun*. 2009:1001–1010.
115. Aman F, Hanif M, Kubanik M, Ashraf A, Soehnel T, Jamieson S, Siddiqui W, Hartinger C. *Chem – Eur J*. 2017; 23:4893–4902. [PubMed: 28198061]
116. Babak MV, Meier SM, Huber KVM, Reynisson J, Legin AA, Jakupec MA, Roller A, Stukalov A, Gridling M, Bennett KL, Colinge J, Berger W, Dyson PJ, Superti-Furga G, Keppler BK, Hartinger CG. *Chem Sci*. 2015; 6:2449–2456.
117. Kilpin KJ, Dyson PJ. *Chem Sci*. 2013; 4:1410–1419.
118. Blanck S, Maksimoska J, Baumeister J, Harms K, Marmorstein R, Meggers E. *Angew Chem, Int Ed*. 2012; 51:5244–5246.
119. Meggers E. *Curr Opin Chem Biol*. 2007; 11:287–292. [PubMed: 17548234]
120. Dwyer FP, Gyrfas EC, Rogers WP, Koch JH. *Nature*. 1952; 170:190. [PubMed: 12982853]
121. Tamaoki T, Nomoto H, Takahashi I, Kato Y, Morimoto M, Tomita F. *Biochem Biophys Res Commun*. 1986; 135:397–402. [PubMed: 3457562]
122. Rüegg UT, Gillian B. *Trends Pharmacol Sci*. 1989; 10:218–220. [PubMed: 2672462]
123. Bregman H, Carroll PJ, Meggers E. *J Am Chem Soc*. 2006; 128:877–884. [PubMed: 16417378]
124. Feng L, Geisselbrecht Y, Blanck S, Wilbuer A, Atilla-Gokcumen GE, Filippakopoulos P, Kräling K, Celik MA, Harms K, Maksimoska J. *J Am Chem Soc*. 2011; 133:5976–5986. [PubMed: 21446733]
125. Bregman H, Meggers E. *Org Lett*. 2006; 8:5465–5468. [PubMed: 17107048]
126. Meggers E, Atilla-Gokcumen GE, Gruendler K, Frias C, Prokop A. *Dalton Trans*. 2009:10882–10888. [PubMed: 20023918]
127. Pagano N, Wong EY, Breiding T, Liu H, Wilbuer A, Bregman H, Shen Q, Diamond SL, Meggers E. *J Org Chem*. 2009; 74:8997–9009. [PubMed: 19886617]

128. Qin J, Rajaratnam R, Feng L, Salami J, Barber-Rotenberg JS, Domsic J, Reyes-Urbe P, Liu H, Dang W, Berger SL, Villanueva J, Meggers E, Marmorstein R. *J Med Chem.* 2015; 58:305–314. [PubMed: 25356520]
129. Vock CA, Ang WH, Scolaro C, Phillips AD, Lagopoulos L, Juillerat-Jeanneret L, Sava G, Scopelliti R, Dyson PJ. *J Med Chem.* 2007; 50:2166–2175. [PubMed: 17419606]
130. Ang WH, De Luca A, Chapuis-Bernasconi C, Juillerat-Jeanneret L, LoBello M, Dyson PJ. *Chemmedchem.* 2007; 2:1799–1806. [PubMed: 17918761]
131. Respondek T, Garner RN, Herroon MK, Podgorski I, Turro C, Kodanko JJ. *J Am Chem Soc.* 2011; 133:17164–17167. [PubMed: 21973207]
132. Tan CP, Lu YY, Ji LN, Mao ZW. *Metallomics.* 2014; 6:978–995. [PubMed: 24668273]
133. Kangdi Z, Qiong W, Chengxi W, Weijun T, Wenjie M. *Anti-Cancer Agent.* 2017; 17:29–39.
134. Cao W, Zheng W, Chen T. *Sci Rep.* 2015; 5:9157. [PubMed: 25778692]
135. Liu Y, Chen T, Liu J, Wong YS. *Medchemcomm.* 2013; 4:865–869.
136. Chen L, Li G, Peng F, Jie X, Dongye G, Cai K, Feng R, Li B, Zeng Q, Lun K, Chen J, Xu B. *Oncotarget.* 2016; 7:80716–80734. [PubMed: 27811372]
137. Majno G, Joris I. *Am J Pathol.* 1995; 146:3–15. [PubMed: 7856735]
138. Castonguay A, Doucet C, Juhas M, Maysinger D. *J Med Chem.* 2012; 55:8799–8806. [PubMed: 22991922]
139. Yuan J, Lei Z, Wang X, Zhu F, Chen D. *Metallomics.* 2015; 7:896–907. [PubMed: 25811406]
140. Mühlgassner G, Bartel C, Schmid WF, Jakupec MA, Arion VB, Keppler BK. *J Inorg Biochem.* 2012; 116:180–187. [PubMed: 23037896]
141. Suss-Fink G. *Dalton Trans.* 2010; 39:1673–1688. [PubMed: 20449402]
142. Murray BS, Babak MV, Hartinger CG, Dyson PJ. *Coord Chem Rev.* 2016; 306:86–114. Part 1.
143. Dougan SJ, Sadler PJ. *Chimia.* 2007; 61:704–715.
144. Wang F, Chen H, Parsons S, Oswald ID, Davidson JE, Sadler PJ. *Chem – Eur J.* 2003; 9:5810–5820. [PubMed: 14673852]
145. Romero-Canelon I, Pizarro AM, Habtemariam A, Sadler PJ. *Metallomics.* 2012; 4:1271–1279. [PubMed: 23138378]
146. Montani M, Pazmay GVB, Hysi A, Lupidi G, Pettinari R, Gambini V, Tilio M, Marchetti F, Pettinari C, Ferraro S, Iezzi M, Marchini C, Amici A. *Pharm Res.* 2016; 107:282–290.
147. Chow MJ, Licon C, Yuan Qiang Wong D, Pastorin G, Gaiddon C, Ang WH. *J Med Chem.* 2014; 57:6043–6059. [PubMed: 25023617]
148. Chow MJ, Licon C, Pastorin G, Mellitzer G, Ang WH, Gaiddon C. *Chem Sci.* 2016; 7:4117–4124.
149. Chow MJ, Babak MV, Wong DYQ, Pastorin G, Gaiddon C, Ang WH. *Mol Pharm.* 2016; 13:2543–2554. [PubMed: 27174050]
150. Grozav A, Balacescu O, Balacescu L, Cheminel T, Berindan-Neagoe I, Therrien B. *J Med Chem.* 2015; 58:8475–8490. [PubMed: 26488797]
151. Betanzos-Lara S, Salassa L, Habtemariam A, Sadler PJ. *Chem Commun.* 2009:6622–6624.
152. Betanzos-Lara S, Salassa L, Habtemariam A, Novakova O, Pizarro AM, Clarkson GJ, Liskova B, Brabec V, Sadler PJ. *Organometallics.* 2012; 31:3466–3479.
153. Wang T, Zhou Q, Zhang Y, Zheng Y, Wang W, Hou Y, Jiang G, Cheng X, Wang X. *RSC Adv.* 2016; 6:45652–45659.
154. Chen Y, Lei W, Hou Y, Li C, Jiang G, Zhang B, Zhou Q, Wang X. *Dalton Trans.* 2015; 44:7347–7354. [PubMed: 25797273]
155. Motswainyana WM, Ajibade PA. *Adv Chem.* 2015; 2015:859730.
156. Chelopo MP, Pawar SA, Sokhela MK, Govender T, Kruger HG, Maguire GE. *Eur J Med Chem.* 2013; 66:407–414. [PubMed: 23827181]
157. Habtemariam A, Melchart M, Fernández R, Parsons S, Oswald ID, Parkin A, Fabbiani FP, Davidson JE, Dawson A, Aird RE. *J Med Chem.* 2006; 49:6858–6868. [PubMed: 17154516]

158. Malgorzata Friks AM, Elie Benelita T, Gonzalo Oscar, Ramírez de Mingo Daniel, Sanaú Mercedes, Sánchez-Delgado roberto, Sadhukha Tanmoy, Prabha Swayam, Ramos Joe W, Marzo Isabel, Contel María. *J Med Chem.* 2014; 57:9995–10012. [PubMed: 25409416]
159. Lord RM, Hebden AJ, Pask CM, Henderson IR, Allison SJ, Shepherd SL, Phillips RM, McGowan PC. *J Med Chem.* 2015; 58:4940–4953. [PubMed: 25906293]
160. Clavel CM, Paunescu E, Nowak-Sliwinska P, Griffioen AW, Scopelliti R, Dyson PJ. *J Med Chem.* 2015; 58:3356–3365. [PubMed: 25812075]
161. Seršen S, Kljun J, Kryeziu K, Panchuk R, Alte B, Körner W, Heffeter P, Berger W, Turel I. *J Med Chem.* 2015; 58:3984–3996. [PubMed: 25856666]
162. Pettinari R, Pettinari C, Marchetti F, Skelton BW, White AH, Bonfili L, Cucciaroni M, Mozzicafreddo M, Cecarini V, Angeletti M, Nabissi M, Eleuteri AM. *J Med Chem.* 2014; 57:4532–4542. [PubMed: 24793593]
163. Yellol GS, Donaire A, Yellol JG, Vasylyeva V, Janiak C, Ruiz J. *Chem Commun.* 2013; 49:11533–11535.
164. Yellol J, Pérez SA, Buceta A, Yellol G, Donaire A, Szumlas P, Bednarski PJ, Makhoulfi G, Janiak C, Espinosa A. *J Med Chem.* 2015; 58:7310–7327. [PubMed: 26313136]
165. Bratsos, I., Gianferrara, T., Alessio, E., Hartinger, CG., Jakupc, MA., Keppler, BK. *Bioinorganic Medicinal Chemistry.* Alessio, E., editor. Wiley-VCH; Weinheim: 2011. p. 151-174.
166. Scolaro C, Bergamo A, Brescacin L, Delfino R, Cocchietto M, Laurenczy G, Geldbach TJ, Sava G, Dyson PJ. *J Med Chem.* 2005; 48:4161–4171. [PubMed: 15943488]
167. Bergamo A, Masi A, Dyson PJ, Sava G. *Int J Oncol.* 2008; 33:1281. [PubMed: 19020762]
168. Weiss A, Berndsen RH, Dubois M, Muller C, Schibli R, Griffioen AW, Dyson PJ, Nowak-Sliwinska P. *Chem Sci.* 2014; 5:4742–4748.
169. Pettinari R, Marchetti F, Condello F, Pettinari C, Lupidi G, Scopelliti R, Mukhopadhyay S, Riedel T, Dyson PJ. *Organometallics.* 2014; 33:3709–3715.
170. Allardice CS, Dyson PJ, Ellis DJ, Heath SL. *Chem Commun.* 2001:1396–1397.
171. Adhireksan Z, Davey GE, Campomanes P, Groessl M, Clavel CM, Yu H, Nazarov AA, Yeo CHF, Ang WH, Dröge P, Rothlisberger U, Dyson PJ, Davey CA. *Nat Commun.* 2014; 5:3462. [PubMed: 24637564]
172. Adhireksan Z, Palermo G, Riedel T, Ma Z, Muhammad R, Rothlisberger U, Dyson PJ, Davey CA. *Nat Commun.* 2017; 8:14860. [PubMed: 28358030]
173. Casini A, Gabbiani C, Sorrentino F, Rigobello MP, Bindoli A, Geldbach TJ, Marrone A, Re N, Hartinger CG, Dyson PJ. *J Med Chem.* 2008; 51:6773–6781. [PubMed: 18834187]
174. Linares F, Galindo MA, Galli S, Romero MA, Navarro JA, Barea E. *Inorg Chem.* 2009; 48:7413–7420. [PubMed: 19586019]
175. Mishra A, Kang SC, Chi KW. *Eur J Inorg Chem.* 2013; 2013:5222–5232.
176. Singh AK, Pandey DS, Xu Q, Braunstein P. *Coord Chem Rev.* 2014; 270:31–56.
177. Mendoza-Ferri MG, Hartinger CG, Mendoza MA, Groessl M, Egger AE, Eichinger RE, Mangrum JB, Farrell NP, Maruszak M, Bednarski PJ. *J Med Chem.* 2009; 52:916–925. [PubMed: 19170599]
178. Mendoza-Ferri MG, Hartinger CG, Eichinger RE, Stolyarova N, Severin K, Jakupc MA, Nazarov AA, Keppler BK. *Organometallics.* 2008; 27:2405–2407.
179. Nováková O, Nazarov AA, Hartinger CG, Keppler BK, Brabec V. *Biochem Pharmacol.* 2009; 77:364–374. [PubMed: 19014908]
180. Gras M, Therrien B, Süß-Fink G, Zava O, Dyson PJ. *Dalton Trans.* 2010; 39:10305–10313. [PubMed: 20890536]
181. Therrien B. *CrystEngComm.* 2015; 17:484–491.
182. Schmitt, Fdr, Freudenreich, J., Barry, NP., Juillerat-Jeanneret, L., Süß-Fink, G., Therrien, B. *J Am Chem Soc.* 2011; 134:754–757. [PubMed: 22185627]
183. Mattsson J, Govindaswamy P, Renfrew AK, Dyson PJ, Štěpnička P, Süß-Fink G, Therrien B. *Organometallics.* 2009; 28:4350–4357.
184. Therrien B. *Chem – Eur J.* 2013; 19:8378–8386. [PubMed: 23737435]

185. Therrien B, Süß-Fink G, Govindaswamy P, Renfrew AK, Dyson PJ. *Angew Chem.* 2008; 120:3833–3836.
186. Mattsson J, Zava O, Renfrew AK, Sei Y, Yamaguchi K, Dyson PJ, Therrien B. *Dalton Trans.* 2010; 39:8248–8255. [PubMed: 20689885]
187. Medlycott EA, Hanan GS. *Chem Soc Rev.* 2005; 34:133–142. [PubMed: 15672177]
188. Gill MR, Thomas JA. *Chem Soc Rev.* 2012; 41:3179–3192. [PubMed: 22314926]
189. Salassa L. *Eur J Inorg Chem.* 2011; 2011:4931–4947.
190. Li G, Sun L, Ji L, Chao H. *Dalton Trans.* 2016; 45:13261–13276. [PubMed: 27426487]
191. Dolmans DE, Fukumura D, Jain RK. *Nat Rev Cancer.* 2003; 3:380–387. [PubMed: 12724736]
192. Kilah NL, Meggers E. *Aust J Chem.* 2012; 65:1325–1332.
193. Tan C, Wu S, Lai S, Wang M, Chen Y, Zhou L, Zhu Y, Lian W, Peng W, Ji L. *Dalton Trans.* 2011; 40:8611–8621. [PubMed: 21804968]
194. Song H, Kaiser JT, Barton JK. *Nat chem.* 2012; 4:615–620. [PubMed: 22824892]
195. Zhu BZ, Chao XJ, Huang CH, Li Y. *Chem Sci.* 2016; 7:4016–4023.
196. Puckett CA, Barton JK. *Biochemistry.* 2008; 47:11711–11716. [PubMed: 18855428]
197. Gill MR, Cecchin D, Walker MG, Mulla RS, Battaglia G, Smythe C, Thomas JA. *Chem Sci.* 2013; 4:4512–4519. [PubMed: 25580209]
198. Zeng ZP, Wu Q, Sun FY, Zheng KD, Mei WJ. *Inorg Chem.* 2016; 55:5710–5718. [PubMed: 27191197]
199. Yu Q, Liu Y, Xu L, Zheng C, Le F, Qin X, Liu Y, Liu J. *Eur J Med Chem.* 2014; 82:82–95. [PubMed: 24878637]
200. Li L, Wong YS, Chen T, Fan C, Zheng W. *Dalton Trans.* 2012; 41:1138–1141. [PubMed: 22159211]
201. Chen T, Mei WJ, Wong YS, Liu J, Liu Y, Xie HS, Zheng WJ. *Medchemcomm.* 2010; 1:73–75.
202. Zhao Z, Luo Z, Wu Q, Zheng W, Feng Y, Chen T. *Dalton Trans.* 2014; 43:17017–17028. [PubMed: 25087850]
203. Du Y, Fu X, Li H, Chen B, Guo Y, Su G, Zhang H, Ning F, Lin Y, Mei W, Chen T. *ChemMedChem.* 2014; 9:714–718. [PubMed: 24403015]
204. Chen T, Liu Y, Zheng WJ, Liu J, Wong YS. *Inorg Chem.* 2010; 49:6366–6368. [PubMed: 20527894]
205. Deng Z, Gao P, Yu L, Ma B, You Y, Chan L, Mei C, Chen T. *Biomaterials.* 2017; 129:111–126. [PubMed: 28340357]
206. Cardoso CR, Lima MVS, Cheleski J, Peterson EJ, Venâncio T, Farrell NP, Carlos RM. *J Med Chem.* 2014; 57:4906–4915. [PubMed: 24831959]
207. Griffith C, Dayoub AS, Jaranatne T, Alatrash N, Mohamedi A, Abayan K, Breitbach ZS, Armstrong DW, MacDonnell FM. *Chem Sci.* 2017; doi: 10.1039/C6SC04094B
208. Wang YC, Qian C, Peng ZL, Hou XJ, Wang LL, Chao H, Ji LN. *J Inorg Biochem.* 2014; 130:15–27. [PubMed: 24145066]
209. Kou JF, Qian C, Wang JQ, Chen X, Wang LL, Chao H, Ji LN. *J Biol Inorg Chem.* 2012; 17:81–96. [PubMed: 21858685]
210. He X, Zeng L, Yang G, Xie L, Sun X, Tan L. *Inorg Chim Acta.* 2013; 408:9–17.
211. Shi S, Xu JH, Gao X, Huang HL, Yao TM. *Chem – Eur J.* 2015; 21:11435–11445. [PubMed: 26118412]
212. Zhang Z, Wu Q, Wu XH, Sun FY, Chen LM, Chen JC, Yang SL, Mei WJ. *Eur J Med Chem.* 2014; 80:316–324. [PubMed: 24793882]
213. Fan C, Wu Q, Chen T, Zhang Y, Zheng W, Wang Q, Mei W. *Medchemcomm.* 2014; 5:597–602.
214. Chen X, Wu JH, Lai YW, Zhao R, Chao H, Ji LN. *Dalton Trans.* 2013; 42:4386–4397. [PubMed: 23400220]
215. Liao G, Chen X, Wu J, Qian C, Wang Y, Ji L, Chao H. *Dalton Trans.* 2015; 44:15145–15156. [PubMed: 25604798]
216. Chen ZF, Qin QP, Qin JL, Zhou J, Li YL, Li N, Liu YC, Liang H. *J Med Chem.* 2015; 58:4771–4789. [PubMed: 25988535]

217. Ye RR, Ke ZF, Tan CP, He L, Ji LN, Mao ZW. *Chem – Eur J*. 2013; 19:10061–10061.
218. Luo Z, Yu L, Yang F, Zhao Z, Yu B, Lai H, Wong KH, Ngai SM, Zheng W, Chen T. *Metallomics*. 2014; 6:1480–1490. [PubMed: 24823440]
219. Ferstl W, Sakodinskaya IK, Beydoun-Sutter N, Le Borgne G, Pfeffer M, Ryabov AD. *Organometallics*. 1997; 16:411–418.
220. Dehand J, Pfeffer M. *Coord Chem Rev*. 1976; 18:327–352.
221. Sortais JB, Pannetier N, Holuigue A, Barloy L, Sirlin C, Pfeffer M, Kyritsakas N. *Organometallics*. 2007; 26:1856–1867.
222. Djukic JP, Sortais JB, Barloy L, Pfeffer M. *Eur J Inorg Chem*. 2009; 2009:817–853.
223. Gaiddon C, Jeannequin P, Bischoff P, Pfeffer M, Sirlin C, Loeffler JP. *J. P. E. T.* 2005; 315:1403–1411.
224. Meng X, Leyva ML, Jenny M, Gross I, Benosman S, Fricker B, Harlepp S, Hébraud P, Boos A, Wlosik P. *Cancer Res*. 2009; 69:5458–5466. [PubMed: 19549908]
225. Licona C, Spaety ME, Capuozzo A, Ali M, Santamaria R, Armant O, Delalande F, Dorselaer AV, Cianferani S, Spencer J, Pfeffer M, Mellitzer G, Gaiddon C. *Oncotarget*. 2017; 8:2568–2584. [PubMed: 27935863]
226. Boff B, Ali M, Alexandrova L, Espinosa-Jalapa NÁ, Saavedra-Díaz RO, Le Lagadec R, Pfeffer M. *Organometallics*. 2013; 32:5092–5097.
227. Leyva L, Sirlin C, Rubio L, Franco C, Le Lagadec R, Spencer J, Bischoff P, Gaiddon C, Loeffler JP, Pfeffer M. *Eur J Inorg Chem*. 2007; 2007:3055–3066.
228. Fetzter L, Boff B, Ali M, Meng X, Collin JP, Sirlin C, Gaiddon C, Pfeffer M. *Dalton Trans*. 2011; 40:8869–8878. [PubMed: 21837342]
229. Pena B, David A, Pavani C, Baptista MS, Pellois JP, Turro C, Dunbar KR. *Organometallics*. 2014; 33:1100–1103.
230. Albani BA, Pena B, Dunbar KR, Turro C. *Photochem Photobiol Sci*. 2014; 13:272–280. [PubMed: 24220236]
231. Huang H, Zhang P, Chen H, Ji L, Chao H. *Chem – Eur J*. 2015; 21:715–725. [PubMed: 25388328]
232. Zeng L, Chen Y, Huang H, Wang J, Zhao D, Ji L, Chao H. *Chem – Eur J*. 2015; 21:15308–15319. [PubMed: 26338207]
233. Zeng L, Chen Y, Liu J, Huang H, Guan R, Ji L, Chao H. *Sci Rep*. 2016; 6:19449. [PubMed: 26763798]
234. Klajner M, Licona C, Fetzter L, Hebraud P, Mellitzer G, Pfeffer M, Harlepp S, Gaiddon C. *Inorg Chem*. 2014; 53:5150–5158. [PubMed: 24786362]
235. Colasson B, Credi A, Ragazzon G. *Coord Chem Rev*. 2016; 325:125–134.
236. Smith NA, Zhang P, Greenough SE, Horbury MD, Clarkson GJ, McFeely D, Habtemariam A, Salassa L, Stavros VG, Dowson CG, Sadler PJ. *Chemical Science*. 2017; 8:395–404. [PubMed: 28451184]
237. Karaoun N, Renfrew AK. *Chem Commun*. 2015; 51:14038–14041.
238. Knoll JD, Turro C. *Coord Chem Rev*. 2015; 282–283:110–126. [PubMed: 25729089]
239. Singh TN, Turro C. *Inorg Chem*. 2004; 43:7260–7262. [PubMed: 15530069]
240. Salassa L, Ruiu T, Garino C, Pizarro AM, Bardelli F, Gianolio D, Westendorf A, Bednarski PJ, Lamberti C, Gobetto R, Sadler PJ. *Organometallics*. 2010; 29:6703–6710.
241. Palmer AM, Peña B, Sears RB, Chen O, El Ojaimi M, Thummel RP, Dunbar KR, Turro C. *Philos Trans R Soc, A*. 2013; 371:20120135.
242. Sgambellone MA, David A, Garner RN, Dunbar KR, Turro C. *J Am Chem Soc*. 2013; 135:11274–11282. [PubMed: 23819591]
243. Albani BA, Peña B, Leed NA, de Paula NABG, Pavani C, Baptista MS, Dunbar KR, Turro C. *J Am Chem Soc*. 2014; 136:17095–17101. [PubMed: 25393595]
244. van Rixel VHS, Siewert B, Hopkins SL, Askes SHC, Busemann A, Siegler MA, Bonnet S. *Chem Sci*. 2016; 7:4922–4929.

245. Siewert B, van Rixel VHS, van Rooden EJ, Hopkins SL, Moester MJB, Ariese F, Siegler MA, Bonnet S. *Chem – Eur J*. 2016; 22:10960–10968. [PubMed: 27373895]
246. Howerton BS, Heidary DK, Glazer EC. *J Am Chem Soc*. 2012; 134:8324–8327. [PubMed: 22553960]
247. Wachter E, Heidary DK, Howerton BS, Parkin S, Glazer EC. *Chem Commun*. 2012; 48:9649–9651.
248. Hidayatullah AN, Wachter E, Heidary DK, Parkin S, Glazer EC. *Inorg Chem*. 2014; 53:10030–10032. [PubMed: 25198057]
249. Wachter E, Zamora A, Heidary DK, Ruiz J, Glazer EC. *Chem Commun*. 2016; 52:10121–10124.
250. Davia K, King D, Hong Y, Swavey S. *Inorg Chem Commun*. 2008; 11:584–586.
251. Rani-Beeram S, Meyer K, McCrate A, Hong Y, Nielsen M, Swavey S. *Inorg Chem*. 2008; 47:11278–11283. [PubMed: 18980373]
252. Ke H, Wang H, Wong WK, Mak NK, Kwong DWJ, Wong KL, Tam HL. *Chem Commun*. 2010; 46:6678–6680.
253. Frei A, Rubbiani R, Tubafard S, Blacque O, Anstaett P, Felgentraeger A, Maisch T, Spiccia L, Gasser G. *J Med Chem*. 2014; 57:7280–7292. [PubMed: 25121347]
254. Pierroz V, Rubbiani R, Gentili C, Patra M, Mari C, Gasser G, Ferrari S. *Chem Sci*. 2016; 7:6115–6124. [PubMed: 27708751]
255. Cloonan SM, Elmes RBP, Erby M, Bright SA, Poynton FE, Nolan DE, Quinn SJ, Gunnlaugsson T, Williams DC. *J Med Chem*. 2015; 58:4494–4505. [PubMed: 25961430]
256. Lameijer LN, Hopkins SL, Brevé TG, Askes SHC, Bonnet S. *Chem – Eur J*. 2016; 22:18484–18491. [PubMed: 27859843]
257. Monro S, Scott J, Chouai A, Lincoln R, Zong R, Thummel RP, McFarland SA. *Inorg Chem*. 2010; 49:2889–2900. [PubMed: 20146527]
258. Lincoln R, Kohler L, Monro S, Yin Hm, Stephenson M, Zong Rf, Chouai A, Dorsey C, Hennigar R, Thummel RP, McFarland SA. *J Am Chem Soc*. 2013; 135:17161–17175. [PubMed: 24127659]
259. Stephenson M, Reichardt C, Pinto M, Wächtler M, Sainuddin T, Shi G, Yin H, Monro S, Sampson E, Dietzek B. *J Phys Chem A*. 2014; 118:10507–10521. [PubMed: 24927113]
260. Arenas Y, Monro S, Shi G, Mandel A, McFarland S, Lilge L. *Photodiagn Photodyn Ther*. 2013; 10:615–625.
261. Yin H, Stephenson M, Gibson J, Sampson E, Shi G, Sainuddin T, Monro S, McFarland SA. *Inorg Chem*. 2014; 53:4548–4559. [PubMed: 24725142]
262. Sainuddin T, McCain J, Pinto M, Yin H, Gibson J, Hetu M, McFarland SA. *Inorg Chem*. 2015; 55:83–95. [PubMed: 26672769]
263. Tabrizi L, Chiniforoshan H. *Dalton Trans*. 2016; 45:18333–18345. [PubMed: 27805201]
264. Liu J, Chen Y, Li G, Zhang P, Jin C, Zeng L, Ji L, Chao H. *Biomaterials*. 2015; 56:140–153. [PubMed: 25934287]
265. Zeng L, Kuang S, Li G, Jin C, Ji L, Chao H. *Chem Commun*. 2017; 53:1977–1980.
266. Zhuang X, Ma X, Xue X, Jiang Q, Song L, Dai L, Zhang C, Jin S, Yang K, Ding B. *ACS Nano*. 2016; 10:3486–3495. [PubMed: 26950644]
267. Jiang Q, Song C, Nangreave J, Liu X, Lin L, Qiu D, Wang ZG, Zou G, Liang X, Yan H. *J Am Chem Soc*. 2012; 134:13396–13403. [PubMed: 22803823]
268. Huang K, Ma H, Liu J, Huo S, Kumar A, Wei T, Zhang X, Jin S, Gan Y, Wang PC. *ACS nano*. 2012; 6:4483–4493. [PubMed: 22540892]
269. Lee CC, MacKay JA, Fréchet JM, Szoka FC. *Nat Biotechnol*. 2005; 23:1517–1526. [PubMed: 16333296]
270. Ahmed F, Pakunlu RI, Brannan A, Bates F, Minko T, Discher DE. *J Controlled Release*. 2006; 116:150–158.
271. Tran PA, Webster TJ. *Int J Nanomed*. 2011; 6:1553–1558.
272. Ramamurthy C, Sampath K, Arunkumar P, Kumar MS, Sujatha V, Premkumar K, Thirunavukkarasu C. *Bioprocess Biosyst Eng*. 2013; 36:1131–1139. [PubMed: 23446776]

273. Liu W, Li X, Wong YS, Zheng W, Zhang Y, Cao W, Chen T. *ACS nano*. 2012; 6:6578–6591. [PubMed: 22823110]
274. Liu T, Zeng L, Jiang W, Fu Y, Zheng W, Chen T. *Nanomedicine*. 2015; 11:947–958. [PubMed: 25680543]
275. Sun D, Liu Y, Yu Q, Zhou Y, Zhang R, Chen X, Hong A, Liu J. *Biomaterials*. 2013; 34:171–180. [PubMed: 23059005]
276. Sun D, Liu Y, Yu Q, Qin X, Yang L, Zhou Y, Chen L, Liu J. *Biomaterials*. 2014; 35:1572–1583. [PubMed: 24268198]
277. Cobley CM, Chen J, Cho EC, Wang LV, Xia Y. *Chem Soc Rev*. 2011; 40:44–56. [PubMed: 20818451]
278. Huang X, Jain PK, El-Sayed IH, El-Sayed MA. *Lasers Med Sci*. 2008; 23:217–228. [PubMed: 17674122]
279. Ghosh P, Han G, De M, Kim CK, Rotello VM. *Adv Drug Deliver Rev*. 2008; 60:1307–1315.
280. De M, Ghosh PS, Rotello VM. *Adv Mater*. 2008; 20:4225–4241.
281. Manea F, Houillon FB, Pasquato L, Scrimin P. *Angew Chem Int Edit*. 2004; 43:6165–6169.
282. Saha K, Agasti SS, Kim C, Li X, Rotello VM. *Chem Rev*. 2012; 112:2739–2779. [PubMed: 22295941]
283. Elmes RBP, Orange KN, Cloonan SM, Williams DC, Gunnlaugsson T. *J Am Chem Soc*. 2011; 133:15862–15865. [PubMed: 21923121]
284. Rogers NJ, Claire S, Harris RM, Farabi S, Zikeli G, Styles IB, Hodges NJ, Pikramenou Z. *Chem Commun*. 2014; 50:617–619.
285. Zhang P, Wang J, Huang H, Chen H, Guan R, Chen Y, Ji L, Chao H. *Biomaterials*. 2014; 35:9003–9011. [PubMed: 25103232]
286. Zhang P, Wang J, Huang H, Yu B, Qiu K, Huang J, Wang S, Jiang L, Gasser G, Ji L, Chao H. *Biomaterials*. 2015; 63:102–114. [PubMed: 26093791]
287. Zhang P, Wang J, Huang H, Qiu K, Huang J, Ji L, Chao H. *J Mater Chem B*. 2017; 5:671–678.
288. Tarn D, Ashley CE, Xue M, Carnes EC, Zink JJ, Brinker CJ. *Acc Chem Res*. 2013; 46:792–801. [PubMed: 23387478]
289. Knežević NŽ, Trewyn BG, Lin VSY. *Chem–Eur J*. 2011; 17:3338–3342. [PubMed: 21337435]
290. Frasconi M, Liu Z, Lei J, Wu Y, Strekalova E, Malin D, Ambrogio MW, Chen X, Botros YY, Cryns VL. *J Am Chem Soc*. 2013; 135:11603–11613. [PubMed: 23815127]
291. He S, Krippes K, Ritz S, Chen Z, Best A, Butt H-J, Mailänder V, Wu S. *Chem Commun*. 2015; 51:431–434.
292. Knežević NŽ, Stojanovic V, Chaix A, Bouffard E, Cheikh KEI, Morère A, Maynadier M, Lemerrier G, Garcia M, Gary-Bobo M. *J Mater Chem B*. 2016; 4:1337–1342.
293. He, Huang Y, Zhu H, Pang G, Zheng W, Wong YS, Chen T. *Adv Funct Mater*. 2014; 24:2754–2763.
294. Baughman RH, Zakhidov AA, de Heer WA. *Science*. 2002; 297:787–792. [PubMed: 12161643]
295. Huang K, Saha A, Dirian K, Jiang C, Chu PLE, Tour JM, Guldi DM, Marti AA. *Nanoscale*. 2016; 8:13488–13497. [PubMed: 27353007]
296. Bianco A, Kostarelos K, Prato M. *Curr Opin Chem Biol*. 2005; 9:674–679. [PubMed: 16233988]
297. Liu Z, Chen K, Davis C, Sherlock S, Cao Q, Chen X, Dai H. *Cancer Res*. 2008; 68:6652–6660. [PubMed: 18701489]
298. Xue X, Yang JY, He Y, Wang LR, Liu P, Yu LS, Bi GH, Zhu MM, Liu YY, Xiang RW. *Nat Nanotechnol*. 2016; 11:613–620. [PubMed: 26974957]
299. Kam NWS, O’Connell M, Wisdom JA, Dai H. *Proc Natl Acad Sci*. 2005; 102:11600–11605. [PubMed: 16087878]
300. Wang N, Feng Y, Zeng L, Zhao Z, Chen T. *ACS Appl Mater Interfaces*. 2015; 7:14933–14945. [PubMed: 26107995]
301. Zhang P, Huang H, Huang J, Chen H, Wang J, Qiu K, Zhao D, Ji L, Chao H. *ACS Appl Mater Interfaces*. 2015; 7:23278–23290. [PubMed: 26430876]

302. Bœuf G, Roullin GV, Moreau J, Van Gulick L, Terryn C, Ploton D, Andry MC, Chuburu F, Dukic S, Molinari M. *ChemPlusChem*. 2014; 79:171–180.
303. Sun W, Li S, Häupler B, Liu J, Jin S, Steffen W, Schubert US, Butt H-J, Liang X-J, Wu S. *Adv Mater*. 2017; 29:1603702.
304. Chen L, Fu C, Deng Y, Wu W, Fu A. *Pharm Res*. 2016; 33:2989–2998. [PubMed: 27590630]
305. Chakraborty S, Agrawalla BK, Stumper A, Vegi NM, Fischer S, Reichardt C, Kögler M, Dietzek B, Feuring-Buske M, Buske C, Rau S, Weil T. *J Am Chem Soc*. 2017; 139:2512–2519. [PubMed: 28097863]
306. Zhang DY, Zheng Y, Tan CP, Sun JH, Zhang W, Ji LN, Mao ZW. *ACS Appl Mater Interfaces*. 2017; 9:6761–6771. [PubMed: 28150943]
307. Valente A, Garcia MH, Marques F, Miao Y, Rousseau C, Zinck P. *J Inorg Biochem*. 2013; 127:79–81. [PubMed: 23896008]
308. Huang Y, Huang W, Chan L, Zhou B, Chen T. *Biomaterials*. 2016; 103:183–196. [PubMed: 27388944]
309. Süß-Fink G, Khan F-A, Juillerat-Jeanneret L, Dyson PJ, Renfrew AK. *J Cluster Sci*. 2010; 21:313–324.
310. Zhang G, Wu C, Ye H, Yan H, Wang X. *J Nanobiotechnol*. 2011; 9:6.
311. Romero-Canelón I, Phoenix B, Pitto-Barry A, Tran J, Soldevila-Barreda JJ, Kirby N, Green S, Sadler PJ, Barry NP. *J Organomet Chem*. 2015; 796:17–25.
312. Völker T, Dempwolff F, Graumann PL, Meggers E. *Angew Chem Int Ed*. 2014; 53:10536–10540.
313. Sasmal PK, Streu CN, Meggers E. *Chem Commun*. 2013; 49:1581–1587.
314. Zheng Y, Tan Y, Harms K, Marsch M, Riedel R, Zhang L, Meggers E. *J Am Chem Soc*. 2017; 139:4322–4325. [PubMed: 28290685]
315. Zhang L, Meggers E. *Acc Chem Res*. 2017; 50:320–330. [PubMed: 28128920]
316. Yang M, Li J, Chen PR. *Chem Soc Rev*. 2014; 43:6511–6526. [PubMed: 24867400]
317. Li J, Chen PR. *Nat Chem Biol*. 2016; 12:129–137. [PubMed: 26881764]
318. Streu C, Meggers E. *Angew Chem, Int Ed*. 2006; 45:5645–5648.
319. Völker T, Meggers E. *Curr Opin Chem Biol*. 2015; 25:48–54. [PubMed: 25561021]
320. Sadhu KK, Lindberg E, Winssinger N. *Chem Commun*. 2015; 51:16664–16666.
321. Hsu HT, Trantow BM, Waymouth RM, Wender PA. *Bioconjugate Chem*. 2016; 27:376–382.
322. Tomas-Gamasa M, Martinez-Calvo M, Couceiro JR, Mascarenas JL. *Nat Commun*. 2016; 7:12538. [PubMed: 27600651]
323. Soldevila-Barreda JJ, Sadler PJ. *Curr Opin Chem Biol*. 2015; 25:172–183. [PubMed: 25765750]
324. Dougan SJ, Habtemariam A, McHale SE, Parsons S, Sadler PJ. *Proc Natl Acad Sci*. 2008; 105:11628–11633. [PubMed: 18687892]
325. Dougan SJ, Melchart M, Habtemariam A, Parsons S, Sadler PJ. *Inorg Chem*. 2006; 45:10882–10894. [PubMed: 17173447]
326. Soldevila-Barreda JJ, Romero-Canelón I, Habtemariam A, Sadler PJ. *Nat Commun*. 2015; 6:6582. [PubMed: 25791197]
327. Wilson YM, Dürrenberger M, Nogueira ES, Ward TR. *J Am Chem Soc*. 2014; 136:8928–8932. [PubMed: 24918731]
328. Ritter C, Nett N, Acevedo-Rocha CG, Lonsdale R, Kräling K, Dempwolff F, Hoebenreich S, Graumann PL, Reetz MT, Meggers E. *Angew Chem, Int Ed*. 2015; 54:13440–13443.
329. Sanchez MI, Penas C, Vazquez ME, Mascarenas JL. *Chem Sci*. 2014; 5:1901–1907. [PubMed: 25632343]
330. Li X, Guo J, Asong J, Wolfert MA, Boons GJ. *J Am Chem Soc*. 2011; 133:11147–11153. [PubMed: 21678979]
331. Koo H, Lee S, Na JH, Kim SH, Hahn SK, Choi K, Kwon IC, Jeong SY, Kim K. *Angew Chem, Int Ed*. 2012; 51:11836–11840.
332. Han Y, Yang X, Liu Y, Ai Q, Liu S, Sun C, Liang F. *Sci Rep*. 2016; 6:22239. [PubMed: 26917240]
333. Unciti-Broceta A. *Nat Chem*. 2015; 7:538–539. [PubMed: 26100798]

334. Tonga GY, Jeong Y, Duncan B, Mizuhara T, Mout R, Das R, Kim ST, Yeh YC, Yan B, Hou S, Rotello VM. *Nat Chem.* 2015; 7:597–603. [PubMed: 26100809]
335. Ji S, Guo H, Yuan X, Li X, Ding H, Gao P, Zhao C, Wu W, Wu W, Zhao J. *Org Lett.* 2010; 12:2876–2879. [PubMed: 20499862]
336. Li G, Sasaki T, Asahina S, Roy MC, Mochizuki T, Koizumi K, Zhang Y. *Chem.* 2017; 2:283–298.
337. Shen J, Kim HC, Wolfram J, Mu C, Zhang W, Liu H, Xie Y, Mai J, Zhang H, Li Z, Guevara M, Mao ZW, Shen H. *Nano Lett.* 2017; 17:2913–2920. [PubMed: 28418672]
338. Wang YM, Liu W, Yin XB. *Chem Sci.* 2017; 8:3891–3897. [PubMed: 28626558]

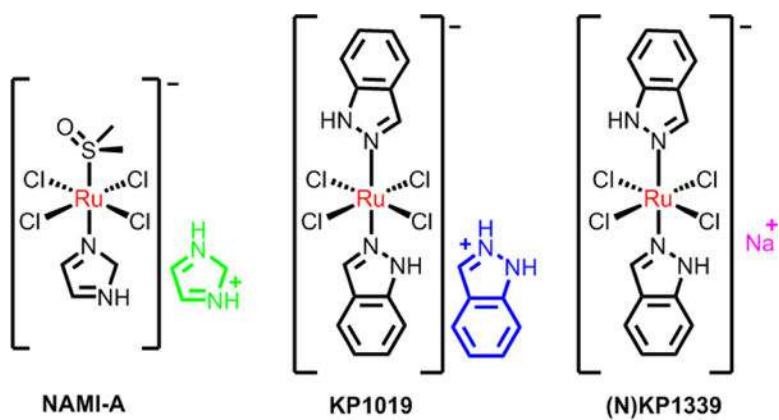


Fig. 1.
Three ruthenium(III) compounds in clinical trials.

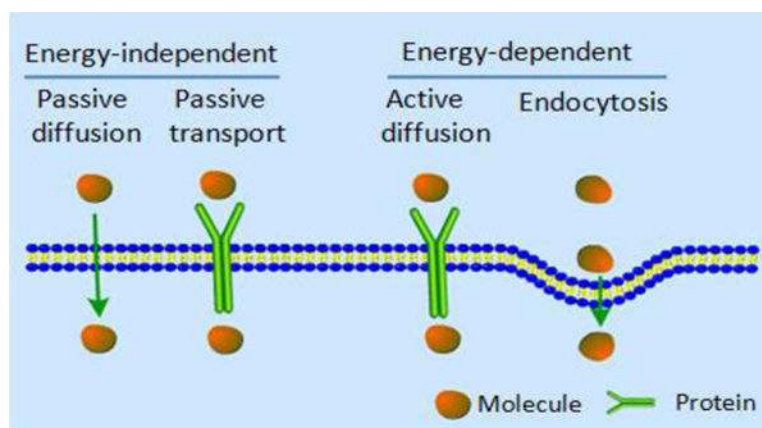


Fig. 2. Common cellular uptake mechanisms of drugs. Reproduced with permission from ref. 71. Copyright 2012, Royal Society of Chemistry.

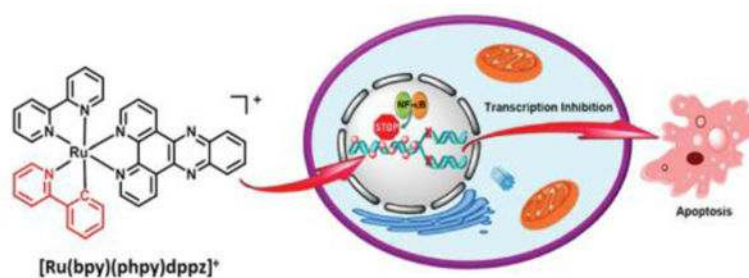
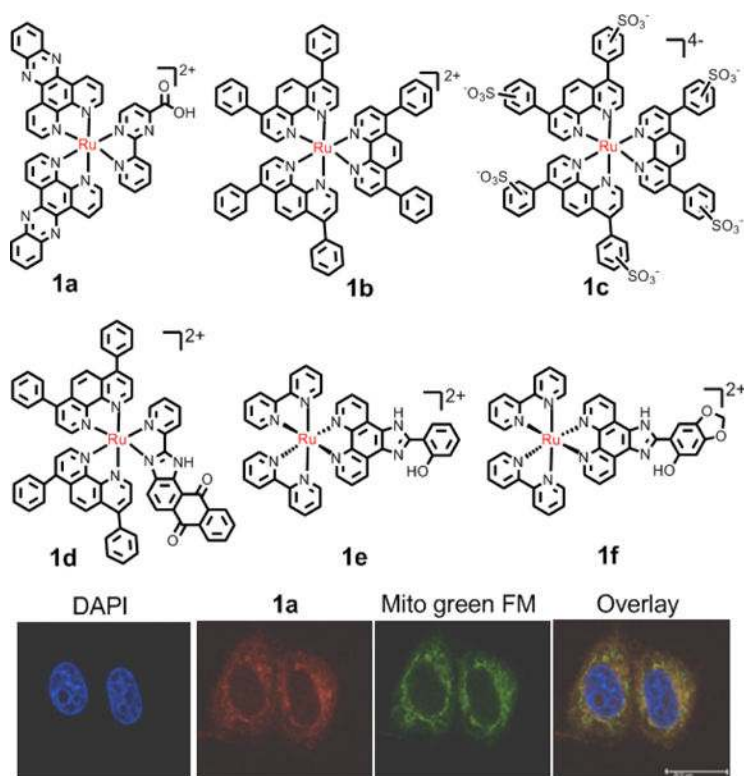


Fig. 3.

The schematic description of the anticancer effect of the nucleic targeting complex $[\text{Ru}(\text{bpy})(\text{phpy})\text{dppz}]^+$. Reproduced with permission from ref. 80. Copyright 2015, American Chemical Society.

**Fig. 4.**

Representation of Ru(II) compounds that accumulate in mitochondria. Bottom image: fluorescence confocal microscopy images of HeLa cells incubated with **1a** with commercial dyes. Reproduced with permission from ref. 86. Copyright 2015, American Chemical Society.

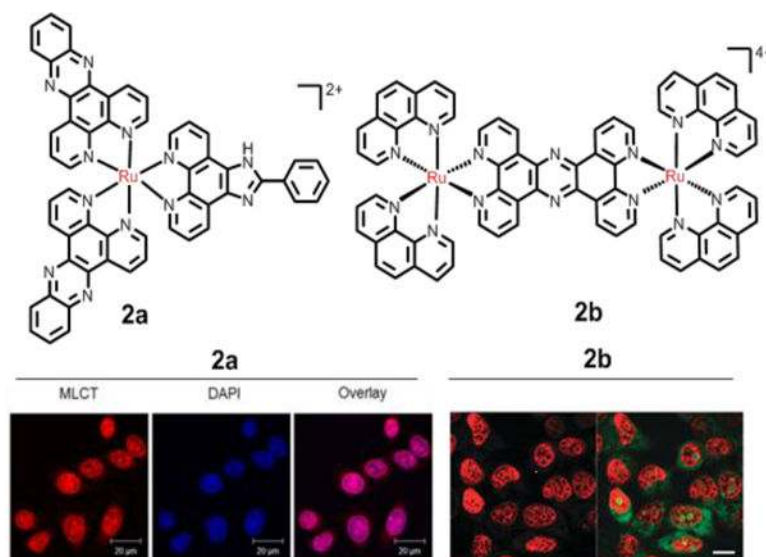


Fig. 5. Representation of Ru(II) compounds that target DNA. Left-hand fluorescence image: the nuclear DNA staining of **2a** in PFA-fixed HeLa cells, as evident by red luminescence, with co-staining by nuclear DNA dye DAPI. Right-hand fluorescence image: the nuclear DNA staining of the dinuclear **2b** in MCF-7 cells, as evident by the red luminescence, with co-staining SYTO-9 (green). Reproduced with permission from ref. ¹⁰⁹ and ¹¹¹, respectively. Copyright 2015, Nature Publishing Group.

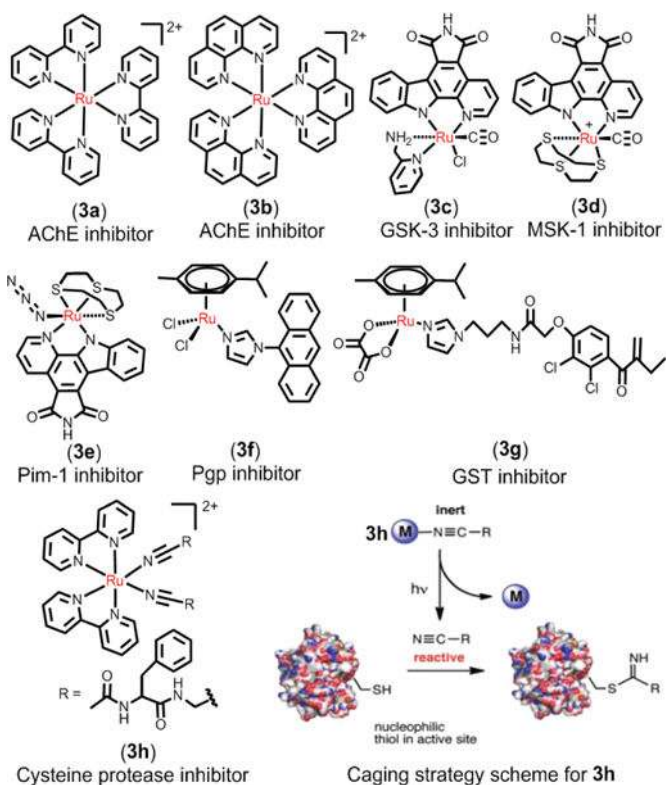


Fig. 6. Representation of Ru(II) compounds that target proteins as enzymes inhibitors. Right-bottom image: caging strategy for compound **3h** as photoinduced cysteine protease inhibitors. Reproduced with permission from ref. ¹³¹. Copyright 2015, American Chemical Society.

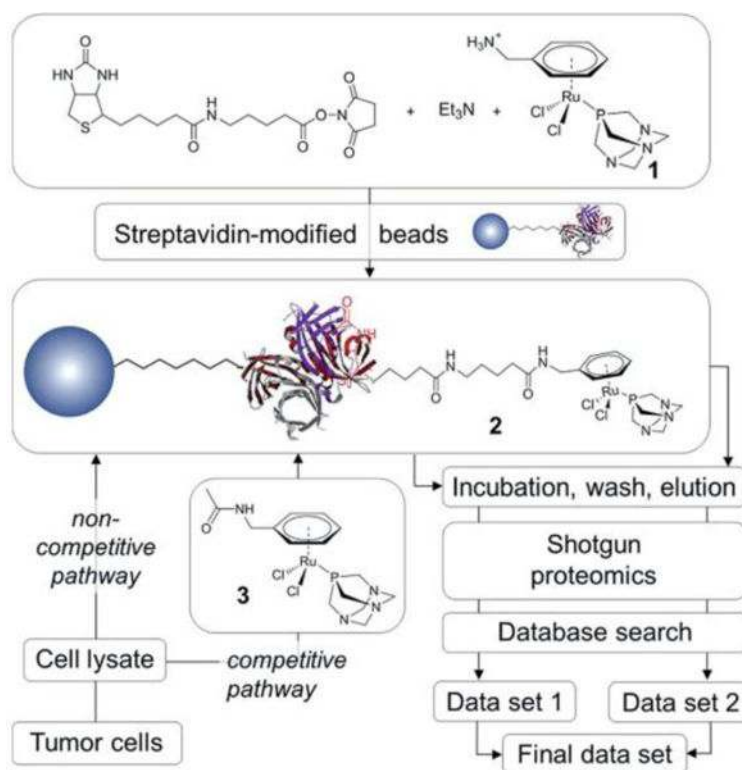


Fig. 7. Schematic representation of the work-flow used in the metallodrug pull-down experiments performed by Hartinger *et al.* Reproduced with permission from ref. ¹¹⁶. Copyright 2012, Royal Society of Chemistry.

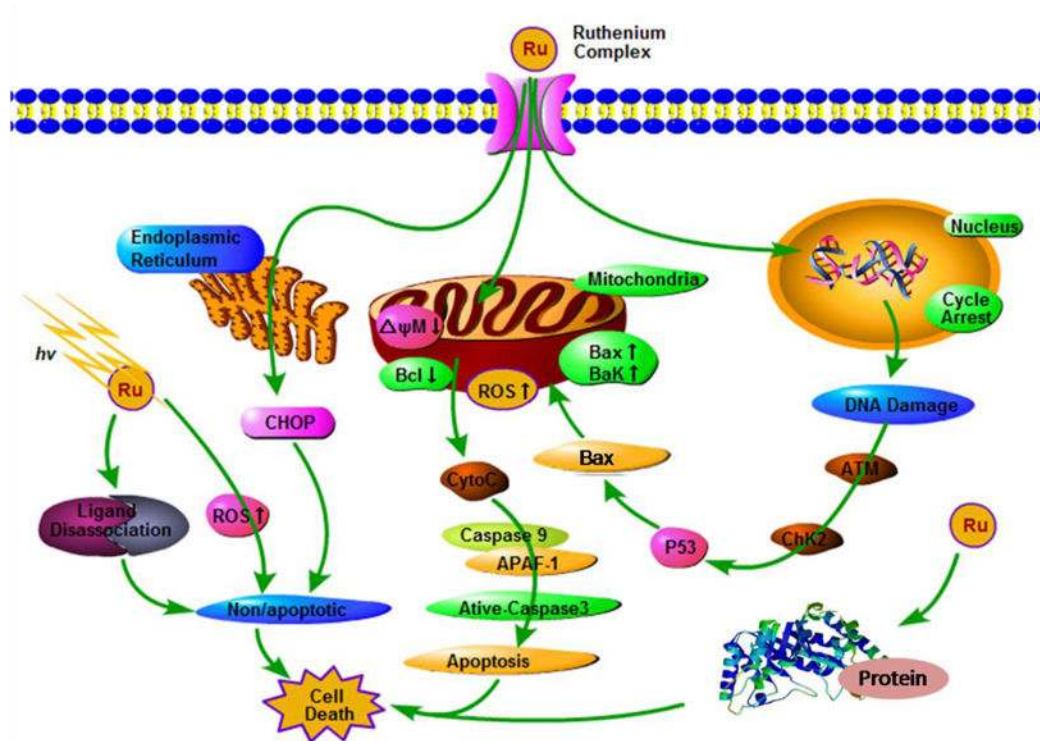


Fig. 8.

General representation of the main targets and proposed mechanisms of action of ruthenium compounds as anticancer drugs.

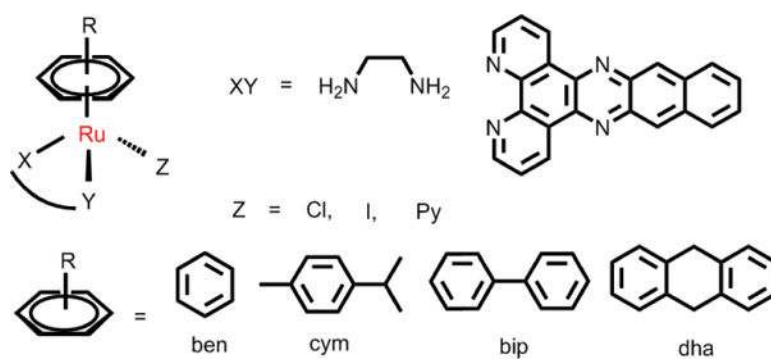


Fig. 9.
Common structures of $[(\eta^6\text{-arene})\text{Ru}(\text{X})(\text{Y})(\text{Z})]$.

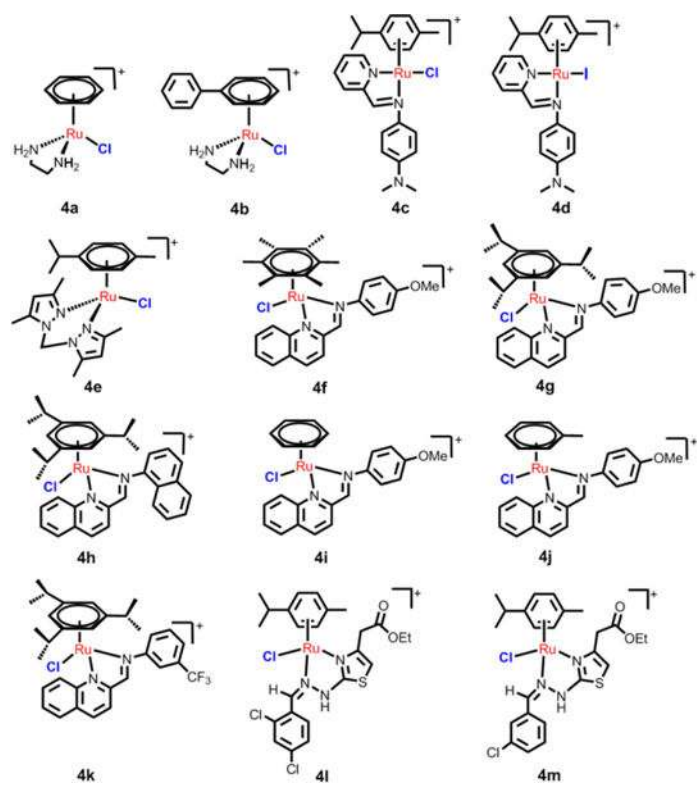
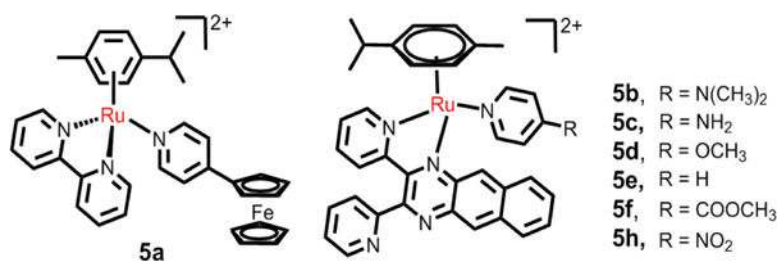


Fig. 10.
Common structures of arene Ru(II) compounds with *N,N*-chelating ligands.

**Fig. 11.**

The *N,N*- ligands are arene Ru(II) compounds with good photoactivity.

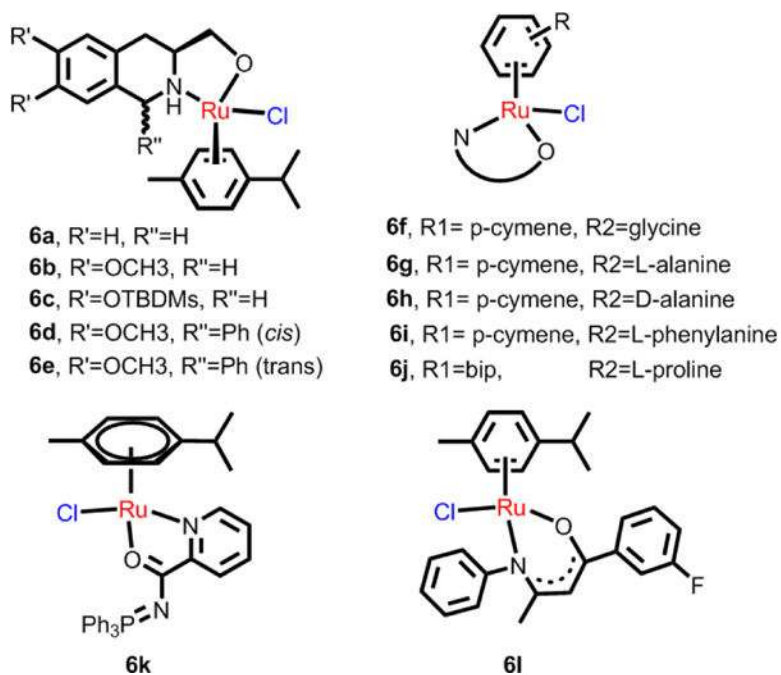
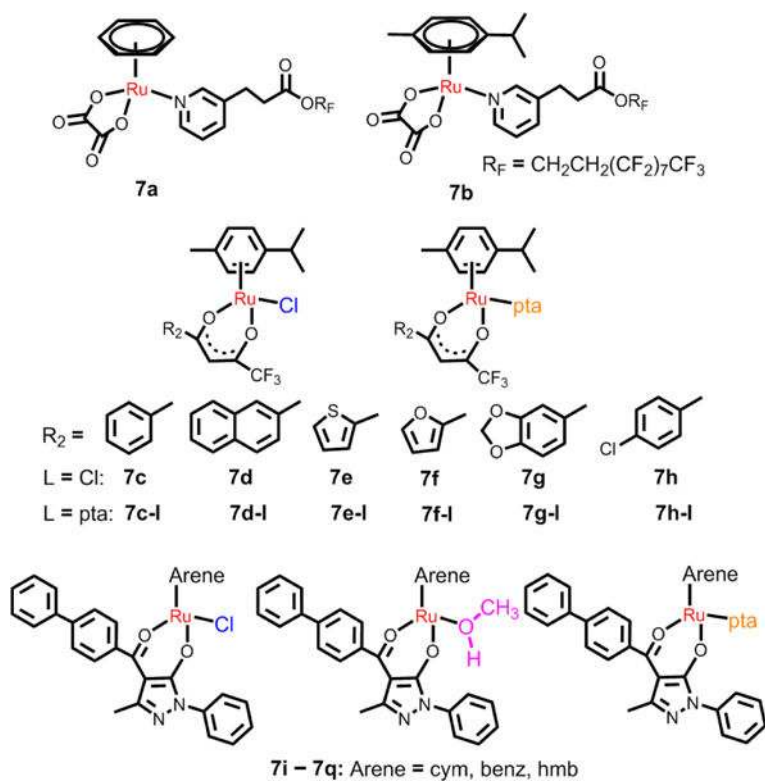


Fig. 12.
Ru(II) arene complexes bearing *N,O*-chelating ligands.

**Fig. 13.**

O,O- ligands arene Ru(II) complexes with different monodentate ligands.

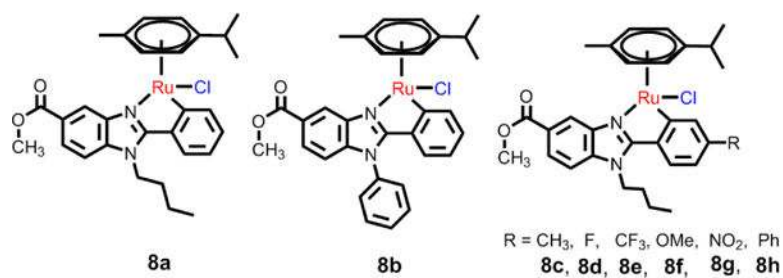
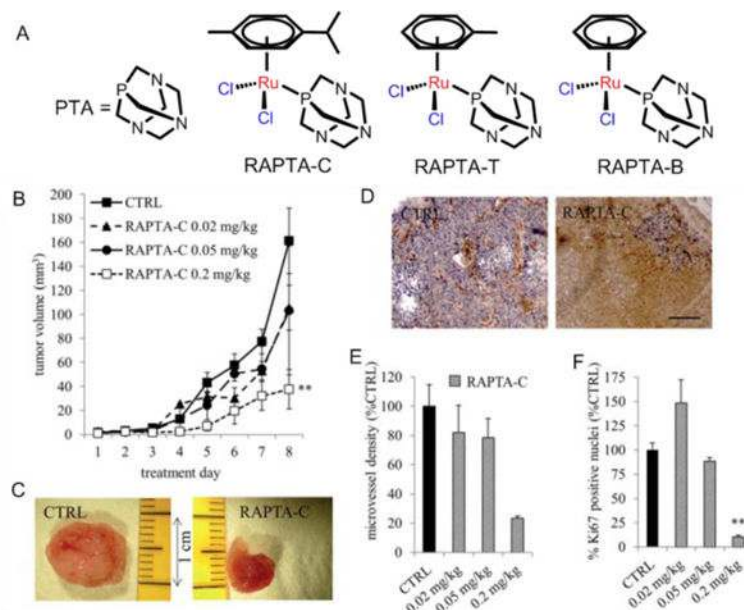


Fig. 14.
C,N-cyclometalated (η^6 -*p*-cymene) Ru(II) complexes.

**Fig. 15.**

(A) The structures of PTA, RAPTA-C, RAPTA-T and RAPTA-B. (B) Growth curve of A2780 tumors with respect to RAPTA-C treatment. (C) Images show representative tumors from the vehicle treated (CTRL) and RAPTA-C (0.2 mg kg⁻¹) treated CAMs. (D) Representative images of the immunohistochemical staining of the endothelial cell marker CD31 (in brown) showing reduced microvessel density per mm² in tumors treated with RAPTA-C normalized to the tumor surface area and provided as a % of the control (E) and Ki-67 positive nuclei (in blue) (D) and quantification of the percentage of the tumor surface area staining positive for Ki-67 (as a % of CTRL) (F). Black bar in the right image of (D) represents 500 μ m and is valid for both images. Reproduced with permission from ref. ¹⁶⁸. Copyright 2012, Royal Society of Chemistry.

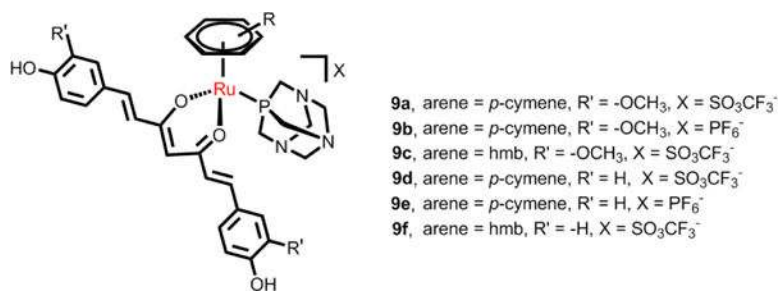


Fig. 16.
Curcumin complexes derived from the RAPTA structure.

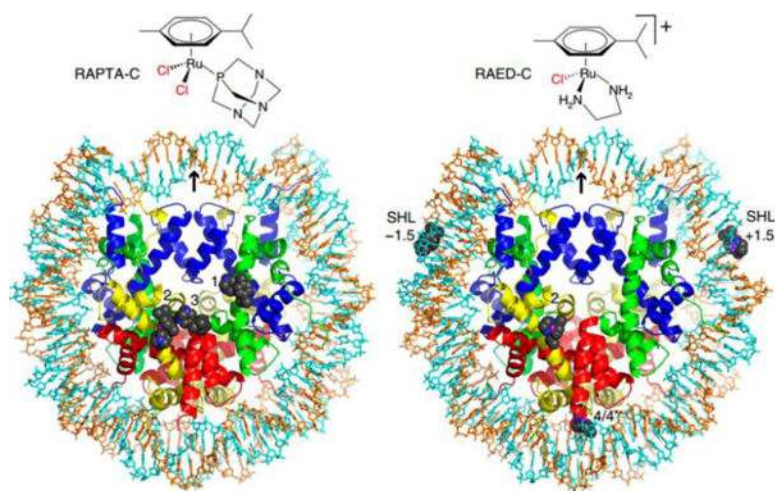
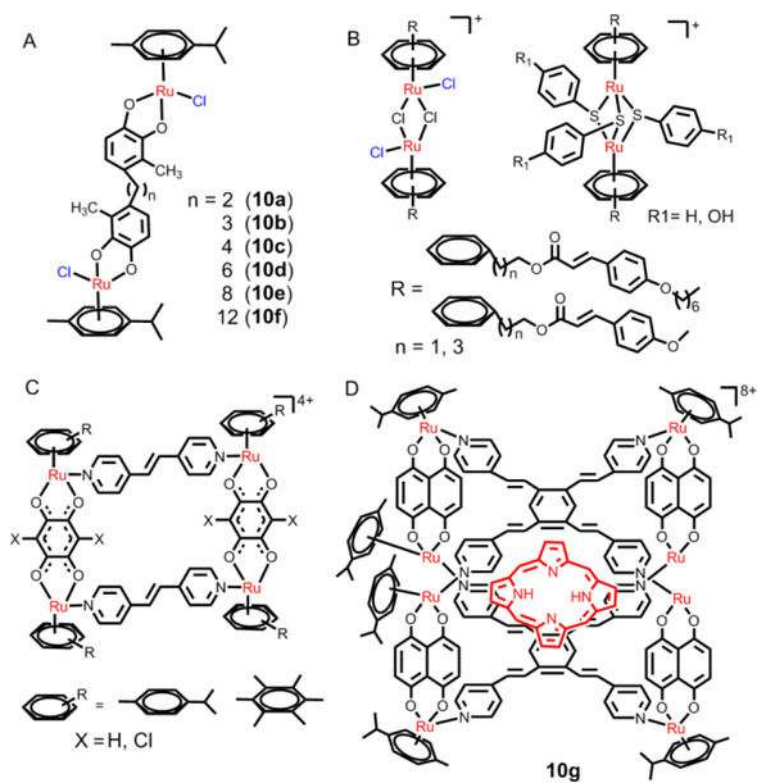


Fig. 17. Chemical structures and nucleosomal adducts of RAPTA-C and RAED-C by X-ray. Reproduced with permission from ref. ¹⁷¹. Copyright 2015, Nature Publishing Group.

**Fig. 18.**

(A), (B), (C) and (D) The structures of selective dinuclear and tetranuclear arene Ru(II) complexes.

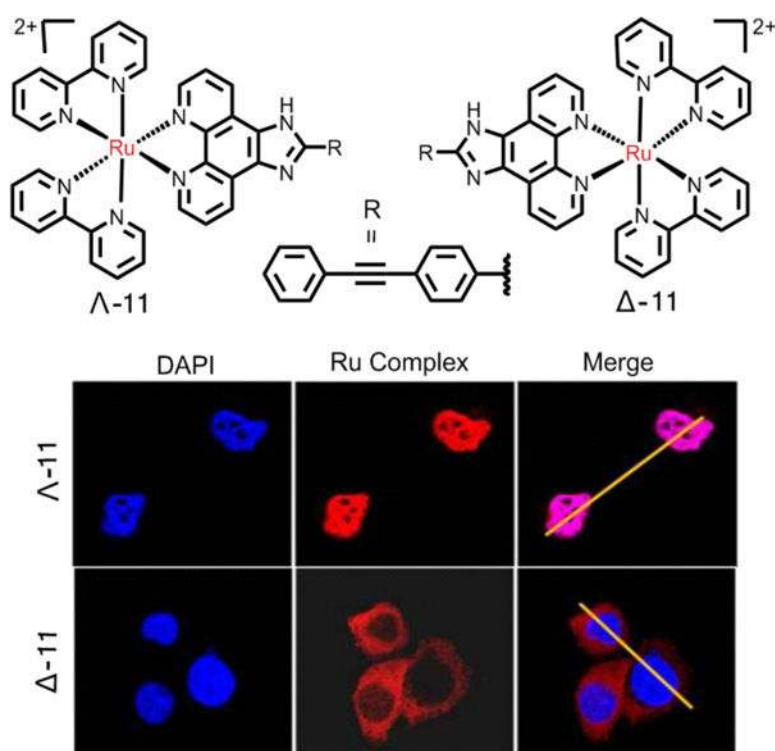


Fig. 19. Cellular localization of Λ - and Δ -11 in MDA-MB-231 cells. Reproduced with permission from ref. ¹⁹⁸. Copyright 2015, American Chemical Society.

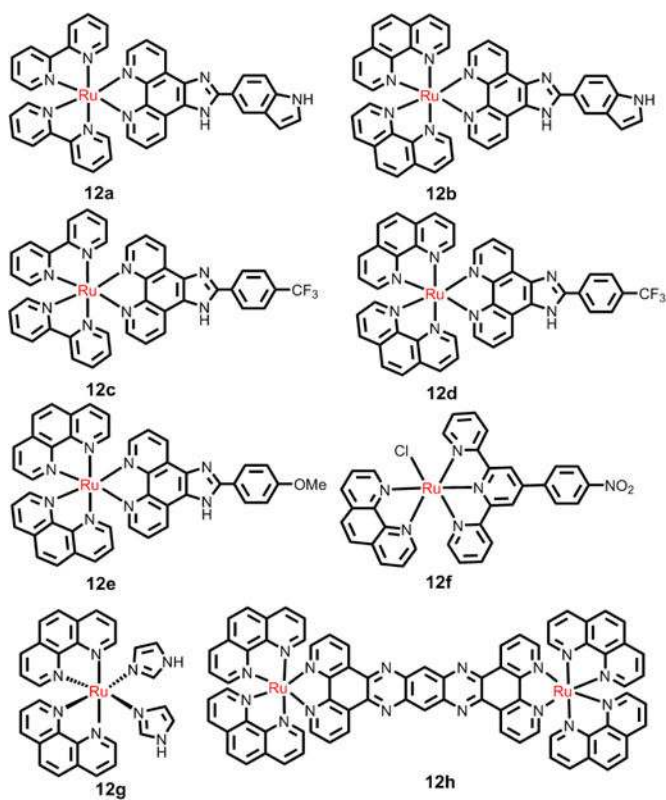
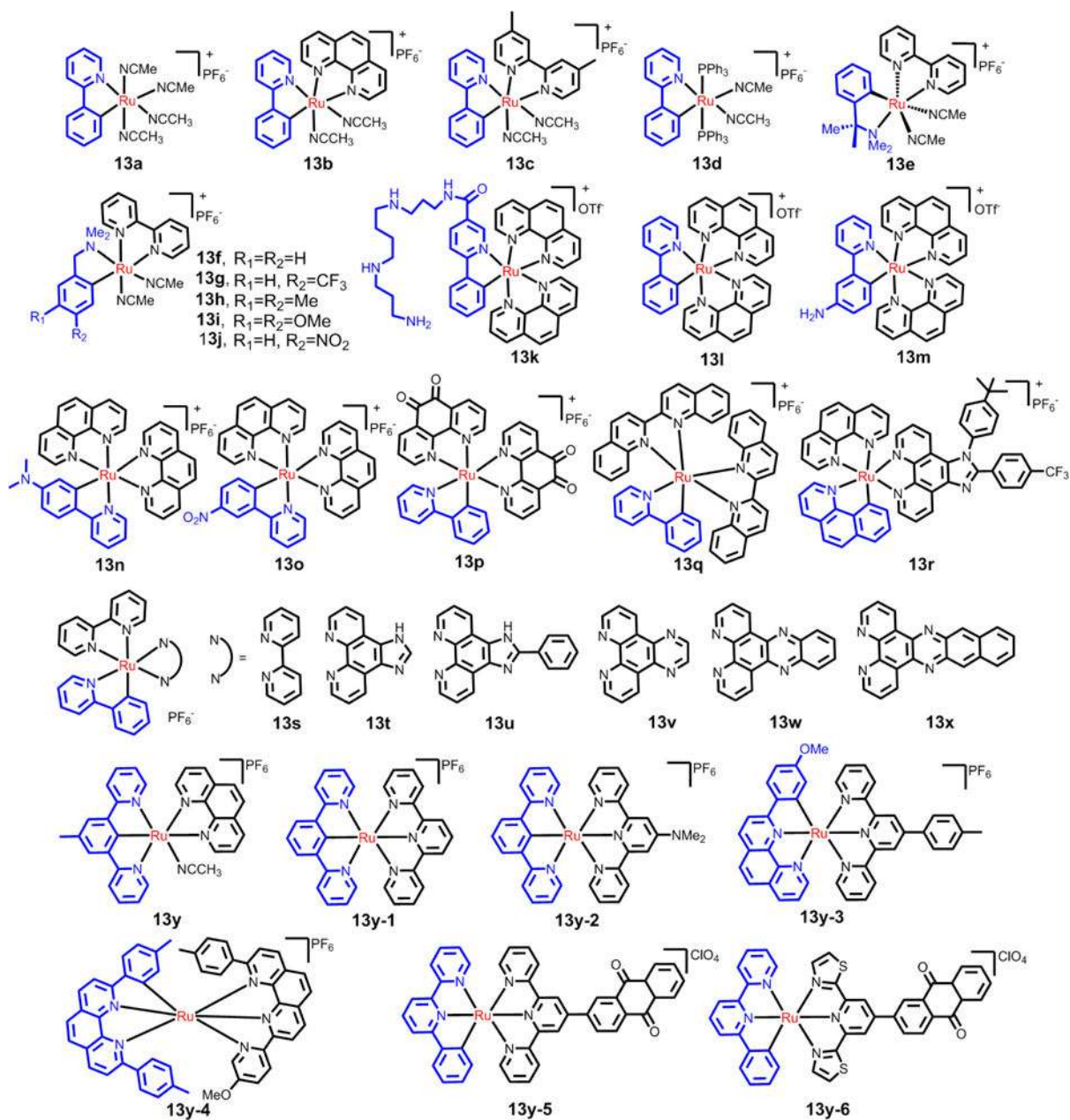


Fig. 20.
The structures of selective Ru(II) polypyridyl compounds as anticancer drugs.

**Fig. 21.**

The structures of the selective cyclothenated compounds used in anticancer drugs.

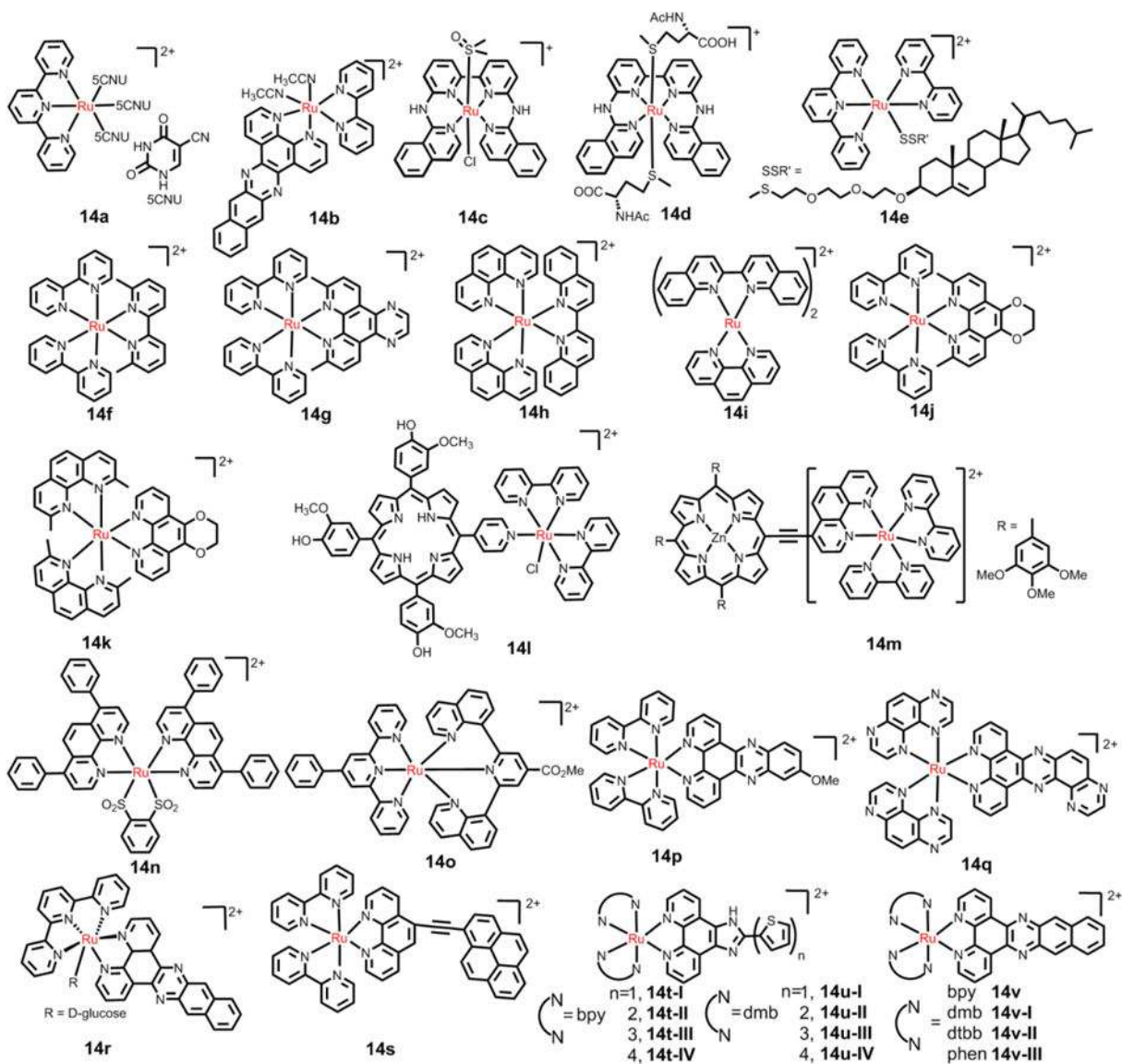


Fig. 22.

The structures of the selective Ru(II) compounds used in PDT

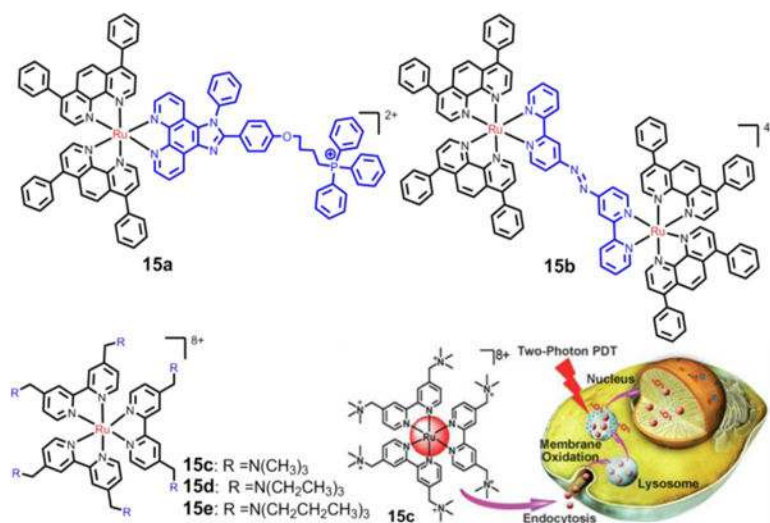
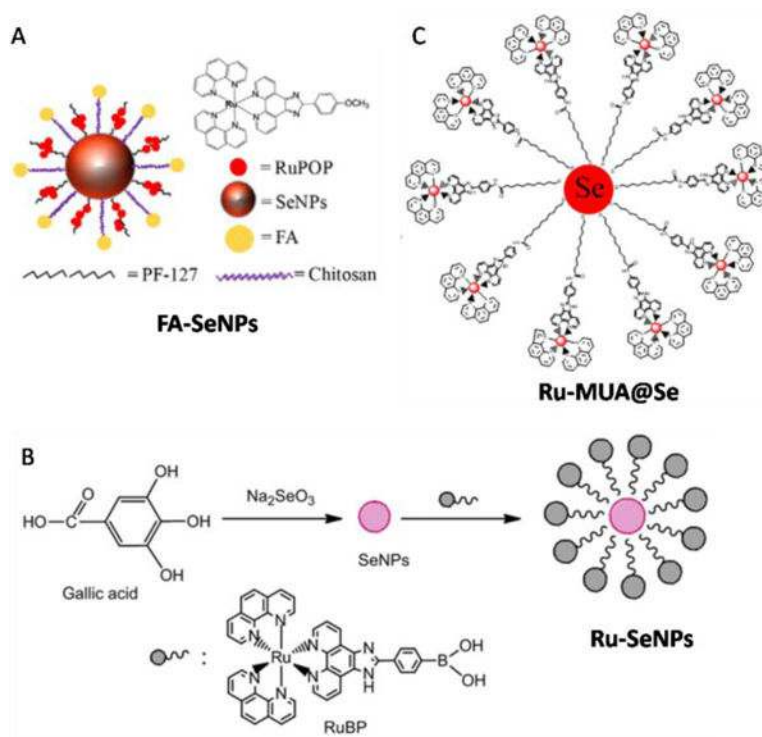


Fig. 23.

The Ru(II) compounds used for two-photon-PDT in Chao's group, and the schematic description of **15c** used for two-photon-PDT. Reproduced with permission from ref. ⁹⁸. Copyright 2015, Wiley-VCH.

**Fig. 24.**

(A) The diagrammatic figure of **FA-SeNPs** and the structure of RuPOP. (B) The method for the synthesis of the **Ru-SeNPs**. (C) The structure of the **Ru-MUA@Se**. Reproduced with permission from ref. ^{274, 275 and 276}, respectively. Copyright 2015, Elsevier.

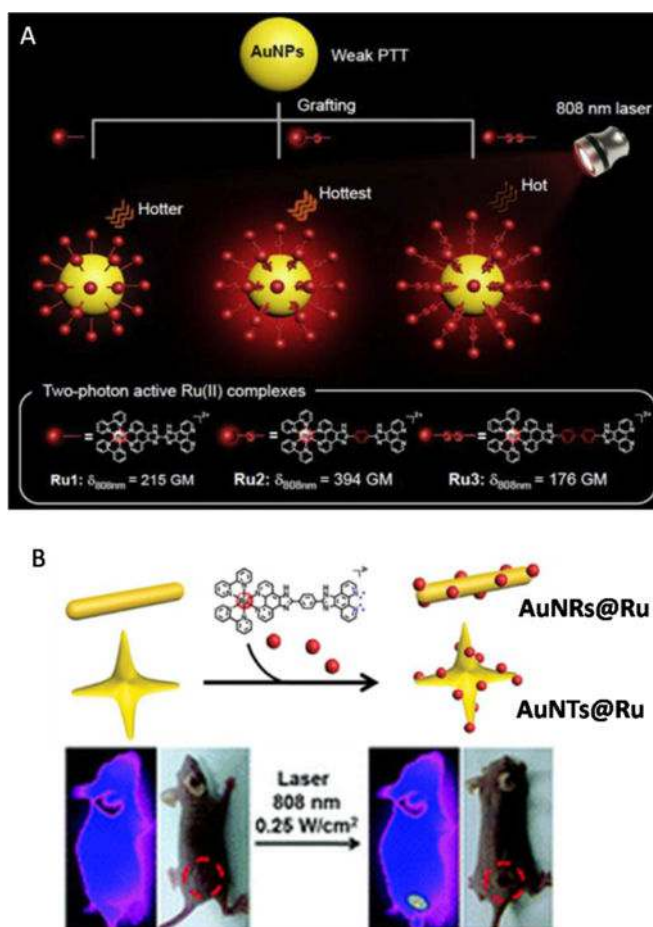


Fig. 25.

(A) Schematic illustration of the photothermal efficiency of **Ru@AuNPs** under two-photon luminescence. (B) The structure of **AuNRs@Ru** and **AuNTs@Ru**, and the schematic illustration of photothermal treatment on mice. Reproduced with permission from ref. ²⁸⁶ (Copyright 2015, Elsevier) and ²⁸⁷ (Copyright 2012, Royal Society of Chemistry), respectively.

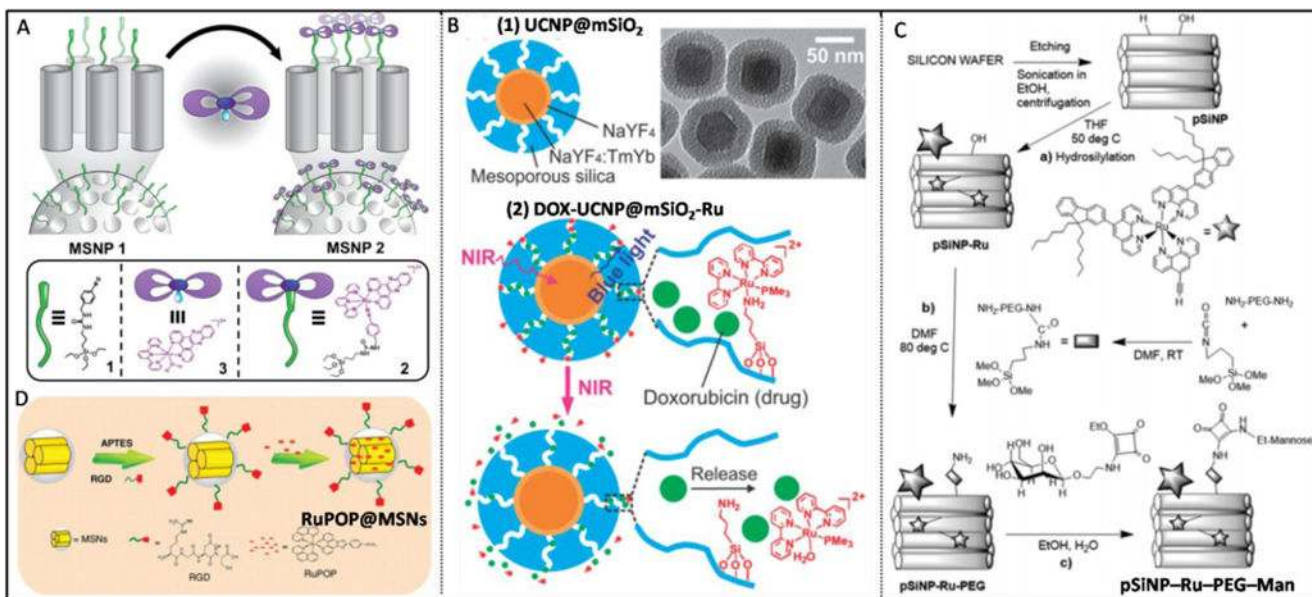


Fig. 26.

(A) Graphical representation for the assembly of mechanized MSNPs. (B) Schematic model and TEM image of UCNP@mSiO₂ nanoparticles (1), the schematic illustration of the drug release from DOX-UCNP@mSiO₂-Ru nanoparticles (2). (C) Synthetic scheme for the pSiNP-Ru-PEG-Man. (D) The reaction pathways for the construction of the materials RuPOP@MSNs. Reproduced with permission from ref. ²⁹⁰ (Copyright 2015, American Chemical Society), ²⁹¹, ²⁹² (Copyright 2012, Royal Society of Chemistry) and ²⁹³ (Copyright 2015, Wiley-VCH), respectively.

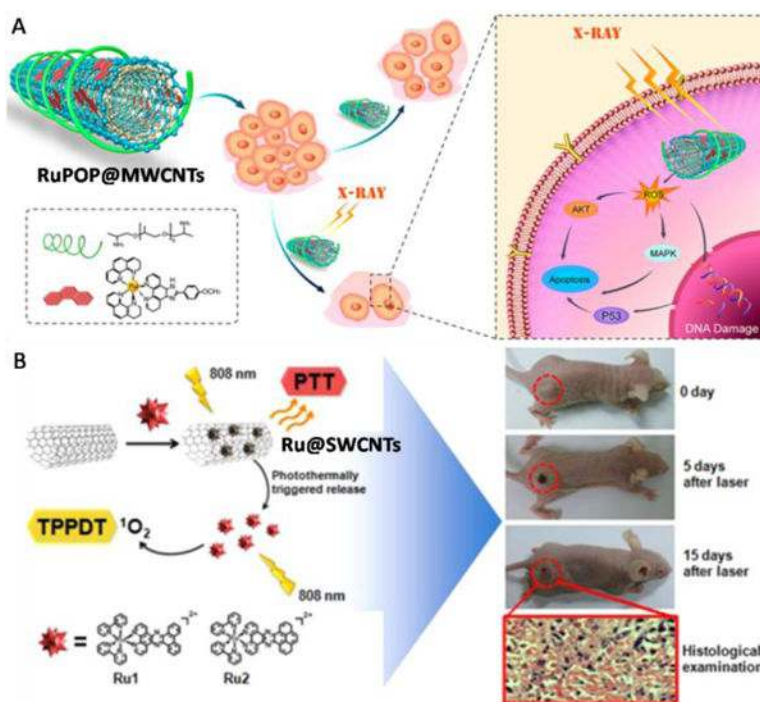


Fig. 27.

(A) The design and radiosensitization action mechanisms of the **RuPOP@MWCNTs** nanosystem. (B) Schematic Design of **Ru@SWCNTs** for bimodal photothermal therapy and two-photon photodynamic therapy with 808 nm Irradiation, and the presentative photographs of HeLa tumors in mice **Ru@SWCNTs** treatments. Reproduced with permission from ref. ³⁰⁰ and ³⁰¹, respectively. Copyright 2015, American Chemical Society.

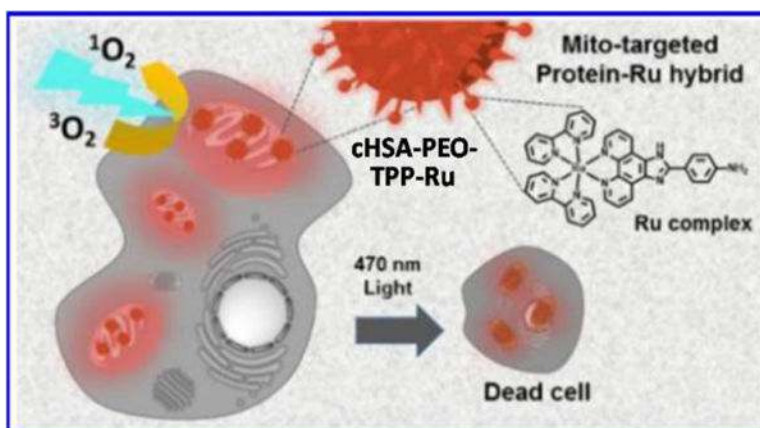
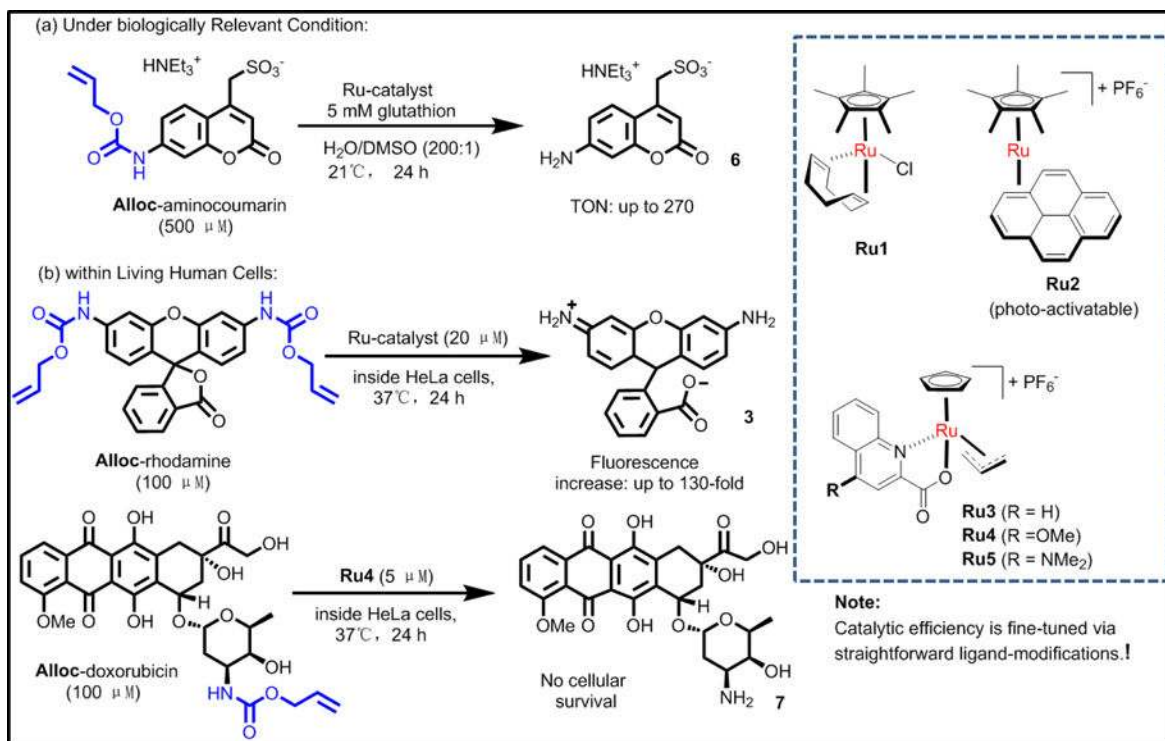
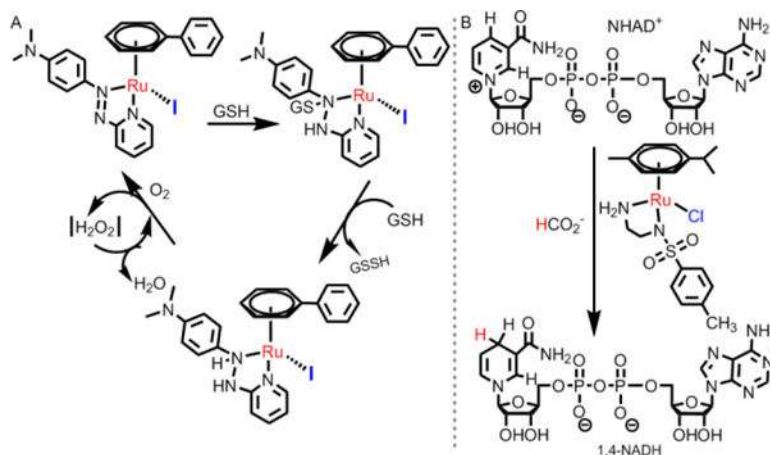


Fig. 28. Schematic design of cHSA-PEO-TPP-Ru for PDT. Reproduced with permission from ref. ³⁰⁵. Copyright 2015, American Chemical Society.

**Fig. 29.**

Uncaging reactions of allyloxycarbonyl (alloc) protected amines under (a) biologically relevant conditions and (b) within living human cells with ruthenium(II) complexes reported by Meggers *et al.* Reproduced with permission from ref. ³¹⁹. Copyright 2015, Elsevier.

**Fig. 30.**

The Ru(II) catalytic reactions reported by Sadler group. Reproduced with permission from ref. ³²⁴ (Copyright 2008, National Academy of Sciences.) and 326 (Copyright 2015, Nature Publishing Group), respectively.

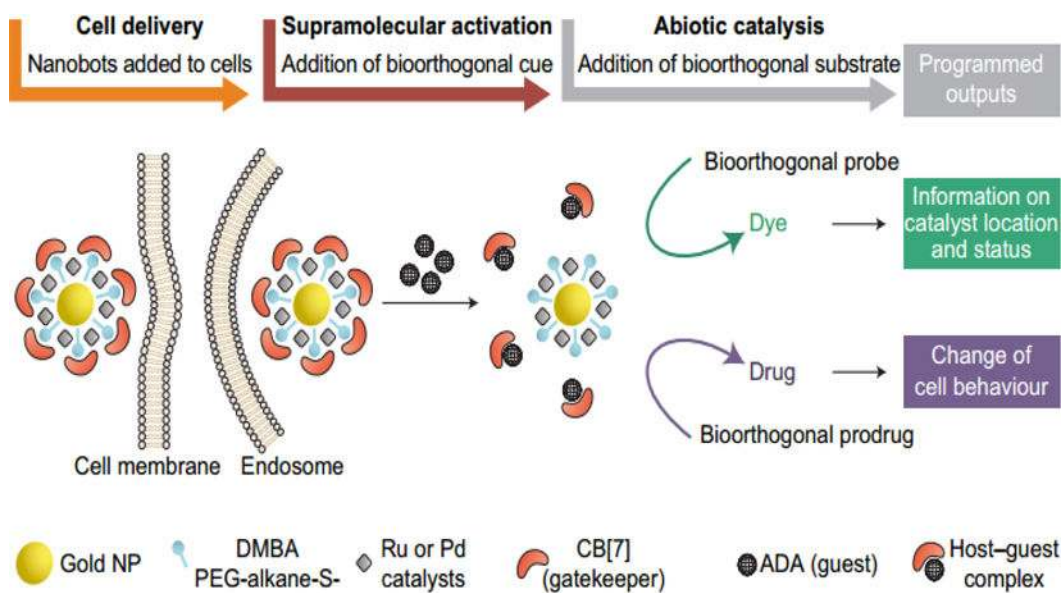


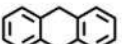
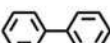
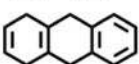


Fig. 31.

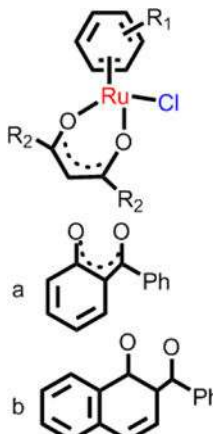
Spatiotemporal resolution of the sequential actions performed by Rotello's nanobots.

Reproduced with permission from ref. ³³³. Copyright 2015, Nature Publishing Group.

Names	η^6 -arene	Reaction rate ($10^{-2}\text{L}/(\text{mol s})$)	IC_{50} (μM)
Ben		1.13	17
Cym		2.29	10
Dha		7.08	20
Bip		8.06	5
Tha		14.72	0.5

Scheme 1.

The reaction rate of $[(\eta^6\text{-C}_6\text{H}_5)\text{Ru}(\text{en})\text{Cl}]^+$ family with cGMP and their cytotoxicity towards A2780 cells. Data originate from ref. ¹⁰³ and ¹⁰⁸.



arene	R ₂	IC ₅₀ (μM)
<i>p</i> -cymene	CH ₃	19
bip	CH ₃	21
benzene (bz)	CH ₃	>50
indan	CH ₃	>50
dha	CH ₃	70
<i>p</i> -cymene	Ph	11
<i>p</i> -cymene	CMe ₃	14
<i>p</i> -cymene	CF ₃	>100
<i>p</i> -cymene	a	>100
<i>p</i> -cymene	b	83

Scheme 2.

Ru(II) arene complexes bearing *O,O*-chelating ligands, and their cytotoxicity towards A2780 cells. Data originate from ref. ¹⁵⁷.

Table 1
The cytotoxicity of the selective cycloruthenated compounds used in anticancer drugs

Compounds	Cell lines	IC ₅₀ (μM)	Ref.
13a	A172	> 50	223
13b	A172	1.9	223
13c	A172	12	223
13d	A172	15	227
13e	A172	> 50	227
13f	A172	12	227
13g	A172	6.0	227
13h	A172	9.0	227
13i	A172	> 50	227
13j	A172	15	227
13k	HCT116	> 50	228
13l	HCT116	0.1	228
13m	HCT116	5.0	228
13n	HCT116	0.2	228
13o	HCT116	0.5	228
13p	HeLa	57	230
13q	HeLa	51	230
13r	HeLa	2.4	233
13s	HeLa	34	230
13t	HeLa	6.1	231
13u	HeLa	3.4	231
13v	HeLa	3.7	80
13w	HeLa	2.0	213
13x	HeLa	7.0	230
13y	HCT116	1.4	228
13y-1	HCT116	0.7	228
13y-2	HCT116	2.5	228

Compounds	Cell lines	IC ₅₀ (μM)	Ref.
13y-3	HCT116	1.0	228
13y-4	HCT116	0.3	228
13y-5	HeLa	0.51	232
13y-6	HeLa	1.05	232

Table 2

The cytotoxicity of the selective polypyridyl Ru(II) complexes used in PDT

Compounds	Cell lines	Dark IC ₅₀ (μM)	light IC ₅₀ (μM)	PI ^a	Irradiation Wavelength (nm)	Mechanism ^b	Ref.
14b	HeLa	334	0.47	1110	466	A+B	243
14c	A431	13	0.6	22	520	A	244
14d	A431	38	7.8	4.9	520	A	244
14f	HL60	> 300	1.6	> 188	VL ^d (> 450)	A	246
14g	HL60	108	2.6	42	VL (> 450)	A	246
14h	HL60	52.5	1.2	43.8	Blue light	A	247
14i	HL60	47.3	2.4	19.7	Blue light	A	247
14j	HL60	34	0.65	52	VL (400)	A	248
14k	HL60	> 300	0.16	1880	VL (400)	A	248
14n	HeLa	49.7	0.62	80	420	B	253
14o	HeLa	> 100	25.3	> 4	420	B	254
14p	HeLa	> 100	20	5	UV ^e	B	254
14q	HeLa	70	8.8	8	VL	B	255
14r	A549	19	0.72	26	454	A+B	256
14s	HL60	262	0.15	1747	White light	B	258
14u-I	HL60	> 300	> 300	N ^c	VL	B	1
14u-III	HL60	> 300	16	> 20	VL	B	1
14v	HL60	135	34	4	625	B	261
14X	HL60	> 300	0.741	> 410	VL	B	262
15a	HeLa	> 100	1.9	> 52	800	B	264
15b	HeLa	> 500	5.71	19	810	B	98
15c	HeLa	> 100	1.9	250	800	B	265

^aPI means IC₅₀(dark)/IC₅₀(light).^bthe ways of producing phototoxicity; A means ligand dissociation, B means ROS/¹O₂.^cN means not.

UV means ultraviolet.

VL means visible light.

Author Manuscript

Author Manuscript

Author Manuscript

Author Manuscript